HOKKAIDO UNIVERSITY

Title	Singing experience-dependent gene regulation for the critical period of vocal learning
Author(s)	早瀬, 晋
Citation	北海道大学. 博士(生命科学) 甲第13387号
Issue Date	2018-12-25
DOI	10.14943/doctoral.k13387
Doc URL	http://hdl.handle.net/2115/76368
Type	theses (doctoral)
File Information	Shin_Hayase.pdf

Instructions for use

Hokkaido University Collection of Scholarly and Academic Papers : HUSCAP

博士学位論文

Singing experience-dependent gene regulation for the critical period of vocal learning

(自発的な発声練習が制御する

ソングバード学習臨界期に関する研究)

早瀬　晋

北海道大学大学院生命科学院

平成 30 年 12 月

博士論文の日本語要旨　博士(生命科学)　氏名　早瀬　晋

Singing experience-dependent gene regulation for the critical period of vocal learning

(自発的な発声練習が制御するソングバード学習臨界期に関する研究)

本研究の目的は発声学習臨界期の終了をもたらす脳内分子基盤の理解である。脳内神経回路における臨界期は、生後未発達な脳に正常な機能を持たせ、維持するために重要である。これまで臨界期に関する研究は視覚系で主に進められ、その感覚経験依存性が明らかになってきた。しかし一般に感覚系の臨界期よりも後に来る運動系（言語の発音・スポーツ技能・楽器の演奏等）の学習臨界期が脳のどこで、何が引き金となり、どういった分子メカニズムにより制御されるのかわかっていない。そこで本研究では感覚運動学習に明確な臨界期をもち、なおかつ分子生物学的な研究が可能なソングバードを対象とし、運動系の臨界期における経験依存性および脳内分子基盤を調べた。

第一章において、キンカチョウの脳内の「どこ」で学習臨界期が制御されているのかを検討した。まず行動学的にキンカチョウの発声パターンが「どの時期・時間帯」に発達するのかを調べ、臨界期中、それも 1 日の轉り始め 3 時間に歌が最も発達することを示した。次に神経可塑性に重要な遺伝子 *Arc* をマーカーとし、歌が発達する発達時期・時間帯のみ神経可塑性が活発な脳部位を探索した。結果、歌に特化した脳内歌神経核の中でも、特に RA の興奮性投射ニューロンにおいて、*Arc* の発声行動に対する発現誘導率と歌の可塑性に相関が観察された。

第二章においては、何が引き金となり臨界期が終了するのかを調べた。幼鳥の発声練習行動を阻害することで、臨界期が単に加齢により制御されるのではなく、日々の発声経験の積み重ねにより終了することを示した。この発声阻害個体を用い、学習能力の調節に重要な脳内遺伝子発現調節を、単なる加齢による変化から切り離すことが可能となった。私は第一章で見つけた脳内神経核 RA に着目し、ゲノムワイドな遺伝子発現解析により経験依存的に制御される遺伝子群を調べた。その結果、臨界期を通じて発現変動する 1811 遺伝子のうちわずか 119 個の遺伝子だけが、経験依存的に発現調節されていた。逆に、これまで学習臨界期に関わると考えられてきた幼鳥から成鳥にかけての数千の遺伝子発現調節のうち殆どは単に加齢による変化であり、学習臨界期調節とは無関係であることが示唆された。キンカチョウで見つかった候補遺伝子群と学習臨界期との関係を、臨界期を毎年繰り返すカナリアを用いて確かめた結果、予想通り、カナリアでは歌に可塑性がある時期特異的に、これら遺伝子が RA において再誘導されていた。以上から、脳内神経核 RA における活動依存的な遺伝子の発現調節により学習臨界期が制御されていることが強く示唆された。

第三章では、キンカチョウ幼鳥の発声行動練習量および二次性徴発達の個体差に着目し、それらの相関を調べた。その結果、キンカチョウ幼鳥の発声練習経験が、二次性徴の 1 つ、オレンジ色の頬への換羽にも影響を与えている可能性を示した。

以上の研究により、発声練習行動という自発的な行動が、発声パターンの発達のみならず、脳内特定領域の遺伝子発現変動やそれに伴う発声学習の臨界期終了、そして二次性徴の発達に極めて重要な役割を果たしていることが明らかになった。

研　究　業　績　一　覧

１．論　文（学位論文関係）

(1)**Shin Hayase** and Kazuhiro Wada, “Singing activity-driven Arc expression associated with vocal acoustic plasticity in juvenile songbird”、 European journal of neuroscience 誌、Vol. 48、p. 1728-1742 (2018)

(2)**Shin Hayase,** Hongdi Wang, Eri Ohgushi, Masahiko Kobayashi, Chihiro Mori, Haruhito Horita, Katsuhiko Mineta, Wan-chun Liu, and Kazuhiro Wada, “Vocal practice regulates singing activity-dependent genes underlying age-independent vocal learning in songbirds.”、PLOS Biology 誌、Vol.16, e2006537 (2018)

２．論　文（その他）

(1)Kazuhiro Wada, **Shin Hayase**, Raimu imai, Chihiro Mori, Masahiko Kobayashi, Wan-chun Liu, Miki Takahashi, Kazuo Okanoya, “Differential androgen receptor expression and DNA methylation state in striatum song nucleus Area X between wild and domesticated songbird strains” European Journal of Neuroscience 誌、 Vol. 38(4)、p. 2600-2610、 (2013)

(2)Raimu Imai, Azusa Sawai, **Shin Hayase**, Hiroyuki Furukawa, Chinweike Norman Asogwa, Miguel Sanchez, Hongdi Wang, Chihiro Mori, Kazuhiro Wada, “A quantitative method for analyzing species-specific vocal sequence pattern and its developmental dynamics” Journal of Neuroscience Methods 誌、 Vol. 271, p. 25–33(2016)

(3)Shinji Yamaguchi, **Shin Hayase**, Naoya Aoki, Akihiko Takehara, Jun Ishigohoka, Toshiya Matsushima, Kazuhiro Wada, Koichi J. Homma, “Sex Differences in Brain Thyroid Hormone Levels during Early Post-Hatching Development in Zebra Finch (Taeniopygia guttata)” PLOS ONE 誌 (2017)

(4)Devin P. Merullo, Chinweike N. Asogwa, Miguel Sanchez-Valpuesta, **Shin Hayase**, Bikash R. Pattnaik, Kazuhiro Wada, Lauren V. Riters, “Neurotensin and neurotensin receptor 1 mRNA expression in song-control regions changes during development in male zebra finches” Developmental Neurobiology 誌、Vol. 78(7), p. 671-686 (2018)

(5)Norman Chinweike Asogwa, Chihiro Mori, Miguel Sanchez-Valpuesta, **Shin Hayase**, and Kazuhiro Wada, “Inter- and intra-specific differences in muscarinic acetylcholine receptor expression in the neural pathways for vocal learning in songbirds” Journal of Comparative Neurology 誌、Accepted (2018)

３．講　演（学位論文関係）

(1)**Shin Hayase** and Kazuhiro Wada, “Regulation of singing-driven genes in the song system during the critical period for vocal learning”, ICN / JSCPB(meeting of the 11th International Congress of Neuroethology) ポスター発表 PO-2089 (2014/7/31, Sapporo Convention Center, Sapporo, Hokkaido)

(2)**Shin Hayase** and Kazuhiro Wada, “Experience-dependent regulation of singing-driven gene expression in the song system during the critical period for vocal learning.” Neuroscience2014 (Society for Neuroscience 44th annual meeting) ポスター発表 779. 04/A37 (2014/11/19, Walter E. Washington Convention Center , Washington, DC, USA)

(3)**Shin Hayase** and Kazuhiro Wada, 「ソングバードにおける発声行動経験依存的な脳内遺伝子発現誘導制御と発声学習臨界期」, NGS 現場の会・第四回研究会、ポスター発表 6-24 (2015/7/1-7/3, つくば国際会議場, Tsukuba, Ibaraki)

(4)**Shin Hayase** and Kazuhiro Wada, "Accumulation of vocal experience regulates the critical period of vocal plasticity during active learning of birdsong", 第 39 回日本神経科学大会、口頭発表 O1-H-1-4 (2016/7/20, パシフィコ横浜, Yokohama, Kanagawa)

(5)**Shin Hayase** and Kazuhiro Wada, "Accumulation of singing experience regulates the critical period of vocal plasticity during birdsong active learning" Society for neuroscience 46th annual meeting Neuroscience2016、ポスター発表 (2016/11/14, San Diego, CA, USA)

(6)**Shin Hayase** and Kazuhiro Wada, "Accumulation of vocal experience regulates the critical period of vocal learning in songbirds" Avian Brain and Behavior; Sapporo Workshop 2016 learning and cognition embedded in animal behaviors、口頭発表 (2016/11/26, 北海道大学, Sapporo, Hokkaido)

(7)**Shin Hayase** and Kazuhiro Wada, "Accumulation of vocal experience regulates the critical period of vocal learning in songbirds", NIPS International Symposium "Towards elucidation of memory engram"、招待講演 (2016/12/6, 生理学研究所, Okazaki, Shizuoka)

Contents

General introduction

Critical periods in central nervous systems and their dependence on experience

Animals are born with immature brains (Davison, 1968; Portman et al., 1972). A number of neural circuits (including sensory and motor area) are rearranged by experience during a specific temporal window called the critical (or sensitive) period (Knudsen, 2004). Synaptic plasticity, the capacity to modify connections among neurons, is down-regulated for the closure of the critical period (Hensch, 2005), and is separately regulated in each circuit at different times in postnatal life (Bardin 2012).

Sensory circuits (*e.g.* visual, somatosensory, and auditory) are dramatically rearranged during the critical periods in various species including rodents, cats, and birds (Lorenz, 1958; Wiesel and Hubel, 1963; O'Leary et al., 1994; Gordon and Stryker, 1996; Chang and Merzenich, 2003). In the visual cortex, dark rearing elongates the critical period (Mower et al., 1981; Stryker and Harris, 1986; Sato and Stryker, 2008), indicating that the critical period in sensory areas is not solely regulated by age, but also by sensory experience from the surrounding environment.

Critical / sensitive periods are also observed in motor skill learning processes in vertebrates, *e.g.* human speech, playing instruments, and birdsong (Show & Hoefnagel-Hohle, 1978; Doupe & Kuhl, 1999; Elbert et al., 1995; Bengtsson et al., 2005). Although motor skills greatly improve through practice during the critical / sensitive period, skill improvement and brain plasticity tend to require more effort afterwards. For motor systems, experience is accumulated by self-generated active movements, but not passively given by the external environment. The contributions of such motor experience to the closure of the critical periods and its molecular mechanisms are still poorly understood.

Songbirds as a model to study the critical period of motor skill learning

Songbirds serve as an adequate animal model to examine the molecular mechanisms underlying the critical period of motor skill learning, based on the following biological characteristics:

(1) Active learning process for song acquisition. Songbirds develop their song through sensorimotor learning via the coordination of auditory inputs and motor outputs (Arnold, 1975; Zann, 1997; Nottebohm, 1985). Sensorimotor learning is achieved by repeated singing practice without any external rewards or punishments (Zann, 1997). For example, juvenile male zebra finch (*Teniopygia guttata*) sings hundreds of times per day to acquire a song pattern (Johnson et al., 2002; Ohgushi et al., 2015). Such active learning process allows us to easily monitor and evaluate daily song plasticity. In addition, thanks to efficient lab-breeding, and a 24 h recording system (Tchernichovski et al., 2000), researchers can track all songs produced by a juvenile bird from hatching to adulthood (Deregnaucourt et al., 2005; Johnson et al., 2002; Ohgushi et al., 2015).

(2) Critical period for song learning: Songbirds dramatically change their song acoustics and sequence only during a species-specific, defined critical period after hatching (Hultsch and Todt, 2004). For example, zebra finch learn a song during the critical period, between 30-90 post-hatching day (phd) (Immelmann, 1969; Arnold, 1975) (Fig. 1A). Their song learning process starts with the generation of subsong with soft and highly variable syllables (30-40 phd). Thereafter, birds start producing plastic song, characterized by the gradual inclusion of recognizable, yet variable syllables. The acoustic features of song syllables substantially develop during the early plastic song stage (40–60 phd). During this time, the acoustic structure of syllables, variance entropy, greatly change in the morning, but remains relatively stable in the afternoon

(Deregnaucourt et al., 2005; Shank & Margoliash, 2009). After the closure of the critical period (> 90 phd), song acoustics and syllable sequence are crystallized and maintained throughout life. Based on this persistent song stabilization, zebra finch is categorized as a “closed-ended” learner. On the other hand, canary (*Serinus canaria*) is referred to as an “open-ended” learner because it seasonally regains song plasticity every fall at adulthood (Fig. 1B). These temporal differences in song plasticity (between different times in a day, developmental stages, and seasons) allow us to examine the specific gene regulation in the brain for song plasticity from several points of view.

(3) Specialized neural circuits. For song learning and production, songbirds possess specialized neural circuits called the song system. This consists of a set of interconnected brain areas called the song nuclei (Nottebohm et al., 1976; Bottjer et al., 1984; Scharff & Nottebohm, 1991, Fig. 1C). The song system is divided into two functional circuits: the posterior vocal motor circuit for song production, and the anterior cortical-basal ganglia circuit for song learning and adult song plasticity (Fig. 1C). The song system is independent from other motor systems, *e.g.* flying or hopping (Feenders et al., 2008). Since learned acoustics and sequences of birdsong are generated by neuronal connections among song nuclei, regulation of neuroplasticity in these brain regions is considered important for the critical period of song development (Jarvis, 2004b). These specific brain circuits permit the evaluation of the effects of age and singing experience at the cellular and molecular level.

Neuronal activity-dependent genes and critical periods

After the critical period of song learning, neuroplasticity mechanisms such as long term depression (LTD), or long term potentiation (LTP) in the song nuclei are down-regulated or modified to stabilize the synaptic connections (Sizemore and Perkel, 2011; Ding and Perkel, 2004). This stabilization may contribute to the closure of the critical period of song plasticity. One of the candidate regulatory mechanisms for neuroplasticity is the induction change of neuroplasticity-related genes in such nuclei. Neural activity-dependent synthesis of mRNA / protein is supposed to either directly or indirectly influence the physiological function and structural maturation of neural circuits (Kelleher III et al., 2004; Greer and Greenberg, 2008, Bramham et al., 2008). In accordance with this, singing behavior induces a set of neuronal activity-dependent genes in the song circuits (Jarvis and Nettebohm, 1997; Wada et al., 2006; Whitney et al., 2014). Intriguingly, some of the activity-dependent genes are differentially induced in the song nuclei between juveniles and adults (Jin and Clayton, 1997; Wada et al., 2006). Another candidate mechanism is the shift in baseline gene expression in the song nuclei. A large variety of genes are developmentally regulated in the song circuits (Mori and Wada, 2015; Kubikova et al., 2010; Matsunaga and Okanoya, 2008).

These differentially regulated genes could be candidate molecules crucial to modulate song plasticity for the closure of the critical period. Since these previous studies focused only on gene expression differences between juveniles and adults, it is still unclear whether this gene regulation is really associated with song plasticity, or merely shifts according to age.

Sexual maturation period and singing experience

Secondary sex characteristics of male songbirds, such as birdsong, plumage coloration, or tail feather are important for courtship (Houtman, 1990; Lifjeld & Slagsvold 1988; Andersson, 1982). Plumage has been suggested to indicate a bird's nutritional conditions, social status, song repertories, or breeding seasons (Hill and Montgomerie, 1994; Senar, 1999; Lampe & Espmark 1994, Moller, 1989). Such correlations between plumage and the internal traits of individuals indicate that plumage does not solely develop by age, but exhibits developmental plasticity.

During the same period of song learning, sexual dimorphic features such as rust-colored cheek plumage (cheek patch), breast bands, and rust-colored side plumage also develop in male zebra finches (Zann, 1997, Fig. 22A). The cheek patches develop by molting the juvenile grey feathers to give rise to the adult rust-colored cheek plumage (Leader and Nottebohm, 2006). This process starts at about 35-40 phd, and is normally completed by 55-60 phd (Zann, 1997). It is known that there is individual variation in the timing of molting. For example, wild zebra finches in south-east Australia which hatched in late fall tend to show a delayed cheek plumage development for several months (Zann, 1997). Another study reported that social isolation or poor nutritional condition during the juvenile stage delays cheek plumage molting (Leader and Nottebohm, 2006; Krause and Naguib, 2014). However, the interaction between singing experience and plumage development has not been examined.

Goal of this thesis

In this thesis, I aimed to understand the closure mechanisms of the critical period of song learning. Therefore, I tried to detect specific gene regulation for song plasticity and examine its singing experience-dependence. However, there are too many song nuclei in songbirds to perform careful genome-wide analysis in all of them.

In Chapter I, to examine the brain region where the critical period is regulated, I elucidated where neuroplasticity is down-regulated during song stabilization using zebra finches. First, I identified when song acoustics changed in a day during the early plastic song stage. Then I elucidated the song nuclei where the induction of neuroplasticity-related genes correlated with song plasticity using juvenile birds it sung different time in a day, and adult birds.

In Chapter II, I examined how the critical period is regulated in the song nuclei. First, I tested the contribution of active motor experience for the closure of the critical period using singing-prevented (SP) zebra finches. Second, I examined singing experience-dependent gene regulation in the song nuclei by genome-wide gene expression analysis. By comparison of these experience-dependent genes between zebra finch and canary, I identified genes that are responsible for song plasticity across species.

In Chapter III, I examined the potential contribution of singing experience to the molting of cheek plumage using normal individual variations and manipulating practice by lesion of song nuclei.

General introduction Figure

(Figure 1)

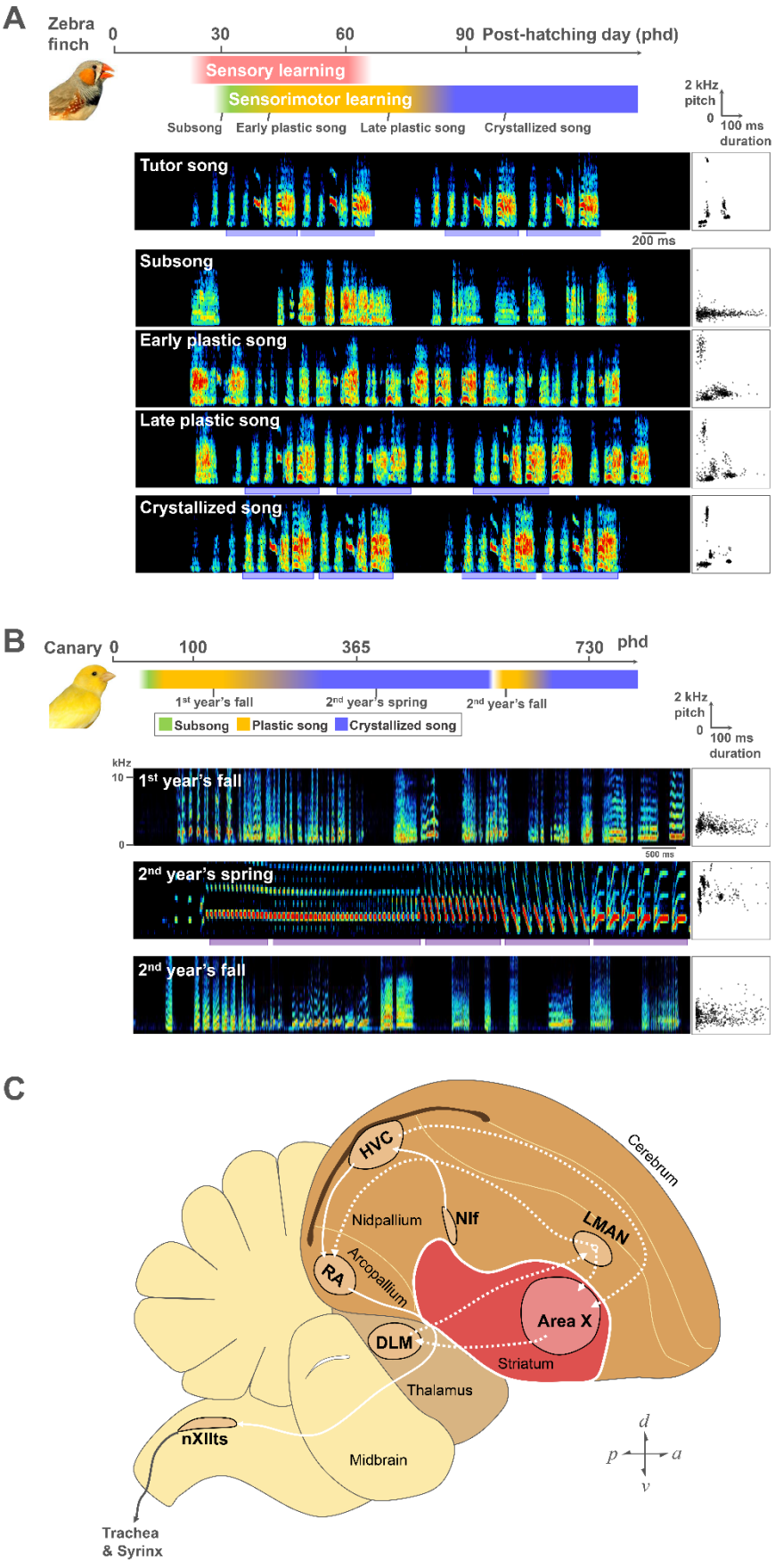

Figure 1. Critical period of vocal learning in songbird and the song circuits

(A) Critical period of vocal learning (upper panel) and song development (lower panels, left) in the zebra finch. Blue bars in the lower panels represent the motif structure of crystallized song. (Lower panels, right) Scatter plots indicate 500 syllable distribution (duration versus pitch).

(B) (Upper panel) The critical period of vocal learning in the canary. Seasonal change of vocal plasticity in canary songs (Lower panels, left). Purple bars: the crystallized repetitive phrase structure of canary song. (Lower panels, right) Scatter plots indicate 500 syllable distribution (duration versus pitch).

(C) Diagram of the song circuits (modified from Jarvis, 2004b). The posterior motor circuit and the anterior cortical-basal ganglia-thalamic circuit (anterior forebrain pathway) are represented as solid and dotted white lines, respectively. HVC (used as a proper name); RA, the robust nucleus of the arcopallium; Area X, Area X of the striatum; DLM, dorsal lateral nucleus of the medial thalamus; LMAN, lateral magnocellular nucleus of the anterior nidopallium; NIf, interfacial nucleus of the nidopallium; nXIIts, tracheosyringeal part of the hypoglossal nucleus.

Chapter I

Song nuclei-specific regulation of singing-induced gene for song plasticity

1.1 Introduction

In this chapter, to estimate where the critical period is regulated in the songbird brain, I identified song nuclei where neuroplasticity is modulated along with song plasticity. First, I evaluated when syllable acoustics developed during the critical period. During the the early-plastic song stage (40–60 phd, Fig. 1A; Fig. 2A), a syllable acoustic feature, variance entropy, greatly shifts especially in the morning (Deregnaucourt et al., 2005; Shank & Margoliash, 2009). As these previous studies focused on a single acoustic feature, it remains unclear whether other acoustic features are similarly and simultaneously modulated. Here, I compared shifts in the distribution of eight acoustic features (duration, variance entropy, pitch, entropy, FM, variance pitch, mean frequency, and pitch goodness) in the morning (9AM vs. 12PM) and afternoon (12PM vs. 7PM) to quantitatively evaluate the diurnal dynamics of syllable acoustics.

To identify the song nuclei where neuroplasticity is modulated along with diurnal song plasticity, I analyzed the induction of a neuroplasticity-related gene by singing. Activity-regulated cytoskeleton-associated protein (*Arc*) is an important effector gene for neuroplasticity (Shepherd & Bear, 2011). Mammalian studies reveal that *Arc* increases the endocytic trafficking of α-amino-3-hydroxy-5-methyl-4-isoxazolepropionic acid (AMPA) receptors in dendritic spines, a crucial regulator of LTD and LTP underlying synaptic plasticity (Steward et al., 1998; Chowdhury et al., 2006; Plath et al., 2006; Messaoudi et al., 2007). *Arc* expression is also induced in songbird song nuclei by singing (Wada et al., 2006). I examined the induction of *Arc* in the song nuclei at different times of the day: morning, afternoon, and evening during the early plastic song stage (Fig. 3A).

To identify the potential regulatory mechanisms behind the diurnal modulation of *Arc* induction in the song nuclei, I examined the effect of circadian rhythm. I prevented birds from singing for 8 hours after lights on, and then allowed them to freely sing for 30 min in the evening (Fig. 5A). To examine the potential contribution of diurnal change in neuronal activity of the upstream brain regions to modulate *Arc* induction, I performed unilateral lesion of the song nuclei.

Exogenous testosterone leads to a precocious stabilization of birdsong (Korsia & Bottjer, 1991; Sizemore & Perkel, 2011). To further examine the correlation between *Arc* induction in the song nuclei and song plasticity, I manipulated juveniles by testosterone (T) implantation to accelerate syllable acoustic stabilization at an earlier developmental stage than sham-operated (blank-implanted) juveniles. Adult birds with crystallized songs were added for comparison. *Arc* induction in the song nuclei was compared among blank-implanted, T-implanted, and adult birds.

Finally, I identified the neuronal subtypes in which *Arc* induction is regulated in a day and through the critical period. The song nuclei are made up of heterogeneous cell populations including glia, vascular, glutamatergic excitatory projection neurons, and GABAergic inhibitory local neurons (Spiro et al., 1999; Vyssotski et al., 2016). I co-labeled *Arc* mRNA with the glutamatergic excitatory neuron marker *Vglut2* (vesicular glutamate transporter 2) and a GABAergic inhibitory neuron marker *Gad2* (glutamic acid decarboxylase 2) by fluorescence *in-situ* hybridization.

1.2 Materials and methods

Animals

Male zebra finches were obtained from our breeding colonies at Hokkaido University. Birds were kept in breeding cages (370 x 415 x 440 mm: HOEI) under a 13 : 11 h light / dark cycle. During song recording sessions, each bird was individually housed in a cage inside a sound-attenuating box. All experiments were conducted under the guidelines and approval of the Committee on Animal Experiments of Hokkaido University (Approved No. 13-0061). These guidelines are based on the national regulations for animal welfare in Japan (Law for the Humane Treatment and Management of Animals with partial amendment No.105, 2011).

Song recording

Songs were recorded using a unidirectional microphone (SM57, Sure) connected to a computer with Sound Analysis Pro (SAP v1.04; http://soundanalysispro.com/) (Tchernichovski et al., 2000). Each song bout was saved as a sound file (wav file), including time information. Low frequency noise (< 0.5 kHz) and mechanical noise were filtered out using avisoft-SASLab (Avisoft Bioacoustics). I visualized syllable distribution patterns (scatter plots) using the SAP program while measuring two acoustic features, syllable duration and pitch. A song bout was defined as the continuous production of syllables followed by at least 200 ms of silence.

Song acoustic shifts

Analysis of syllables acoustic features was performed using SAP program while measuring eight acoustic features; syllable duration, variance entropy, pitch, entropy,

frequency modulation (FM), variance pitch, mean frequency, and pitch goodness. For quantitative evaluation of diurnal acoustic dynamics of juveniles (n = 17, 45–53 phd, mean = 49.7 phd), T-implanted juveniles (n = 10, 44–51 phd, mean = 46.9 phd), and adults (n = 12, 123–512 phd, mean = 198.3 phd), 500 syllables were sampled from the first 0–1 h, 3–4 h, and 8–10 h after the birds started singing and were analyzed. To measure shifts of syllable acoustics between each time point, probability density distributions were derived for each acoustic feature by the statistics software R program (R core team, 2012). For calculation of syllable acoustic shifts (%) of morning (comparison between 0–1 and 3–4 h after birds start singing) and afternoon (comparison between 3–4 and 8–10 h after birds start singing) period, areas in probability density distributions that were not overlaid were measured. The *p* values for comparison of acoustic shifts between morning and afternoon periods during juvenile singing were obtained by applying the Wilcoxon signed-rank test with Bonferroni correction. The *p* values for comparisons of acoustic shifts (%) during morning period among normal juveniles, T-implanted juveniles, and normal adults were obtained by applying the ANOVA with Bonferroni correction and subsequently the unpaired *t* test with Bonferroni correction as post hoc test.

Brain sampling

Male zebra finch juveniles were split into eleven experimental groups: (I) 30 min silence (n = 5, 50–55 phd, mean = 53.4); (II) 30 min singing as morning singing (n = 12, 45–54 phd, mean = 48.7); (III) 3 h singing + 1 h silence + 30 min singing as afternoon singing (n = 8, 43–60 phd, mean = 51.8); (IV) 7 h singing + 1 h silence + 30 min singing as evening singing (n = 8, 45–55 phd, mean = 50.5); (V) 8 h silence + 30 min singing as diurnal singing-prevented (n = 9, 45–54 phd, mean = 49.7); (VI) 7 h singing + 1 h silence

(n = 4, 49-53 phd, mean = 51.25); (VII) unilateral LMAN lesioned + 30 min singing (n = 4, 47–52 phd, mean = 49.8); (VIII) unilateral HVC lesioned + 30 min singing (n = 7, 47–52 phd, mean = 49.6); (IX) testosterone-implanted + 30 min singing (n = 12, 43–53 phd, mean = 47.6); (X) blank tube-implanted + 30 min singing (n = 9, 45–51 phd, mean = 47.4);, and (XI) adult 30 min silent/singing (n = 17, 103–512 phd, mean = 153). Each bird was individually placed in a sound-attenuating box overnight, and singing behavior was recorded during the next morning after lights on. For brain sampling of silent conditions, birds were prevented from singing by tapping cages when the birds started singing. For accurate estimation of the induction of *Arc* at afternoon and evening periods, I kept birds silent for more than 1 hour to ensure cell clearance of previously-accumulated *Arc* mRNA (Fig. 4), and then I performed brain sampling after 30 min of singing. Singing duration was defined as the total amount of singing during the last 30 min before brain sampling. Brains were embedded in OCT compound (Sakura Fine Technical) and stored at −80°C until use.

In-situ **hybridization**

cDNA fragments used for the synthesis of i*n-situ* hybridization probes were cloned from a whole-brain cDNA mixture of a male zebra finch. Total RNA was transcribed to cDNA using Superscript Reverse Transcriptase (Invitrogen) with oligo dT primers. The cDNAs were amplified by PCR using oligo DNA primers directed to conserved regions of the coding sequence from the NCBI cDNA database. PCR products were ligated into the pGEM-T Easy plasmid (Promega) (Chapter II, Table. 2, p. 81). The cloned sequences were searched using BLAST against the NCBI nucleotide database to identify homologies to other species. For radioisotope *in-situ* hybridization, 12-μm thick frozen sections were

cut in the sagittal plane. Brain sections for a given experiment were simultaneously fixed in 3% paraformaldehyde/1× PBS (pH7.4), washed in 1× PBS, acetylated, dehydrated in an ascending ethanol series, air dried, and processed for *in-situ* hybridization with antisense 35S-UTP labeled riboprobes of genes. To generate the riboprobes, gene inserts in the pGEM-T Easy vector were PCR amplified with plasmid M13 forward and reverse primers, and then gel purified. The amplified DNA fragments and Sp6 or T7 RNA polymerase was used to transcribe the antisense 35S-riboprobes. A total of 1×10^6 cpm of the 35S-probe was added to a hybridization solution (50% formamide, 10% dextran, 1× Denhardt's solution, 12 mM EDTA (pH8.0), 10 mM Tris-HCl (pH8.0), 300 mM NaCl, 0.5 mg/mL yeast tRNA, and 10 mM dithiothreitol). Hybridization was performed at 65°C for 12–14 h in same time for each probes to reduce experimental biases. The slides were washed in 2× SSPE and 0.1% β-mercaptoethanol at room temperature for 1 h, 2× SSPE, 50% formamide, and 0.1% β-mercaptoethanol at 65°C for 1 h, and 0.1× SSPE twice at 65°C for 30 min each. Slides were dehydrated in an ascending ethanol series, and exposed to X-ray film (Biomax MR, Kodak) for 1-14 days. The slides were then dipped in an autoradiographic emulsion (NTB2, Kodak), incubated for 1-8 weeks, and processed with D-19 developer (Kodak) and fixer (Kodak). Developed slides were Nissl-stained with a cresyl violet acetate solution (Sigma). The high resolution silver-dipped glasses were used for graphic representation. But due to uneven staining of some sections on the silver-dipped glass slides, we used X-ray films to measure the expression intensity of genes in song nuclei. To minimize experimental bias, we performed hybridization and film exposure at the same time for each comparison. The exposed X-ray films of brain images were digitally scanned from a dissecting microscope (Leica, Z16 APO) connected to a CCD camera (Leica, DFC490) with Application Suite V3 imaging software (Leica). The

same light settings were used across all images from each experiment. Photoshop (Adobe Systems) was used to measure the mean pixel intensities in the brain areas of interest from sections after conversion to 256 grayscale images. For statistical analysis of the expression of each gene, I presumed linear induction curve to singing duration an ANCOVA was performed to examine the homoscedasticity from the regression line of the gene induction. For fluorescent *in-situ* hybridization, dinitrophenyl (DNP)- and digoxigenin (DIG)-labeled riboprobes were used. A total of 100–200 ng of the DNP/DIG-labeled riboprobe was mixed with the hybridization solution (50% formamide, 10% dextran, 1× Denhardt's solution, 1 mM EDTA (pH8.0), 33 mM Tris-HCl (pH8.0), 600 mM NaCl, 0.2 mg/mL yeast tRNA, 80 mM dithiothreitol, and 0.1% N-lauroylsarcosine). Hybridization was performed at 68^{o}C for 6–13 hr. Washing steps were performed as follows: 5× SSC solution at 68^{o}C for 30min, formamide-I solution (4× SSC, 50% formamide, and 0.005% Tween20) at 68^{o}C for 40min, formamide-II solution (2× SSC, 50% formamide, and 0.005% Tween20) at 68^{o}C for 40min, 0.1× SSC 68^{o}C 15min × 3, NTE buffer at RT for 20min, and TNT buffer × 3, and TNB buffer [0.5% blocking reagent (Perkin Elmer)/1× TNT buffer] at RT for 30 min. DNP-labeled probes were detected with an anti-DNP horseradish peroxidase (HRP)-conjugated antibody using a TSA DNP system (Perkin Elmer) and anti-DNP KLH AlexaFluor488 (Molecular Probes, cat#A-11097). Following treatment with 1% H_2O_2/1× PBS for 30 min, DIG-labeled probes were detected with anti-DIG HRP-conjugated antibody (Jackson Laboratory, cat#200-032-156) and a TSA Plus Cy3 system (Perkin Elmer). Signal images were obtained by fluorescence microscopy (EVOS FL; Thermo Fisher Science).

Unilateral HVC or LMAN lesion

Juvenile zebra finches (35–40 phd; n = 4 for left HVC lesion, n = 3 for right HVC lesion, n = 2 for left LMAN lesion, and n = 2 for right LMAN lesion) were anesthetized with pentobarbital and lesioned by the local injection of 240 nL of 1 % ibotenic acid dissolved in 1 M NaCl using a Nanoject 2 injector (Drummond Scientific) at least 6 days before sacrifice. HVC or LMAN were targeted with stereotaxic coordinates in mm: HVC; 0–0.5 rostral, 2.2–2.4 lateral, and 0.8–1.0 ventral, LMAN; 5.0 rostral, 2.0 lateral, and 1.6 ventral from the bifurcation of the central sinus at the border of the forebrain and cerebellum. To measure the lesioned area, 12-μm thick coronal frozen sections were fixed with 4% paraformaldehyde/1× PBS (pH7.4), washed in 1× PBS, and Nissl-stained with a Cresyl violet acetate solution (Sigma). Complete-lesioned animals were used for *in-situ* hybridization experiments. Paired t test was performed for *Arc* expression intensity in RA in ipsilateral and contralateral of lesioned sites to examine the effect of unilateral HVC or LMAN lesion.

Exogenous testosterone administration

Juvenile birds were subcutaneously implanted with a silastic tube (inner diameter, 1.0 mm; outer diameter, 2.0 mm) containing either 10 mm of crystalline testosterone (T-implanted; n = 13) or 10 mm of silicon (blank-implant; n = 9) from 30 phd. To measure serum testosterone of T-implanted juveniles and blank-implanted juveniles, blood was sampled from the jugular vein when birds were euthanized, and then serum testosterone was assessed using a testosterone enzyme-linked immunosorbent assay kit (Enzo ADI-900-097). Sampling of brains and blood was performed by 9AM after lights were turned on at 8AM at 43–53 phd (T-implanted, mean = 47.64; black-implanted mean = 47.7).

Retrograde labeling of projection neurons in RA and NIf

nXIIts and HVC of juvenile birds (30–34 phd, n = 2 for nXIIts; n = 2 for HVC) were targeted with stereotaxic coordinates (range in mm: -0.8 rostral, 0.2 lateral, 5.9-6.0 ventral for nXIIts; 0.2-0.4 rostral, 2.2-2.5 lateral, 0.8-1.0 ventral for HVC, from the bifurcation of the central sinus at the border of the forebrain and cerebellum). The retrograde tracer DiI (SIGMA, 70 mg/ml dissolved in N, N-dimethylformamide; 100 nl / nXIIts) or or Cholera Toxin B subunit-AlexaFluor555 conjugated (CTB, Invitrogen, 1 mg/ul; 100 nl / HVC) was injected into the nXIIts or HVC 10 days before euthanasia. Birds were euthanized after 30 min of singing, and brains were processed for fluorescence *in-situ* hybridization.

1.3 Results

Diurnal shift and stabilization of syllable acoustic features

Syllable acoustics developed mainly during the first 3 hours in a day and the altered features were maintained until sleep during the early plastic song stage. First I traced the trajectories of two acoustic features, variance entropy and pitch, of all syllables produced by a juvenile for two successive days during the early plastic song stage (50-51 phd, Fig. 2B). Although these two acoustic features consistently fluctuated in a daily fashion, the average and distribution of the acoustic features largely shifted within the first 3 hours after the start of singing and remained relatively stable during the afternoon until sleep (Fig. 2B and C). Each juvenile modified individually a unique set of syllable acoustic features with different changing rate during a day (Fig. 2D). However, the shifts in the distribution of acoustic features were significantly larger in the morning than in the afternoon (Fig. 2E).

Diurnal change of *Arc* induction in the song nuclei

The induction intensity of *Arc* attenuated diurnally in RA and NIf during the early plastic song stage. I examined *Arc* induction at different times during the day: morning, afternoon, and evening at the early plastic song stage (Fig. 3A). I ensured that the 1 h silence period before singing session was enough to reverse the *Arc* expression level to baseline (Fig. 4A, B, and C). In the premotor song nucleus HVC and the cortical-basal ganglia circuit nuclei LMAN and Area X, *Arc* mRNA was consistently induced at similar intensities by singing at each time in the day (Fig. 3B and C). In contrast, in the song nuclei RA and NIf in the vocal motor circuit, *Arc* induction was significantly down-regulated in the afternoon and evening compared with its level in the morning (Fig. 3C;

Bonferroni-corrected ANCOVA: morning: afternoon (RA), $F(1,24) = 26.98$, $p = 8.7e\text{-}5$; morning: evening (RA), $F(1,24) = 19.85$, $p = 4.0e\text{-}4$; morning: afternoon (NIf), $F(1,24) = 50.53$, $p = 9.2e\text{-}7$; morning: evening (NIf), $F(1,24) = 32.24$, $p = 1.5e\text{-}5$). These result indicate a correlation between song acoustic plasticity and *Arc* induction in RA and NIf.

Diurnal singing experience-dependent attenuation of *Arc* inducibility in RA and NIf

The diurnal change of *Arc* inducibility in RA is neither modulated by the circadian rhythm nor by neuronal activity in upstream brain regions, but by cumulative singing experience in RA. The diurnal singing-prevented juveniles (8 hr singing prevention + 30 min singing) induced *Arc* in all song nuclei, including RA and NIf, with similar induction intensities during the morning singing (Fig. 5B and C). To examine a potential contribution of neuronal activity of the RA upstream brain regions in modulating *Arc* induction in RA, I unilaterally lesioned HVC or LMAN and compared *Arc* induction in ipsilateral and contralateral RAs, respectively (Fig. 6A and B). I found that unilateral lesion of HVC or LMAN did not affect the induction of *Arc* in ipsilateral RA compared with the contralateral side after morning singing (Fig. 6A and B).

Testosterone implant-induced song stabilization or closure of the critical period is accompanied by attenuation of *Arc* inducibility in RA and NIf

Arc induction was also attenuated in RA and NIf in song-stabilized birds; T-implanted juveniles and adults. I ensured that T-implantation significantly increased the circulating testosterone levels when compared to blank implants (T-implanted: 10.7 ± 1.3 ng/mL, n = 11 birds, and blank-implanted: 0.95 ± 0.68 ng/mL, n = 9 birds, respectively; unpaired t test, $p = 6.0$ e-13). As I speculated, the shifts in distribution of syllable acoustic

features in the morning were significantly lower in T-implanted juveniles (43-53 phd) compared with intact birds of the similar age (Fig. 7A, F). These artificially suppressed acoustic shifts by T-implantation were similar to normal adults with crystalized songs (Fig. 7B-F). When the T-implanted juveniles were compared with blank tube-implanted birds, *Arc* induction was significantly attenuated in the RA of T-implanted birds (ANCOVA: RA, $F(1,23) = 9.97$, $p = 0.013$) (Fig. 8A and B). The T-implant effect on attenuation of *Arc* inducibility in NIf was milder than in RA (Fig. 8B). In normal adult birds, *Arc* induction by morning singing was significantly attenuated in RA and NIf when compared with intact and T-implanted juveniles (Bonferroni-corrected ANCOVA: blank-implanted juvenile: adult (RA), $F(1,28) = 34.8$, $p = 8.2$ e-6, blank-implanted juvenile : adult (NIf), $F(1,28) = 16.17$, $p = 0.0013$) (Fig. 8A and B). These results indicate a strong correlation between song plasticity and *Arc* induction in the song nuclei RA and NIf.

Identification of *Arc*-inducing neurons in RA and NIf

Arc mRNA was induced by singing in the glutamatergic projection neurons in RA and NIf. Molecular markers, *Vglut2* and *Gad2* (Fig. 9A) were not co-expressed in RA (Fig. 9B). By co-labeling *Arc* with *Vglut2* or *Gad2*, I found that *Arc* was specifically induced in the glutamatergic excitatory neurons in both RA and NIf by juvenile singing (RA: 99.1% co-labeled, NIf: 97.5%) (Fig. 9C and D). By co-labeling *Arc* with DiI retrograded from nXIIts (Fig. 9E) or Cholera Toxin B subunit (CTB) conjugated with Alexa-Fluor555 retrograded from HVC (Fig. 9G), I identified that *Arc* was induced in the projection neurons in both RA and NIf (RA: 95% co-labeled, NIf: 95.7%) (Fig. 9F and H).

1.4 Discussion

In this Chapter I, I aimed to elucidate the song nuclei where neuroplasticity is modulated to effect the closure of the critical period. During the early plastic song stage, juvenile birds developed song acoustics dramatically within the first 3 hours in a day, and the altered features were maintained until the end of the day (Fig. 2). Diurnal song stabilization was accompanied by the down-regulation of *Arc* induction, in projection neurons in RA and NIf (Fig. 3; Fig. 7). This diurnal induction change was regulated by singing experience, not circadian rhythm (Fig. 5). Especially in RA, *Arc* induction was attenuated in both adults and T-implanted juveniles with stabilized songs (Fig. 7; Fig. 8). These results suggest that the change in the induction of *Arc* in RA and NIf contribute to the diurnal song stabilization and closure of the critical period of song learning.

Internal regulation mechanisms of *Arc* induction

In RA and NIf, singing-dependent neuronal excitation is generated in both juveniles and adults (Ölveczky et al., 2011; Vyssotski et al., 2016). These facts indicate that the changes in induction rate of *Arc* in RA and NIf do not depend on a developmental decrease in neuronal firing rate during singing in RA and NIf. Additionally, lesion of upstream regions of RA did not affect *Arc* induction in RA (Fig. 6), even through such lesions should influence the firing pattern of RA neurons. Therefore, singing-dependent neuronal activity is necessary, but not sufficient to regulate *Arc* expression dynamics in RA and NIf, due to intracellular molecular mechanisms that modulate gene induction strength in song nuclei-specific manner.

Presumed functions of singing-induced genes in projection neurons in RA

In the projection neurons in RA, *Arc* induction strength correlated with song plasticity, daily and developmentally (Fig. 10A). Based on previous electrophysiological studies, I propose a potential function of *Arc* induction in these neurons for song plasticity (Fig. 10B, C, D, and E). As the final telencephalic output nucleus of the song system, RA neurons project to motor neurons of the hypoglossal nucleus (nXIIts) which directly innervate syringeal muscles (Vicario & Nottebohm, 1988, Wild, 1993) to generate song pattern. During singing, the firing rate of RA neurons can be correlated with syllable acoustic features, including pitch, amplitude and entropy (Sober et al., 2008). Therefore, the firing rate of RA neurons is crucial in the production of learned song. RA receives two premotor inputs: a motor exploration signal from LMAN as the cortical-basal ganglia-thalamic circuit output and a time-locked sequence signal from HVC of the motor circuit (Hahnloser et al., 2003; Fee et al., 2004; Kao et al., 2005; Ölveczky et al., 2011; Okubo et al., 2015). In the early plastic song stage, immature syllables are produced by random firing activity of RA neurons owing to a larger number of HVC-RA connections. (Garst-Orozco et al., 2014, Fig. 10B). Through song practice, the motor circuit is refined by the strengthening and pruning of HVC to RA connections, but not the LMAN to RA connections (Garst-Orozco et al., 2014; Stark and Perkel, 1999). These circuit changes in RA are regulated by activity-dependent synaptic plasticity (Mehaffey and Doupe, 2015). Intense *Arc* induction may contribute to such synaptic plasticity during morning singing in the early plastic song stage (Fig. 10C).

After song development, stereotyped syllables are produced by the bursting activity of selective RA neurons due to refined HVC-RA connections (Fig. 10C). The attenuation of *Arc* induction in RA neurons may reduce the synaptic plasticity between

HVC and RA and then fix the syllable acoustics (Fig. 10D). Indeed, LTD between HVC-RA connections is down-regulated after the critical period (Sizemore and Perkel, 2011). However, not only *Arc*, but many other genes should contribute to such developmental change in neuroplasticity. To deeply understand the molecular mechanisms for the closure of the critical period, further genome-wide gene expression analysis is needed.

1.5 Figures

(Figure 2)

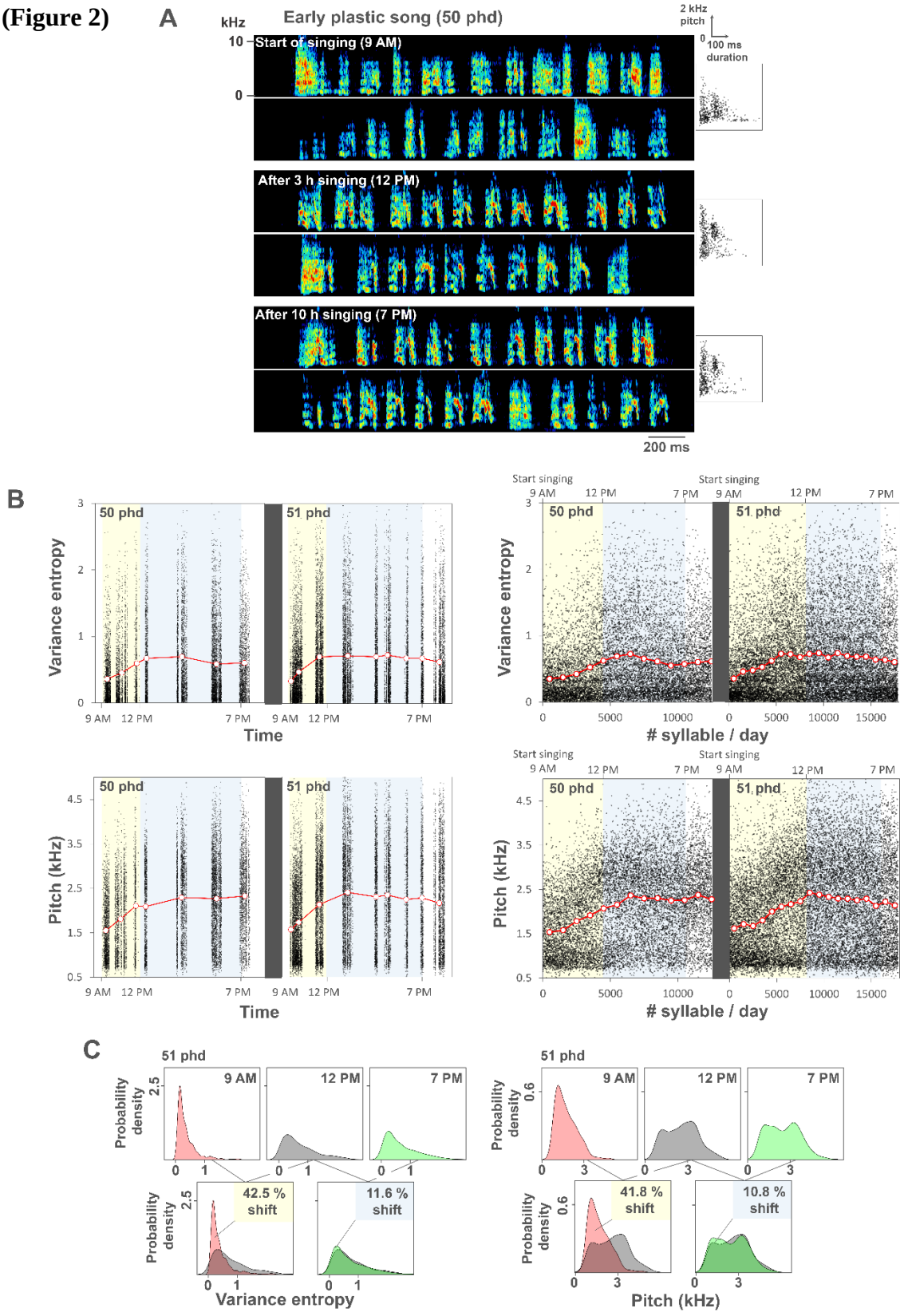

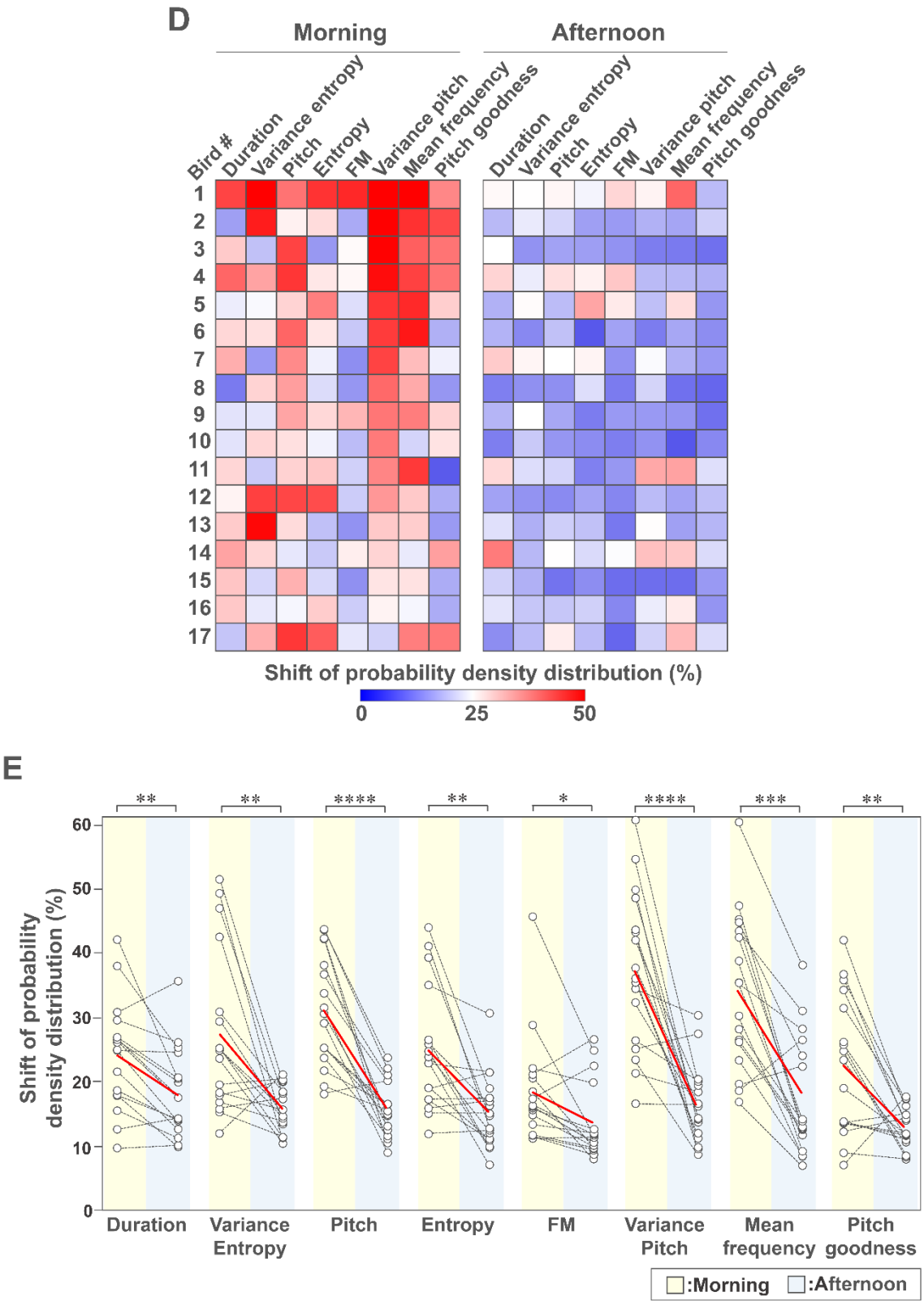
D
Morning
Afternoon
Bird #
Duration
Variance entropy
Pitch
Entropy
FM
Variance pitch
Mean frequency
Pitch goodness
1
2
3
4
5
6
7
8
9
10
11
12
13
14
15
16
17
Shift of probability density distribution (%)
0
25
50
E
**
**
****
**
*
****
***
**
Shift of probability density distribution (%)
60
50
40
30
20
10
0
Duration
Variance Entropy
Pitch
Entropy
FM
Variance Pitch
Mean frequency
Pitch goodness
:Morning
:Afternoon

Figure 2. Diurnal shift and stabilization of song syllable acoustics during the early-plastic song stage in the zebra finch

(A) Early plastic songs of a zebra finch juvenile (50 phd) in the morning (9AM), afternoon (12PM), and evening (7PM) in a day.

(B) Trajectory plots of variance entropy and pitch of all song syllables during 2 successive days produced by the same bird shown in **(A)** (12,506 syllables at 50 phd; 17,845 syllables at 51 phd). Acoustic features were plotted against time (left panels) or the order of syllables (right panels). Red-lined circles indicate the average of each song cluster (left panels) or each 1,000 syllables (right panels).

(C) Distribution of probability density of variance entropy and pitch in morning (9AM), afternoon (12PM), and evening (7PM) using 500 syllables at each time point (upper panels). Comparison of probability densities of the two acoustic features for the assessment of the acoustic shifts (%) during morning and afternoon periods (lower panels).

(D) Individual variations of acoustic shifts (%) during morning and afternoon period for eight acoustic features (duration, variance entropy, pitch, entropy, FM, variance pitch, mean frequency, and pitch goodness), n= 17 birds.

(E) Comparison of the acoustic shifts (%) between morning and afternoon periods during the early-plastic song stage (45 - 53 phd, n = 17). Black lines indicate acoustics shifts for individual bird. Red lines indicate average of 17 birds. *$p < 0.05$, **$p < 0.01$, ***$p < 0.001$, ****$p < 0.0001$; Wilcoxon signed-rank test.

(Figure 3)

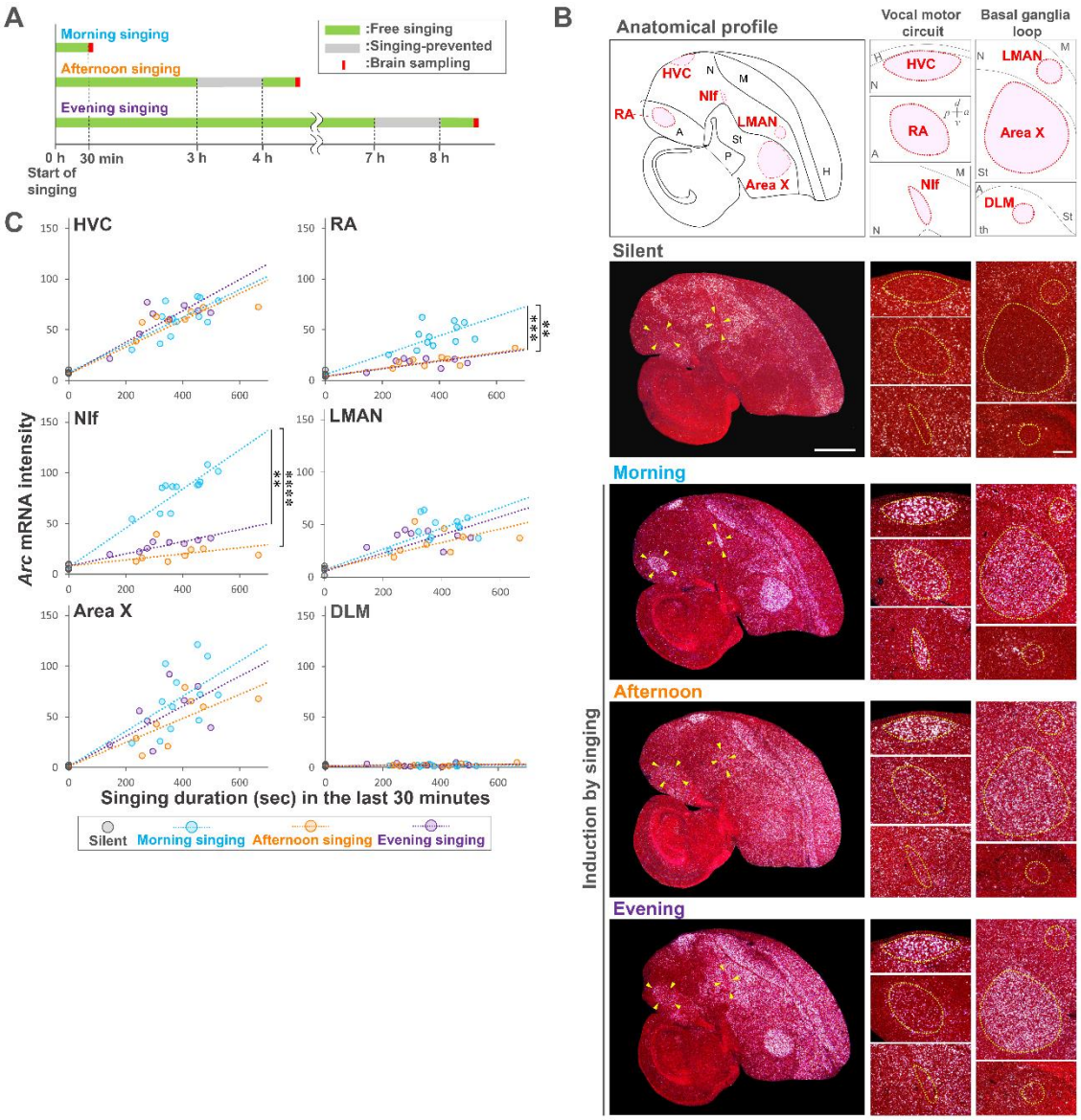
A
Morning singing
Afternoon singing
Evening singing
:Free singing
:Singing-prevented
:Brain sampling
0 h
30 min
3 h
4 h
7 h
8 h
Start of singing
B
Anatomical profile
Vocal motor circuit
Basal ganglia loop
HVC
RA
NIf
LMAN
Area X
DLM
Silent
Morning
Afternoon
Evening
Induction by singing
C
HVC
RA
NIf
LMAN
Area X
DLM
Arc mRNA intensity
Singing duration (sec) in the last 30 minutes
Silent
Morning singing
Afternoon singing
Evening singing

Figure 3. Diurnal change of *Arc* inducibility during singing of the early-plastic songs in song nuclei RA and NIf

(A) Experimental paradigm for brain sampling to test the diurnal regulation of *Arc* in song system.

(B) (left panel) Typical examples of expression of *Arc* mRNA in silence (50 phd) and singing during morning (47 phd, 328 sec singing), afternoon (52 phd, 348 sec singing), and evening periods (51 phd, 405 sec singing). White signals: *Arc* mRNA expression. Red: Cresyl-violet counter-stained cells. Sections are sagittal. Scale bar = 1.5 mm. (right panel) Higher magnification images of *Arc* mRNA expression in song nuclei. A, arcopallium; H, hyperpallium; M, mesopallium; N, nidopallium; P, pallidum ;St, striatum; Th, thalamus. Scale bar = 200 μm.

(C) Induction rate of *Arc* mRNA in song nuclei during singing in the morning (light blue; n = 12 birds, 45–54 phd, mean = 48.7), afternoon (orange; n = 8 birds, 43–60 phd, mean = 51.8), and evening (purple; n = 8 birds, 45–55 phd, mean = 50.5). Silent condition (black; n = 5 birds, 50–55 phd, mean = 53.4). $^{**}p < 0.001$, $^{***}p < 0.0001$, $^{****}p < 0.00001$; ANCOVA with Bonferroni correction.

(Figure 4)

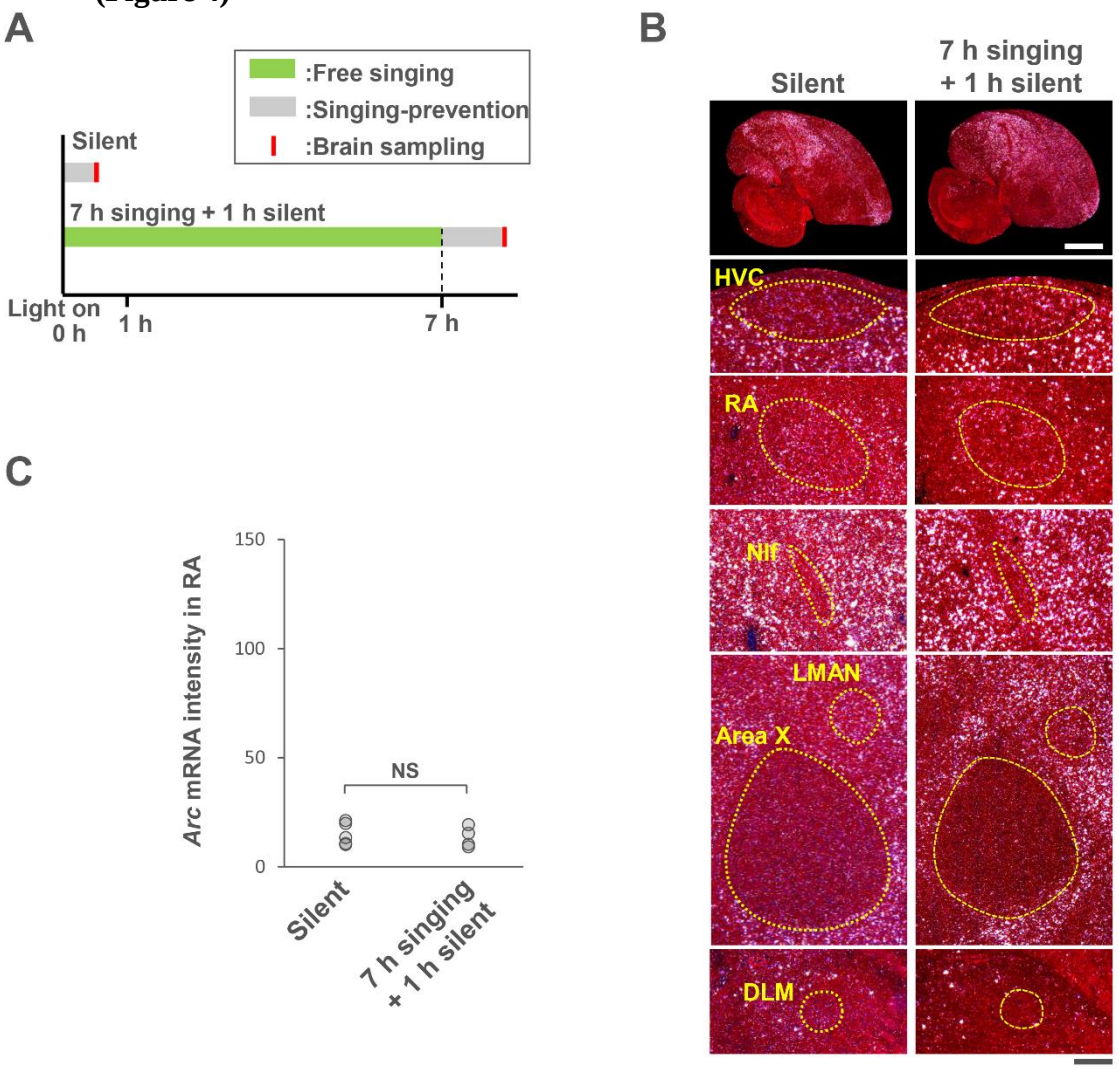

Figure 4. 1 h silence period was enough for the reduction of *Arc* expression level to basal level in song nuclei.

(A) Experimental paradigm for brain sampling to test the reduction of *Arc* mRNA expression in song nuclei by 1 h silence after continuous singing.

(B) Typical examples of expression of *Arc* mRNA in the silent condition (50 phd) and 7 h singing + 1 h silent condition (49 phd). Scale bar = 1.5 mm, 200 μm.

(C) Expression level of *Arc* mRNA in RA of silent (n = 5 birds, 50–55 phd, mean = 53.4) and 7 h singing + 1 h silent (n = 4 birds, 49-53 phd, mean = 51.25). $^{NS}p > 0.1$, Mann-Whitney *U* test.

(Figure 5)

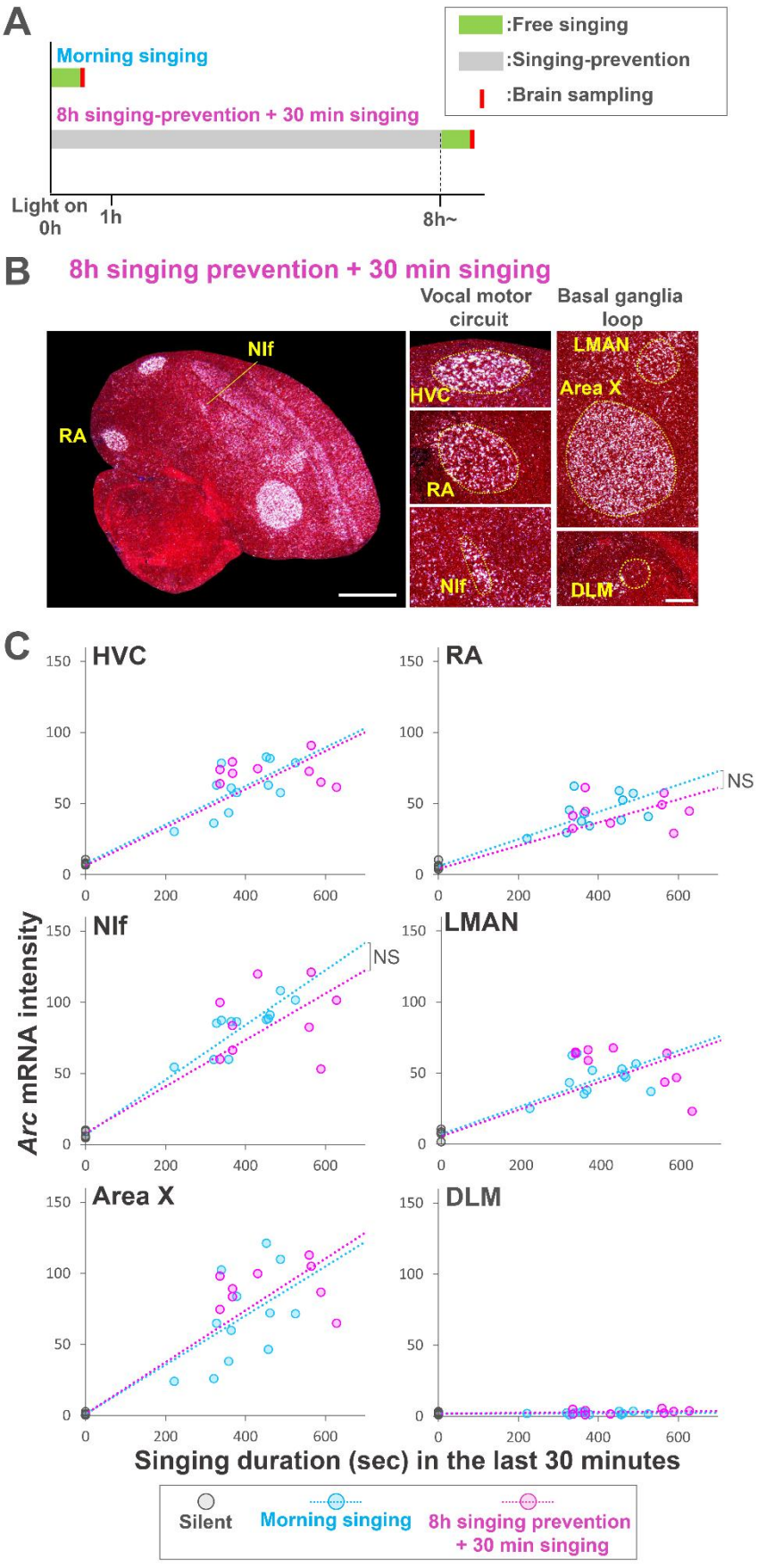
A
Morning singing
8h singing-prevention + 30 min singing
:Free singing
:Singing-prevention
:Brain sampling
Light on
0h
1h
8h~
B
8h singing prevention + 30 min singing
Vocal motor circuit
Basal ganglia loop
NIf
RA
HVC
LMAN
Area X
DLM
C
HVC
RA
NIf
LMAN
Area X
DLM
NS
Arc mRNA intensity
Singing duration (sec) in the last 30 minutes
Silent
Morning singing
8h singing prevention + 30 min singing

Figure 5. Daily singing practice, not circadian rhythm, changes *Arc* inducibility

(A) Experimental paradigm of brain sampling to test singing experience-dependent regulation of *Arc* inducibility.

(B) A typical example of induction of *Arc* mRNA after 30 min free singing following 8h singing prevention (50 phd, 366 sec singing). Scale bar = 1.5 mm (left panel) and 200 μm (right panels).

(C) Induction rate of *Arc* mRNA during normal morning singing (light blue; n = 12 birds, 45–54 phd, mean = 48.7) and free singing in the afternoon after 8 h singing prevention (pink; n = 9 birds, 45–54 phd, mean = 49.7). Silent condition (black; n = 5 birds, 50–55 phd, mean = 53.4). $^{NS}p > 0.1$; ANCOVA.

(Figure 6)

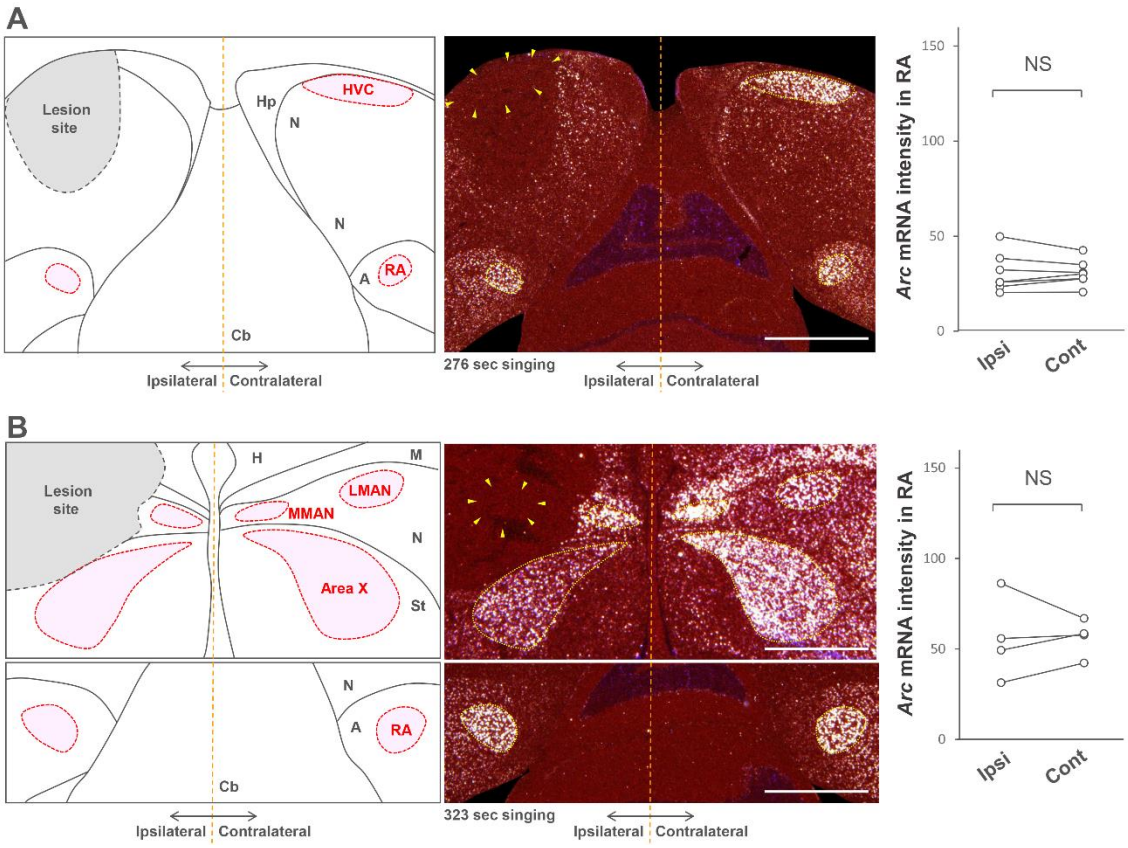

Figure 6. HVC, or LMAN lesion does not affect *Arc* mRNA induction in RA

(A) *Arc* induction by singing after unilateral HVC lesion. No significant difference ($^{NS}p > 0.1$; paired *t* test) between ipsilateral (ipsi) and contralateral (cont) lesioned sites (right HVC lesion, n = 4 birds; left HVC lesion, n = 3 birds). Coronal sections. Scale bars = 1 mm.

(B) *Arc* induction by singing after unilateral LMAN lesion. No significant differences ($^{NS}p > 0.1$; paired *t* test) between ipsi and cont lesioned sites (right LMAN lesion, n = 2 birds; left LMAN lesion, n = 2 birds). Coronal sections. Scale bars = 1 mm.

(Figure 7)

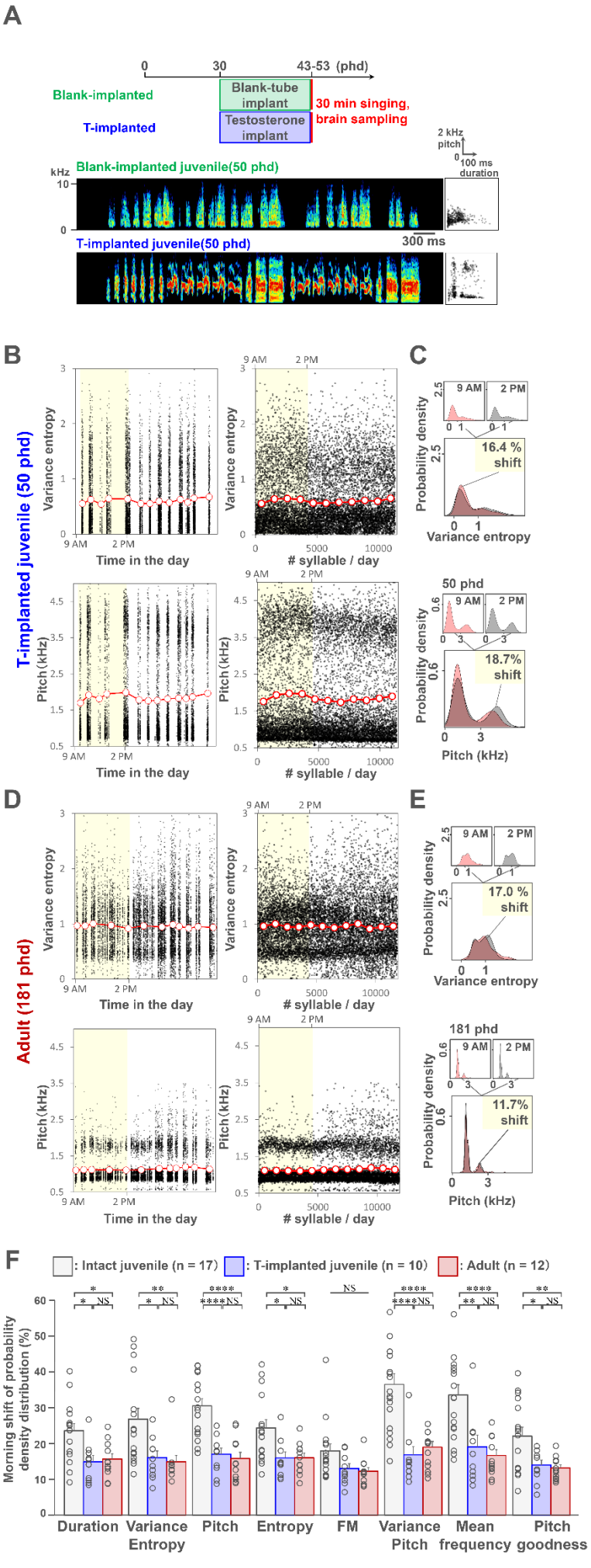
A
0
30
43-53 (phd)
Blank-implanted
Blank-tube implant
30 min singing, brain sampling
T-implanted
Testosterone implant
2 kHz pitch
100 ms duration
kHz
Blank-implanted juvenile(50 phd)
10
0
300 ms
T-implanted juvenile(50 phd)
B
C
T-implanted juvenile (50 phd)
Variance entropy
Time in the day
syllable / day
9 AM
2 PM
Probability density
16.4 % shift
Variance entropy
50 phd
Pitch (kHz)
18.7% shift
D
E
Adult (181 phd)
17.0 % shift
181 phd
11.7% shift
F
: Intact juvenile (n = 17)
: T-implanted juvenile (n = 10)
: Adult (n = 12)
Morning shift of probability density distribution (%)
Duration
Variance Entropy
Pitch
Entropy
FM
Variance Pitch
Mean frequency
Pitch goodness
NS

Figure 7. Song stabilization by exogenous testosterone administration

(A) (upper panel) Experimental timeline for testosterone (T)-implant and brain sampling. (lower panel) Song spectrograms of blank tube- and T-implanted juveniles at 50 phd.

(B) Diurnal trajectory plots of variance entropy and pitch of all song syllables produced by a T-implanted juvenile (50 phd, 11,367 syllables). Acoustic features were plotted against time (left panels), or the order of syllables (right panels). Red-lined circles indicate the average of each song cluster (left panels) or each 1,000 syllables (right panels).

(C) Distribution of probability density of variance entropy and pitch in the morning (9 AM) and afternoon (2PM) using 500 syllables at each time point (upper panels). Comparison of probability densities of the two acoustic features for assessment of the acoustic shifts (%) between morning and afternoon periods (lower panels).

(D) Diurnal trajectory plots of variance entropy and pitch of all song syllables produced by adult (181 phd, 11,864 syllables).

(E) Distribution of probability density of variance entropy and pitch at morning (9 AM) and afternoon (2 PM) using 500 syllables at each time point (upper panels).

(F) Comparison of acoustic shifts (%) during morning period between intact (n = 17 birds) and T-implanted (n = 10 birds) juveniles, and adults (n = 12 birds). *$p < 0.05$, **$p < 0.01$, ***$p < 0.001$, ****$p < 0.0001$; unpaired *t* test with Bonferroni correction.

(Figure 8)

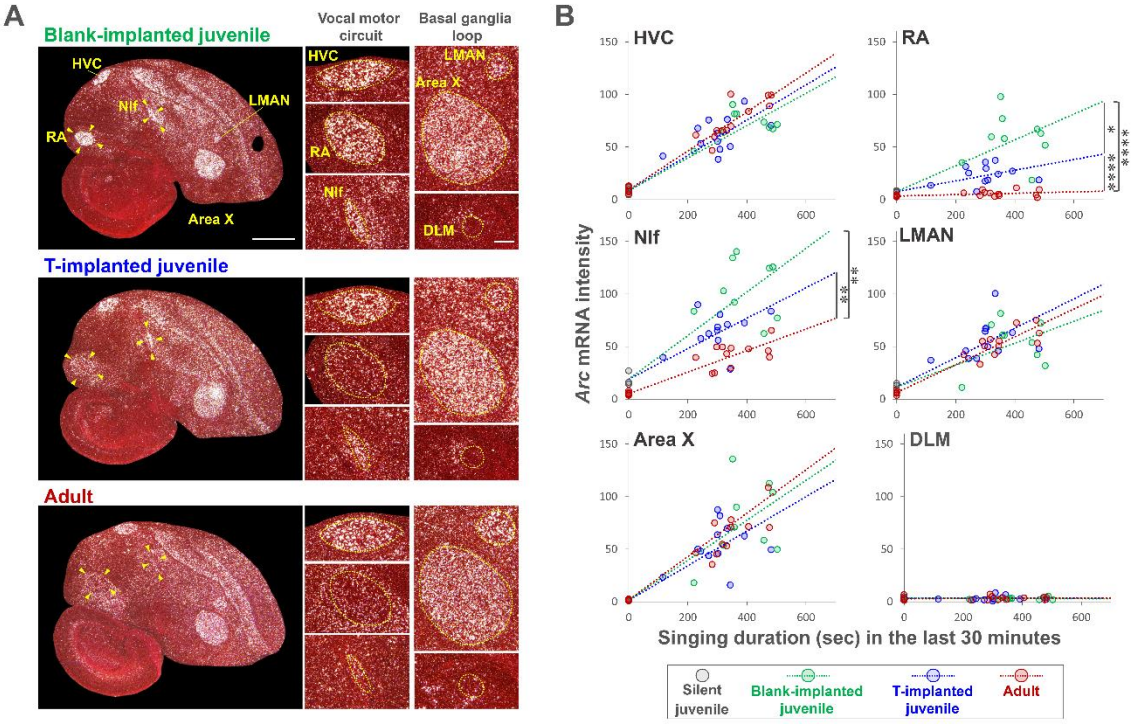

Figure 8. Reduction of *Arc* inducibility in the song-stabilized juvenile by exogenous testosterone administration

(A) *Arc* mRNA induction in blank tube- and testosterone-implanted (482 sec singing) juveniles (358 sec singing) and adults (405 sec singing). Singing duration (sec) in the last 30 min is shown at the bottom. Scale bar = 1.5 mm and 200 μm.

(B) Induction of *Arc* in song nuclei during singing at morning in blank tube-implanted juveniles (green; n = 9 birds, 45–51 phd, mena = 47.4) and T-implanted juveniles (blue; n = 12 birds, 43–53 phd, mean = 47.6), and adults (red; n = 17 birds, 103–512 phd, mean = 153). Silent juveniles (n = 3 birds, 48–53 phd, mean = 50.3) *$p < 0.01$, **$p < 0.001$, ****$p < 0.00001$; ANCOVA with Bonferroni correction.

(Figure 9)

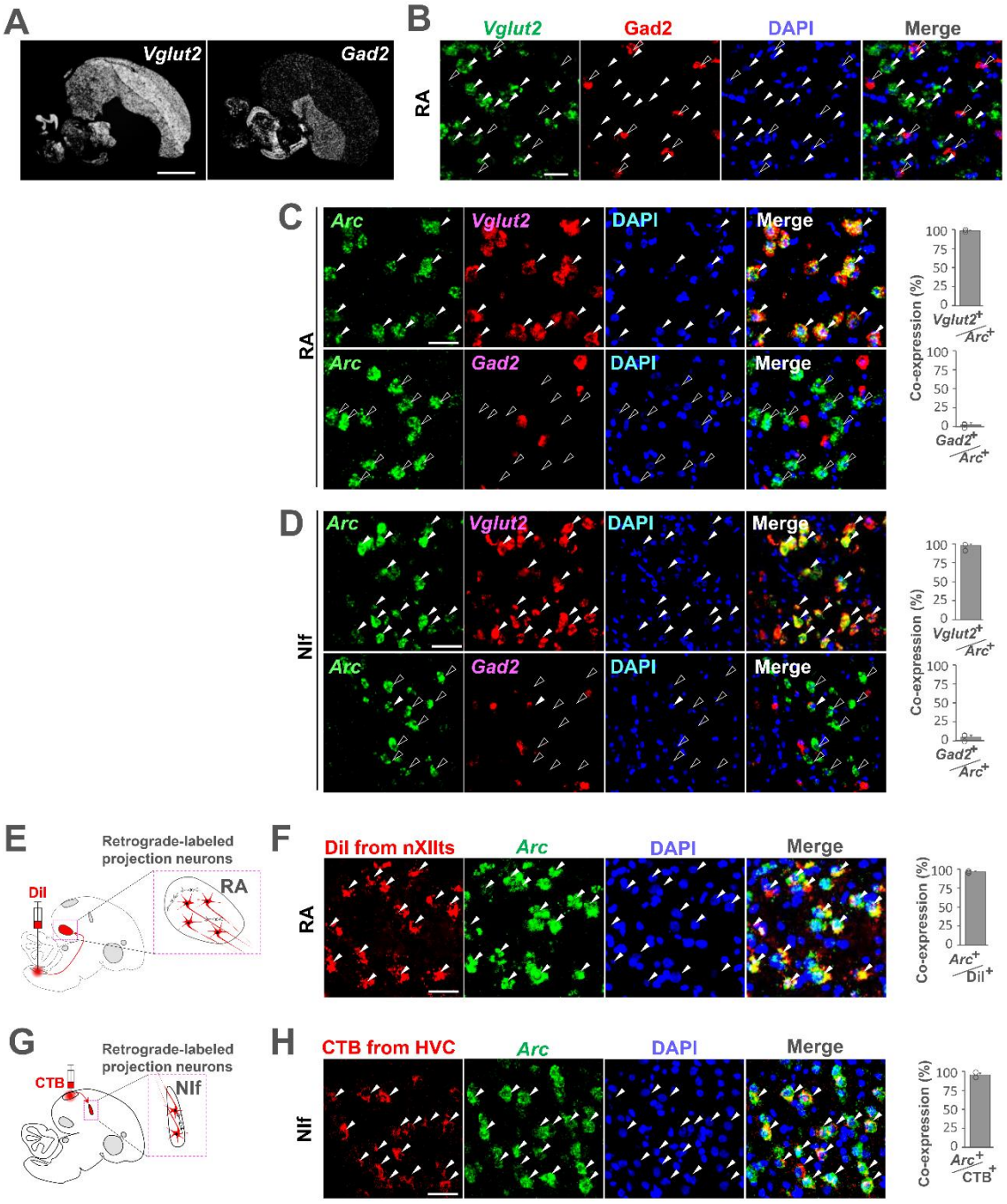
A
Vglut2
Gad2
B
Vglut2
Gad2
DAPI
Merge
RA
C
Arc
Vglut2
DAPI
Merge
Arc
Gad2
DAPI
Merge
RA
Co-expression (%)
100
75
50
25
0
Vglut2+ Arc+
Gad2+ Arc+
D
Arc
Vglut2
DAPI
Merge
Arc
Gad2
DAPI
Merge
NIf
Co-expression (%)
Vglut2+ Arc+
Gad2+ Arc+
E
Retrograde-labeled projection neurons
DiI
RA
F
DiI from nXIIts
Arc
DAPI
Merge
RA
Co-expression (%)
Arc+ DiI+
G
Retrograde-labeled projection neurons
CTB
NIf
H
CTB from HVC
Arc
DAPI
Merge
NIf
Co-expression (%)
Arc+ CTB+

Figure 9. Cell-type specific *Arc* induction in projection neurons of RA and NIf

(A) mRNA expressing pattern of molecular markers for neuron types (marker for glutamatergic neurons: *Vglut2* and marker for GABAergic neurons: *Gad2)* in a zebra finch brain. Scale bar = 2mm.

(B) *Vglut2* (green) and *Gad2* (red) are expressed separately in RA. Cell nuclei (blue, DAPI). Scale bar = 40 μm.

(C, D) (Left panels) Co-induction of *Arc* in *Vglut2* (+) cells, but not *Gad2* (+) cells in RA **(C)** and NIf **(D)**. Cell nuclei (blue, DAPI). Filled arrowheads: cells that co-expressed with *Arc* and marker genes. Empty arrowheads: cells that expressed *Arc* but not marker genes. Scale bar = 40 μm. (Right bar graphs) Proportion of each subpopulation in cells that express *Arc* (n = 80–208 cells).

(E, G) Diagram of retrograde labelling for the projection neurons in RA or NIf. Retrograde dye (DiI or CTB) injected to nXIIts or HVC.

(F, H) Specific induction of *Arc* mRNA (green) in retrograde-labeled projection neurons of RA **(F)** and NIf **(H)**. Cell nuclei (blue, DAPI). (Right bar graphs) Proportion of retrograde-labeled projection neurons that express *Arc* (n = 80–130 cells).

(Figure 10)

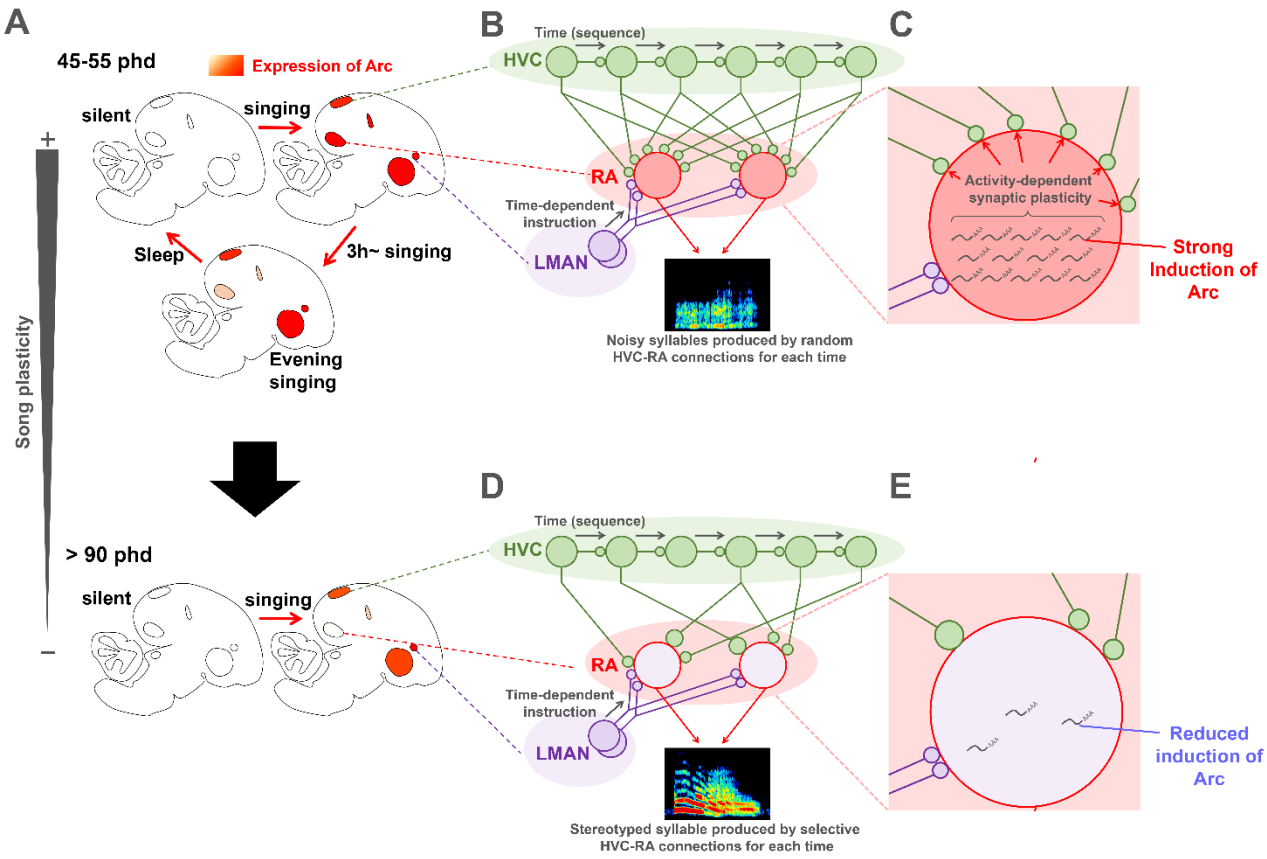

Figure 10. Presumed function of different induction rate of *Arc* in RA during the critical period of vocal learning

A functional model of *Arc* induction differences applied to the circuit model from previous electrophysiological studies (Okubo et al., 2015; Garst-Orozco et al., 2014; Stark and Perkel, 1999; Sizemore and Perkel, 2011; Fee et al., 2004; Fee and Goldberg, 2011).

Chapter II

Cumulative singing experience regulate activity-dependent genes for age-independent vocal plasticity in songbirds

2.1 Introduction

In the projection neurons of RA and NIf, the induction of *Arc* was attenuated both in a short-term way daily (morning vs. afternoon, during the early plastic song stage) and in a long-term way developmentally (juvenile [45-55 phd] vs. adult [> 90 phd]) (Chapter I). Induction of *Arc* and song plasticity were strongest in the morning, then down-regulated in the afternoon during the juvenile stage, and finally diminished at adulthood. The short-term diurnal attenuation of *Arc* induction depended on daily singing experience, instead of circadian rhythm. These results suggest the possibility that the long-term developmental attenuation of *Arc* induction and song plasticity may also depend on singing experience, instead of age. To test this possibility, in this Chapter II, I examined contributions of singing experience to song plasticity and gene expression dynamics in the song nuclei.

To separate the contribution of age from singing experience, I prevented juvenile zebra finches from singing until adulthood (singing-prevented [SP] adults, 91-131 phd, Fig. 11A). First, I evaluated the song phenotype of SP birds at adult age. To test whether SP adults retained the ability to crystallize and mimic the tutor song, I recorded song development of SP adults from when they were allowed to freely sing (100–104 phd, Fig. 12A). I calculated similarity score of syllable acoustics and sequence (motif) features of SP bird's song toward their tutor song.

In the song nuclei, a number of genes are known to be differentially-regulated between juvenile and adult: expression under silent condition (Mori and Wada, 2015; Kubikova et al., 2010; Matsunaga and Okanoya, 2008) or induction by singing (Jin and Clayton, 1997; Wada et al., 2006; Chapter I). Although these gene expression dynamics are probable candidates for the closure mechanisms of the critical period, it is still unclear

which factor, age or singing experience, contributes to such changes. To separate singing-experience dependent gene regulation from mere age-dependent shifts, I performed transcriptome analysis on a genome wide scale in the song nuclei using juveniles, normal adults, and SP adults (Fig. 14B; Table 1). I analyzed gene expression profiles in RA, where *Arc* was most strongly down-regulated in adults (Chapter I, Fig. 8), and HVC as a control region, where *Arc* was similarly induced in juvenile and adults (Chapter I, Fig. 8). I could not dissect NIf from the brain tissue due to its small size and unclear boundaries. I identified differentially-expressed genes in RA and HVC by comparing the expression profiles of 12,156 genes (materials and methods, p. 49) among juveniles and adults under silent, or singing condition (materials and methods, p. 50). Then I evaluated the contribution of singing experience to these differentially-expressed genes by including the gene expression profiles of SP adults into the comparison. I clustered the differentially-expressed genes using weighted gene co-expression network analysis (WGCNA) (materials and methods, p. 50), which allows for the identification of co-expressed gene clusters (Mori and Wada, 2015; Hilliard et al., 2012; Drnevich et al., 2012). To examine the brain-region specificity of experience-dependent regulation, I further analyzed gene expression pattern in the song nuclei by *in-situ* hybridization. To identify which neuron types express the experience-dependent genes, I performed fluorescent *in-situ* hybridization with gene markers (*Vglut2*, or *Gad2*).

In the projection neurons of RA, the number of dendritic spines and synaptic connection from HVC decrease from juvenile stage to adulthood (Kittelberger and Mooney, 1999; Garst-Orozco et al., 2014). This spine pruning is considered important to construct learned syllable acoustics (Fee, 2004, Fig. 10). To examine which factor, age or singing experience contributes to such morphological changes, I quantified the number

of dendritic spines of the projection neurons in RA by Golgi staining using juveniles, adults, and SP adults. Due to the low-efficiency of Golgi staining for the projection neurons in RA, I elongated the incubation time for the staining. This experimental procedure caused overcrowded staining in other song nuclei. Therefore, I could not identify or analyze the projection neurons in NIf or neurons in other song nuclei.

As an open-ended song learner, canary annually re-develops new song elements each fall (Fig. 1C). However, the molecular mechanisms for the seasonal plasticity is still unclear. I examined the relationship between experience-dependent genes and seasonal song plasticity in canary. If the expression changes of experience-dependent genes are important for the song plasticity of songbirds, they should be re-induced in each fall in the canary.

2.2 Materials and methods

Animals

About zebra finch, see (Materials and methods, p. 12). Male canaries at each season (1st year fall, 2nd year spring, and 2nd year fall) were obtained from the breeding colony at the Center for Field Research in Ethology and Ecology at the Rockefeller University and from the colony at Hokkaido University. Canaries were kept in indoor breeding cages under a light / dark cycle that mimics the natural environment (gradually changed 15 min per week).

Singing prevention

Juvenile male zebra finches were prevented from singing during sensorimotor learning period (n = 20, from 30 phd until adulthood, 91-133 phd, 101.2 mean). Singing prevention was performed during light-on time by restricting vertical movement (stretching of neck) for initiation of singing. A padlock (11 × 12 mm, size: 9 × 18 × 23 mm, weight: 16.5 g or 24 g, shell was made from plastic and core was made from metal) was attached to birds during singing prevention. The padlock slightly shifted their head positions downward (approximately at 0.5 – 1.5 cm lower than the normal height). The padlock was usually on the ground and its whole weight did not burden the bird. However, it restricted the bird's posture when they tried to stretch their necks to start singing. During this procedure, birds freely moved horizontally by jumping, produced calls, drank, and ate. The padlock was removed from birds during light-off time and for at least 1 h per day during light-on time to reduce potential stress as much as possible. Body weight was carefully monitored every 2-3 days and it was ensured that birds maintained above 80% of the average weights of intact birds at similar age.

For analysis of song development of the singing -prevented (SP) adults (shown in Fig. 12), birds were kept with their biological fathers after hatching until 30 phd and subsequently exposed to the biological father every 2–4 days during singing prevention and free singing periods at adulthood. The father birds sang at least 20 bouts per day.

Song motif consistency

To evaluate the song motif consistency, similarity score within 20 randomly-selected motifs (total 190 comparison for each developmental stage) were calculated with the default setting in the SAP software. The similarity score was calculated by comparing syllable acoustic features within 9 ms sliding time windows. *p* values for comparisons of motif consistency were obtained using unpaired *t* test for different conditions and a paired *t* test for developmental stages with Bonferroni correction.

Song syllable similarity/ Song motif similarity

For the motif similarity analysis, twenty bouts of songs were randomly selected and analyzed at each developmental time point. Song similarity scores were calculated by whole-motif comparison against each pupil's tutor songs using the SAP software. For the syllable-based song similarity analysis, we used 50 syllables from the same song bouts which were analyzed for the motif-based song similarity. Introductory notes in a song were not included for analyses. The series of separated syllable files of songs were transferred to the CORRELATOR program of Avisoft SASLab pro (Avisoft Bioacoustics, Berlin Germany) for calculating the similarity scores between the syllables from pupil's and tutor's songs by the round-robin comparison. The highest similarity score for each syllables of pupil songs against tutor's syllables was averaged as the similarity score of

total syllables for each individual.

Measurement of serum corticosterone concentration and body weight

To measure serum corticosterone concentration, blood was sampled from the carotid vein when birds were euthanized. Subsequently, serum corticosterone was determined using a corticosterone enzyme-linked immunosorbent assay kit (Enzo ADI-900-097), according to manufacturer's instructions. Juveniles (n = 7; 45–51 phd, mean = 47.7), adults (n = 7; 102–125 phd, mean = 109.4), and SP adults (n = 7; 100–101 phd, mean = 100.8) were used. To avoid the effects of circadian rhythm on serum corticosterone, sampling of blood was completed before 9:00 AM following lights were turned on at 8:00 AM. Serum corticosterone concentration was compared among conditions using one-way ANOVA. Body weight was measured from juveniles (n = 10; 45–51 phd, mean = 47.5), adults (n = 10; 102–310 phd, mean = 139.5), and SP adults (n = 10; 100–101 phd, mean = 100.6) before lights on time (7:30 AM) to remove the effects from eating or drinking. Body weight was compared among conditions using one-way ANOVA.

Brain sampling

Male zebra finch juveniles (n = 17, 45–55 phd, mean = 47.9 phd), adults (n = 19, 103–512 phd, mean = 153.7 phd), and SP adults (n = 12, 91–133 phd, mean = 102.2 phd) were split into six experimental groups: (I) juvenile 30 min silence (n = 3–5 for each genes), (II) adult 30 min silence (n = 3-5), (III) juvenile 30 min singing (n = 7–10), (IV) adult 30 min singing (n = 7–10), (V) SP adults with 30 min silence (n = 4), and (VI) SP adults with 30 min singing (n = 6–8). Male canaries at each season were split into six

experimental conditions: (I) 1st year fall with 30 min silence as silent control (sampled in early October 2010, n =4), (II) 1st year fall with 30 min singing (late September 2010, n = 4), (III) 2nd year spring with 30 min silence (early June 2010, n = 4–5), (IV) 2nd year spring with 30 min singing (early June 2010 and 2015, n = 6), (V) 2nd year fall with 30 min silence (early September 2010 and October 2015, n = 3–4), and (VI) 2nd year fall with 30 min singing (early October 2006 and 2015, n = 5–6).

Golgi staining

Zebra finch male juveniles (n = 6, 46–55 phd, mean = 51.7), adults (n = 5, 106–796 phd, mean = 331.6), and SP adults (n = 5, 100–101 phd, mean = 100.2) were used for Golgi staining. Brains were removed under silent and dark conditions and incubated in the impregnation solution from a FD Rapid GolgiStainTM kit (FD NeuroTechnologies) for two weeks in the dark, incubated in a replacement solution for 3 days, embedded in OCT compound (Sakura Fine Technical), and stored at –80°C until sectioning. Brain sections with a thickness of 100 μm were cut in the sagittal plane. Sections were dried at RT, rinsed with water, and stained in a staining solution (FD NeuroTechnologies). After staining, sections were dehydrated in an EtOH series and xylene and then mounted with Permount. Dendritic spines were counted using photo images taken at 100× magnification with a BZ-X710 Microscope (Keyence). Z-stacked images were formed using 100 sections with a 20-μm depth. Dendritic spine density was calculated for three RA projection neurons and three surrounding neurons in the arcopallium for each bird (n = 18 neurons from 6 juveniles, n = 15 neurons from 5 adults, and n = 15 neurons from 5 SP adults). RA projection neurons were distinguished from interneurons by their characteristic mossy dendritic and axonal morphologies (Spiro et al., 1999).

Sampling of the song nuclei and RNA extraction for Quartz RNA seq

Male zebra finch juveniles after 45 min silence (n = 3, 47–48 phd), juveniles with 45 min singing (n = 3, 40–50 phd), adults with 45 min silence (n = 2, 101–104 phd), adults with 45 min singing (n = 4, 110–338 phd), and SP adults with 45 min singing (n = 3, 96–101 phd) were used (Table 1). For identification of clear RA and HVC boundaries against surrounding non-vocal areas under microscope observation, a fluorescent-retrograde tracer, Cholera Toxin B subunit conjugated with AlexaFluor555 (Invitrogen, 1 mg/μl in 1× PBS, 100nl/hemisphere), was injected into RA 10 days before euthanasia. After behavioral observations, birds were decapitated, and brains were removed and stored at −80°C until sectioning. Brain sections were cut at a 20 μm-thickness in the sagittal plane and mounted onto glass slides with a handmade membrane system for laser microdissection. Fluorescent-labeled RA and HVC tissues were microdissected from 14 to 20 brain slices using a laser capture microscope ArcturusXT (Arcturus Bioscience). The collected tissue was dissolved in Qiagen RLT buffer. Total RNA was purified using a column-based method (RNeasy Micro kit; Qiagen) and treated with DNase in the column to avoid contamination of genomic DNA. RNA integrity number (RIN) and concentration were measured with a Bioanalyzer2100 (Agilent Technologies) to confirm RNA quality (RIN: 6.4–7.4, RNA concentration: 3.5–10 ng/μl).

cDNA synthesis, amplification, and library preparation for Quartz RNA-seq

cDNA was amplified from purified total RNA using previously reported methods (Sasagawa et al., 2013). 10 ng of total RNA was used for synthesis of first strand cDNA. The following PCR amplification was performed with 14 PCR cycles at 98°C for 10

seconds, 65°C for 15 seconds, and 68°C for 5 minutes. The amplified cDNA samples were purified using a PCR purification column (MiniElute PCR Purification Kit; Qiagen). To check the quality of amplified cDNA, concentrations and smearing patterns of cDNA samples were measured with a Bioanalyzer 2100 (cDNA amount, 72–434 ng). 10 ng of amplified cDNA samples were fragmented to 100–300 bp in size using a DNA Shearing System LE220 (peak incident power 450W, duty factor 30%, cycle/burst 200, and treatment time of 700 sec) (Covaris) and then purified by a Zymo DNA 5 column. After end-repair of DNA fragments, adaptors were ligated, and amplified using a ligation-based Illumina multiplex library preparation method (LIMprep) with a KAPA Hyper Prep Kit (Nippon genetics) and 7 PCR cycles. All libraries were then sequenced using a Illumina Hiseq 2500 Sequencer, for 100 bp single-end sequencing. Library preparation was performed in the Bioinformatics Research Unit at RIKEN Advanced Center for Computing and Communication under supervision by Drs. Y. Sasagawa and A. Nikaido. All Quartz RNA-seq data from zebra finches were deposited in the DDBJ Sequence Read Archive (submission number DRA005559).

Improvement of gene annotation file of zebra finch brain transcripts

The previous gene annotation file from Ensemble (Taeniopygia_guttata taeGut3.2.4.76.gtf) did not include 3' UTR information. For annotation of read-sequences obtained from the RNA-seq data, the lack of 3' UTR information decreases the chances of accurate estimations of gene expression. Therefore, I elongated the annotation information with our RNA-seq data from zebra finch whole-brain samples. Total RNA was isolated from the pallium and pallidum regions of adult male zebra finches under silent and dark conditions (n = 5, 234–786 phd) using TRIzol Reagent (Invitrogen)

according to manufacturer's protocol (Invitrogen) and then column-purified using a RNeasy Micro kit (Qiagen). Samples were treated with DNase. The total RNA samples were used for library synthesis with TruSeq DNA Sample Prep Kits (Illumina). All libraries were then sequenced using the Illumina Hiseq 2500 Sequencer for 100 bp paired-ends. These experimental steps were performed in Dr. Y. Suzuki's laboratory in the Department of Computational Biology at the University of Tokyo. The 33.5–47.0 M reads for each telencephalon brain sample were output from the Illumina Hiseq 2500. Sequencing reads were mapped onto the ZF reference genome obtained from Ensemble (Taeniopygia_guttata taeGut3.2.4.dna.fa) with the Tophat2 program and assembled to predicted-transcripts with the Cufflinks program. By comparison with the previous annotation file using cuffcompare program, 12,156 transcripts were identified as predicted RNA transcripts expressed in the zebra finch telencephalon. The RNA-seq data from the zebra finch telencephalon were deposited in the DDBJ Sequence Read Archive (Table 1).

Identification of differentially-expressed genes in RA and HVC

The 9.7–20.9 M RNA-seq reads from zebra finch juveniles after 45 min silence, juveniles with 45 min singing, adults with 45 min silence, and adults with 45 min singing were used. First, RNA-seq reads were mapped onto the zebra finch reference genome with the Tophat2 program, and then the FPKM (Fragments Per Kilobase of exon per Million mapped fragments) of each transcript (12,156 genes) was calculated using the Cufflinks program. Principal component analysis (PCA) using the prcomp package in R was used to check whether there were outliers of quality of RNA-seq. A Bonferroni-corrected DEseq2 was used to identify the differentially-expressed genes between

juveniles and adults ($P < 0.05$; 1,352 genes in RA and 1,540 genes in HVC), singing and silent conditions ($P < 0.05$; 266 genes in RA and 385 genes in HVC), and juvenile singing and adult singing conditions ($P < 0.05$; 937 genes in RA and 2,443 genes in HVC) in normal birds. A total of 1,811 genes in RA and 3,214 genes in HVC were detected as differentially-expressed genes.

Weighted gene co-expression network analysis (WGCNA)

A WGCNA was performed using the WGCNA R package to further investigate the relationship between biological traits (singing experience, age, and/or singing induction) and identify co-regulated Gene Clusters (Langfelder and Horvath, 2008). General information about network analysis methodology and WGCNA software is available at http://labs.genetics.ucla.edu/horvath/htdocs/CoexpressionNetwork/. Pair-wise Pearson correlation coefficients were calculated for all detected genes. The resulting Pearson correlation matrix was transformed into a matrix of connection strength (an adjacency matrix) using the power function [(1 + correlation) / (2 × Soft threshold power)], which was then converted to a topological overlap matrix. WGCNA identified modules of densely interconnected genes by hierarchical clustering was based on topological overlap, a biologically meaningful measure of the similarity of expression pattern among all pairs of genes spanning across all experimental conditions, and then assigning each gene to a "Cluster (module)" was based on shared expression patterns. A preliminary network was built to assess overall connectivity. From this network, 1,811 and 3,214 genes in RA and HVC, respectively, with the highest connectivity were retained for subsequent WGCNA (Soft threshold power = 10, corType = pearson, minModuleSize = 30, detectCutHeight = 0.98, and merge CutHeight = 0.4). Modules were defined as

branches of the dendrogram obtained from clustering and were labeled with colors beneath the dendrograms. To study the relationship between expression variability within the modules and behavioral trait variability, correlations were computed between the principal components of each module and traits. *p* values were computed for each correlation.

2.3 Results

Singing prevention extended song plasticity into adulthood. During the critical period (30-90 phd), successfully singing-prevented (SP) birds (17 out of 20 birds) sang only a total of 20-451 song bouts (mean = 225.2 bouts), which was less than 1% of the total singing amount of normal birds during the same period (Ohgushi et al., 2015). When SP birds were allowed to freely sing, they produced immature subsong-like songs, with highly variable acoustics and syllable sequence even at adulthood (100-101 phd) (Fig. 11B). Body weight and serum corticosterone levels of singing-prevented birds were not significantly different compared with those of normal adults (Fig. 11C and D). These results indicate that age alone is not sufficient for song maturation, but rather that singing experience must be involved.

I observed that 3 of 24 birds in the singing-prevented group continued to sing (more than 5,000 bouts of total singing). They developed crystallized songs with typical motif structure and copied song traits from their tutors in the same way as normal adults (Fig. 13B), indicating that absence of singing experience, but not the experimental handling, influences song development and learning.

Development of song acoustics and sequence of SP birds from adult stage

SP adults retained the ability to mimic the tutor song. All SP adults (> 100 phd, n = 5) developed crystallized songs composed of syllables learned from tutor songs. Their crystallized songs were composed of the typical species-specific motif structure of the zebra finch ((Bonferroni corrected paired *t* test: intact 50-60 phd: intact 100-104 phd, $t(4) = 17.77$, $p = 0.00029$; SP adult 100-104 phd: SP adult 119-130 phd, $t(4) = 18.07$, $p = 0.00027$; Bonferroni corrected unpaired *t* test: intact 100-104 phd: SP adult 100-104 phd,

t(8) = 9.47, *p* = 6.3e-5) (Fig. 12B and C). SP birds quickly crystallized their songs within one month following free singing. This time was shorter than half the normal critical period in zebra finches (Fig. 12B). The syllables produced by the SP birds had the same acoustic features that were observed in intact adults (Fig. 12D). SP adults mimicked their tutor songs at the levels of both syllable acoustics (Fig. 12E) and sequence (motif) features (Fig. 12G). Comparison between the songs produced at just after release (phd 100–103) and ones after 3–4 weeks (phd 119–126) revealed a significant increase of syllable and motif similarity scores toward their tutor songs (paired *t* test: syllable, *t*(4) =7.7, *P* = 0.0015; motif, *t*(4) =5.8, *P* = 0.0044) (Fig, 12F, H). Two of the five birds almost perfectly learned all syllable acoustic structure and sequence of the tutor song (Fig. 12A; Fig. 13A). Consistently, the SP birds showed a similar imitation accuracy of their acquired songs against tutor songs as did the birds which persistently continued singing (Welch's *t* test: syllable, *t*(6) =0.68, *P* = 0.52; motif, *t*(6) =1.2, P = 0.27) (Fig, 12F, H).

Cumulative singing experience regulates the induction of a cluster of singing-induced genes

A cluster of singing-induced genes was extracted as experience-dependent, but age-independent genes in RA. The global gene expression profiles (12,156 genes) of each sample was successfully divided between HVC and RA by principal component analysis (PCA) (Fig. 14A). Using 1,811 differentially-expressed genes in RA (Materials and methods, p. 50), four clusters (I-IV) of co-expressed genes were identified (Fig. 14C). Only Gene Cluster I (119 genes including *Arc*), met criteria for genes significantly regulated by the accumulation of singing experience, but not age (Fig. 14C). In contrast, in the premotor nucleus HVC, no gene clusters were regulated solely by singing

experience (Fig. 14 D). Gene Cluster I (RA) were induced by singing (p = 0.03, Fig. 14C and E). Indeed, all in-situ hybridization tested genes in Cluster I (RA), including *Arc*, *Atf3*, *c-fos*, *Egr1*, *Nr4a1*, *Crem*, *Sik1*, *Dusp5*, *Dusp6*, *Odc*, *Fam60a*, *H3.3b*, and *Gadd45b*, were induced by singing significantly higher in both juveniles and SP adults when compared with intact adults (Fig. 14F; Fig. 15; Fig. 16; Table2). By comparing the induction difference of Cluster I genes among the song nuclei, RA was a "hot spot" for the singing experience-dependent regulation of the activity-dependent genes (Fig. 18). These genes were mainly induced in the projection neurons in RA (Fig. 19).

WGCNA revealed age-regulated Clusters II and III genes (836 and 793 genes, respectively) in RA (Fig. 14C). In SP adults, Cluster II genes showed adult-like expression pattern (Fig. 14E). In line with this, *Gabra5*, *Evl*, *Dpysl3*, and *Il1rapl2*, from Gene Cluster II (RA) whose expression were higher in juveniles than adults, showed similar expression intensities between SP adults and normal adults (Fig. 14F; Fig. 17). These results indicate that cumulative singing experience selectively changed the induction of Cluster I (RA) genes against the expression of age-dependent genes in RA.

Dendritic spine changes in RA neurons by cumulative singing experience

Cumulative singing experience changes dendritic spine morphology in the projection neurons in RA. In line with the neuron type-specific expression of *Arc* as a potential contribution to synaptic development, SP adults retained higher dendritic spine density in the RA projection neurons as juveniles compared with normal adults (Bonferroni-corrected unpaired t test: juvenile:normal adult, $t(31) = 9.14$, p = 2.6e-10; SP adult:normal adult, $t(28) = 6.59$, p = 3.8e-7) (Fig. 20A). In contrast, the arcopallial region surrounding RA, which is a non-vocalization-related area, did not show any significant

changes in the number of dendritic spines among the three groups (Fig. 20B).

Transcriptional plasticity of the activity-dependent genes in an open-ended learner

I analyzed gene induction by singing for 9 Cluster I (RA) genes (*Arc*, *Atf3*, *c-fos*, *Egr1*, *Nr4a1*, *Sik1*, *Dusp5*, *Dusp6*, and *Gadd45b*) in canary. Among these genes, *ATF3* and *Dusp5* did not show clear singing-induced expression in the canary song nuclei (data not shown). Therefore, I analyzed gene induction for other 7 genes. As a result, the induction of genes was attenuated during the production of crystallized songs during the 2nd year's spring in the canary, similar to adult zebra finches with crystallized songs (Fig. 21A and B). In contrast, during the 2nd plastic song phase (2nd year's fall) for seasonal song plasticity in adults, these genes were re-induced by singing with a similar intensity as observed during the juvenile 1st plastic song phase (1st year's fall) (Fig. 21B). These results indicate that the induction intensity of activity-dependent genes is regulated along with song plasticity across species with different learning strategies.

2.4 Discussion

Cumulative motor experience-dependent closure of the critical period

I have revealed song plasticity and the ability to mimic memorized songs in SP adults (Fig. 12; Fig. 13). These results indicate that cumulative singing experience, not age, closes the critical period of song learning in zebra finch. Previous studies showed that auditory deprivation by deafening, or white noise treatment delayed song crystallization in zebra finch (Price et al., 1979; Funabiki and Konishi, 2003; Mori and Wada; 2015), suggesting that hearing is important for song crystallization. Since SP adults which heard tutor songs retained song plasticity, hearing of song was not sufficient for song crystallization. Furthermore, white noise treated birds could not maintain the song learning ability completely in adulthood (Funabiki and Konishi, 2003), whereas some SP adults learned both acoustics and sequence of tutor. To the best of our knowledge, SP adults are the first instance of adult (> 100 phd) birds with sufficient song plasticity for vocal learning. Based on these, I conclude that the singing experience with normal auditory feedback closes the critical period for song learning.

Potential regulatory mechanisms of the singing-induced genes in RA

In RA, a cluster of singing activity-induced genes (Cluster I genes) were down-regulated by cumulative singing experience (Fig. 14; Fig. 15; Fig. 16; Fig. 18) despite many other genes being regulated by age (Cluster II and III gene, Fig. 14; Fig. 17; Fig. 18). The singing experience-dependent regulations of Cluster I genes are likely mechanisms for the closure of the critical period. Then, what could be the molecular bases underlying such experience-dependent and brain region-specific regulation of Cluster I genes?

(1) Neuronal activity-dependent epigenetic regulation

A potential regulatory mechanism for Cluster I genes is activity-dependent epigenetic modifications. Previous studies in rodents revealed that activity-induced mechanisms change the epigenetic states (such as DNA methylation or demethylation) in the upstream regions of other activity-dependent genes within few hours (Guo et al., 2011). As member of the Cluster I genes, I identified the DNA methylation regulator *Gadd45b* (Ma et al., 2009; Kigar et al., 2015) and replacement histone *H3.3b* (Mase et al., 2015). Therefore, these singing-induced epigenetic regulators could directly change the epigenetic states of the regulatory regions of Cluster I genes. Future studies on DNA methylation or histone modification in RA may reveal the experience-dependent epigenetic regulation for the induction of Cluster I genes in a brain region-specific manner.

(2) Contributions of neuromodulators in RA

Modifications of neural activity by neuromodulatory systems are also considerable mechanisms for the down-regulation of Cluster I genes. RA neurons express various receptors for neuromodulators and receive projections from each system in the periaqueductal gray and ventral tegmental area, *e.g.* dopaminergic (Kubikova et al., 2010; Bottjer, 1993; Soha et al., 1995), noradrenergic (Sizemore & Perkel 2008; Mello et al., 1998), and serotonergic (Wood et al., 2011). Intriguingly, dopaminergic input into RA is enriched through the critical period (Bottjer, 1993). Activity of neuromodulators can regulate activity-dependent gene induction rate in rodents (Ye et al., 2016). Future studies with focus on the effects of direct injection for inhibitors for such neuromodulators may reveal the neuromodulatory contributions to the induction of Custer I genes and song plasticity.

(3) Hormonal-mediated regulation

The induction of *Arc* was significantly down-regulated in RA through song stabilization mediated by T-implantation in the early plastic song stage (Chapter I). Previous research revealed a relationship between testosterone secretion and seasonal song plasticity in open-ended learners, including the canary (Marler et al., 1988). Indeed, exogenous testosterone application induces fast, but abnormal song crystallization (Korsia & Bottjer., 1991, Sizemore & Perkel., 2011) and castration of juvenile zebra finches slows down song crystallization (Arnold, 1975). These studies suggests that serum testosterone level also contribute to song plasticity in closed-ended learners, including zebra finches. However, since castrated zebra finches eventually crystallize their songs without testosterone secretion (Arnold 1975) as older adults (150-200 phd), it is not likely that testosterone solely regulates gene induction and song plasticity. It is possible, however, that strong Cluster I gene induction and dramatic song plasticity are only permissible under low testosterone states such as during the early plastic song stage.

Presently, it is still unclear how testosterone affects song plasticity, or the induction of Cluster I genes in RA. Song nuclei including RA strongly express androgen receptor (AR) compared with surrounding region (Arnold, 1981), suggesting a potential mechanism by which serum testosterone could modify epigenetic state or neural activity via AR in the song nuclei. To elucidate which song nucleus is crucial for hormonal regulation, region-specific knock down of AR is required. In the future, genomic editing techniques may help the elucidation of direct causality between developmental hormone regulation in particular song nucleus and the induction of Cluster I genes in RA, or song plasticity.

Potential functions of individual gene regulation in each song nucleus

RA was a "hotspot" for the experience-dependent regulation of Cluster I genes among the song nuclei (Fig. 18). However, there were regulatory variations in Cluster I genes among the song nuclei (Fig. 15; Fig. 16; Fig. 18). For example, *Dusp6* and *Odc* were clearly down-regulated in normal adult HVC compared with juveniles or SP adults (Fig. 16), whereas other cluster I genes, *Arc*, *c-fos*, *Egr1*, *NR4a1*, *Crem*, *Sik1*, *Dusp5*, *Fam60a*, *H3.3b*, and *Gadd45b* were strongly induced by singing even in the same set of normal adults (Fig. 15; Fig. 16). Likewise, the induction of a different set of genes, *Arc*, *Egr1*, and *Dusp6*, was selectively attenuated in NIf in normal adults (Fig. 15; Fig. 16). These results indicate that multiple transcriptional regulation mechanisms control these genes in each song nucleus. Such nuclei- and gene-specific regulatory mechanisms may play a functional roles the song stabilization.

Age-dependent regulations of cluster II/III genes and fast crystallization of song in SP adults

Based on WGCNA and *in-situ* hybridization results, the gene expression state of SP adults was not totally juvenile-like, but rather age-matched expression state for hundreds of age-dependent genes (CluterII/III genes, Fig. 14E and F; Fig. 17). Although SP adults maintained juvenile-like dendritic spine density (Fig. 20) and high inducibility of Cluster I genes in RA projection neurons (Fig. 14F; Fig. 19), their gene expression state under silent conditions was fundamentally adult-like. At least I can say that these adult-like gene expression of Cluster II/III genes including *Gabra5*, a subunit of $GABA_A$ receptor, were not sufficient for song crystallization (Chapter I). However, such adult-like gene expression pattern might influence song development in SP adults. This may explain

why SP adults crystalized their songs about twice faster than normal juveniles (Fig. 12). The accelerated crystallization of song might be as a result of such adult-like gene expression states in the song nuclei.

Can we re-induce the critical period for song plasticity?

Unlike zebra finches, canaries repeat the critical period for song plasticity seasonally (Fig. 21A). Induction of Cluster I genes in RA was recovered in adult canary during seasonal plasticity (Fig. 21B). This result indicates that canaries could reset the long-term mechanisms for the down-regulation of Cluster I genes in RA during seasonal plasticity. How these genes are re-induced in canary RA? Previous studies found that hormonal regulation is important for seasonal plasticity (Nottebohm et al., 1987; Marler et al., 1988) which is accompanied by neurogenesis in HVC neurons that project to RA (Goldman and Nottebohm, 1983; Alvarez-Buylla et al., 1990; Brenowitz and Larson, 2015). These newly-generated HVC-RA connections may contribute to the the re-induction of Cluster I genes and seasonal plasticity. A recent study in mice successfully demonstrated that transplantation of immature inhibitory neurons induces new plasticity in adult mouse visual cortex (Davis et al., 2015), indicating that new connections in a particular brain region can induce a new plasticity. Manipulation of these genes in RA and/or neurogenesis in HVC may re-induce the critical period of song plasticity in closed-ended learners such as the zebra finch.

2.5 Figures

(Figure 11)

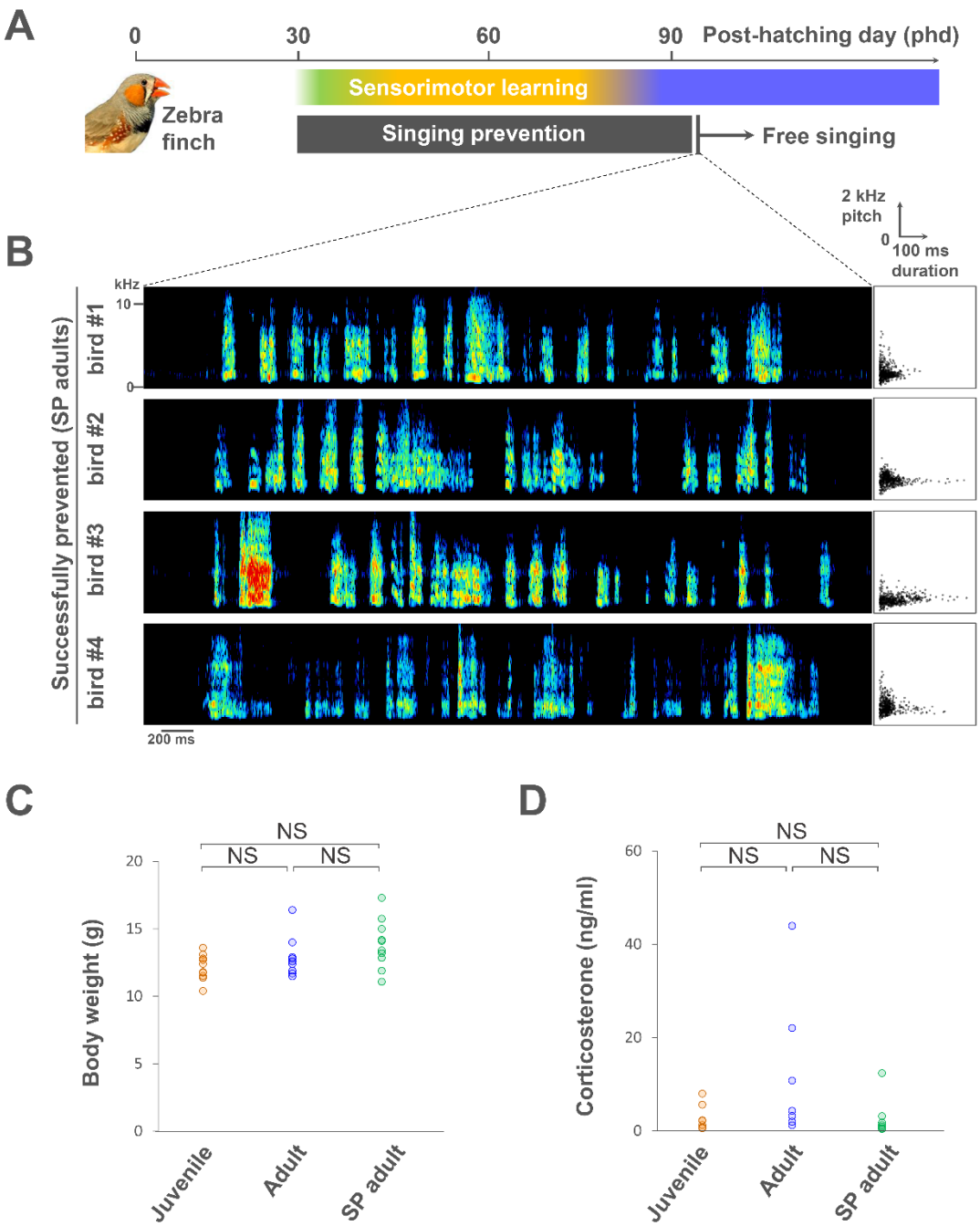

Figure 11. Singing prevention during the critical period extends song plasticity until adulthood

(A) Singing prevention beginning at 30 phd before the initiation of singing. The singing-prevented (SP) birds were then allowed to freely sing as adults (91–131 phd).

(B) Examples of songs of SP adults. Right scatter plots indicate 500 syllable distribution (duration versus pitch).

(C) There was no significant difference in body weight among juveniles (n = 10; 45–51 phd, mean = 47.5), adults (n = 10; 102–310 phd, mean = 139.5), and SP adults (n = 10; 100–101 phd, mean = 100.6) (NS: $P > 0.05$, one-way ANOVA).

(D) There was no significant difference in serum corticosterone levels among juveniles (n = 7; 45–51 phd, mean = 47.7), adults (n = 7; 102–125 phd, mean = 109.4), and SP adults (n = 7; 100–101 phd, mean = 100.8) (NS: $P > 0.05$, one-way ANOVA).

(Figure 12)

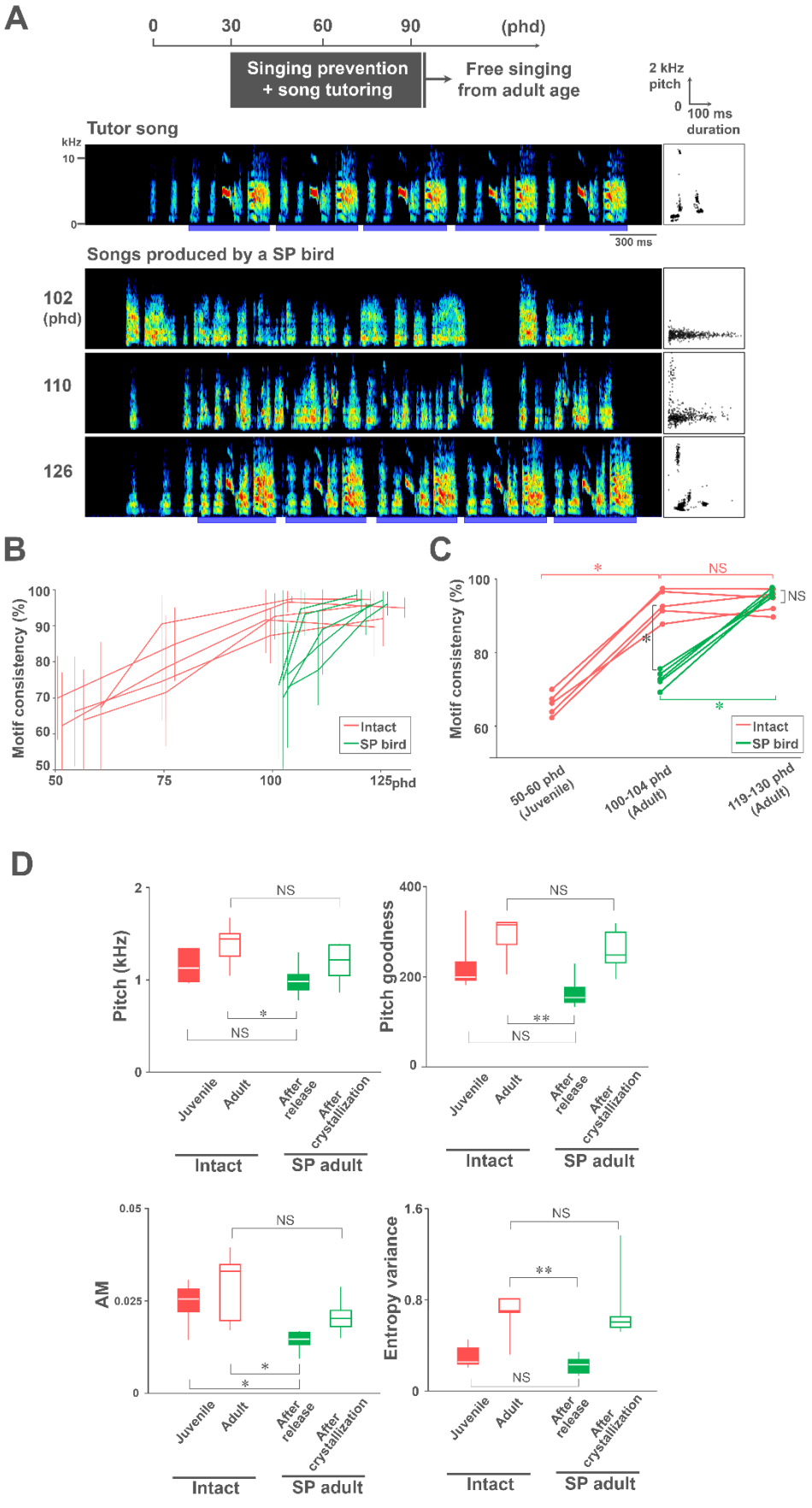
A
0
30
60
90
(phd)
Singing prevention
+ song tutoring
Free singing
from adult age
2 kHz
pitch
0
100 ms
duration
Tutor song
kHz
10
0
300 ms
Songs produced by a SP bird
102
(phd)
110
126
B
Motif consistency (%)
100
90
80
70
60
50
50
75
100
125phd
Intact
SP bird
C
Motif consistency (%)
100
80
60
*
NS
]NS
*
*
Intact
SP bird
50-60 phd
(Juvenile)
100-104 phd
(Adult)
119-130 phd
(Adult)
D
Pitch (kHz)
2
1
0
NS
*
NS
Pitch goodness
400
200
0
NS
**
NS
Juvenile
Adult
After release
After crystallization
Intact
SP adult
AM
0.05
0.025
0
NS
*
*
Entropy variance
1.6
0.8
0
NS
**
NS

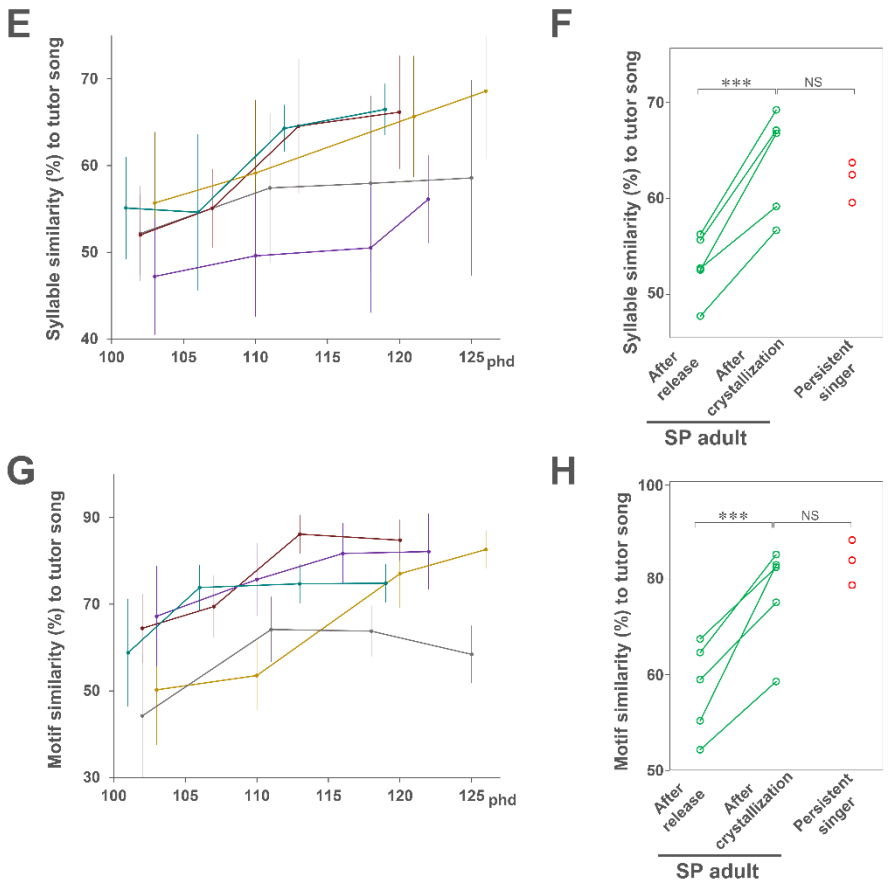

Figure 12. Song development from adult stage in singing-prevented zebra finches

(A) Song development of a SP bird after free singing in adult stage. Blue bars indicate the motif structure of crystallized song.

(B) Development of song motif consistency in intact (red, n = 5) and SP birds (green, n = 5). Vertical bars: standard deviation of motif similarity.

(C) The mean motif consistency of intact and SP birds (red and green, respectively) at 50–60 phd (juvenile), 100–104 phd (adult), and 119–130 phd (adult), $*p < 0.001$. Unpaired *t* test for different conditions and paired *t* test with Bonferroni correction for multiple comparisons.

(D) Development of song acoustic features of SP birds. Comparison of syllable acoustic features, pitch, pitch goodness, AM, and entropy variance, among intact juveniles (n=5, 40–50 phd), intact adults (n =5, 100–104 phd), SP birds after release (n=5, 100–103 phd), and SP birds after song crystallization (n=5, 119–126 phd). $*p < 0.05$, $**p$

< 0.01; Welch's *t* test.

(E, G) Development of syllable and motif similarities of songs in SP birds after release from singing prevention (n=5). Error bar: SD

(F, H) Comparison of mean syllable and motif similarities against tutor song between SP birds after release (n=5, 100–103 phd) and after song crystallization (n=5, 119–126 phd), and singing persistent birds (n=3, 101–103 phd. ***$p < 0.005$; Welch's *t* test. NS: $p > 0.05$; Unpaired *t* test.

(Figure 13)

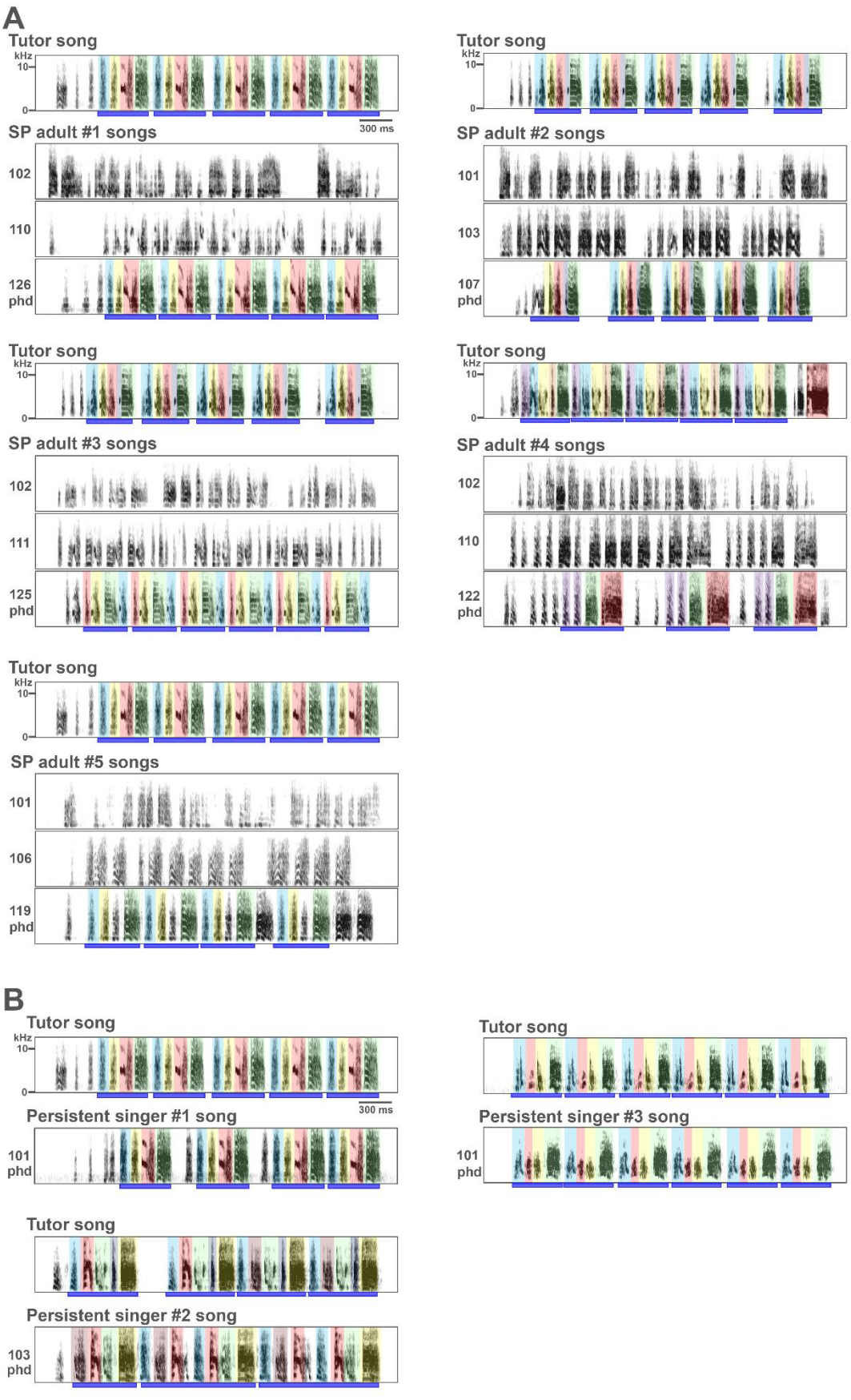
A
Tutor song
kHz
10
0
300 ms
SP adult #1 songs
102
110
126
phd
Tutor song
SP adult #2 songs
101
103
107
phd
Tutor song
SP adult #3 songs
102
111
125
phd
Tutor song
SP adult #4 songs
102
110
122
phd
Tutor song
SP adult #5 songs
101
106
119
phd
B
Tutor song
Persistent singer #1 song
101
phd
Tutor song
Persistent singer #3 song
101
phd
Tutor song
Persistent singer #2 song
103
phd

Figure 13. Song development from adult stage in SP zebra finches

(A) Song development of SP adults (n = 5) and their tutor songs. Blue lines indicate the motif structure of songs. Colored syllables were learned from the same colored syllables of their tutor songs. SP bird #1 and #2 excellently mimicked the syllable acoustics and sequence order of their tutor songs.

(B) Examples of the songs in three persistent singers under singing prevention. Top panels: their tutor songs. Blue lines indicate the motif structure of songs. Colored syllables were learned from the same colored syllables of their tutor songs.

(Figure 14)

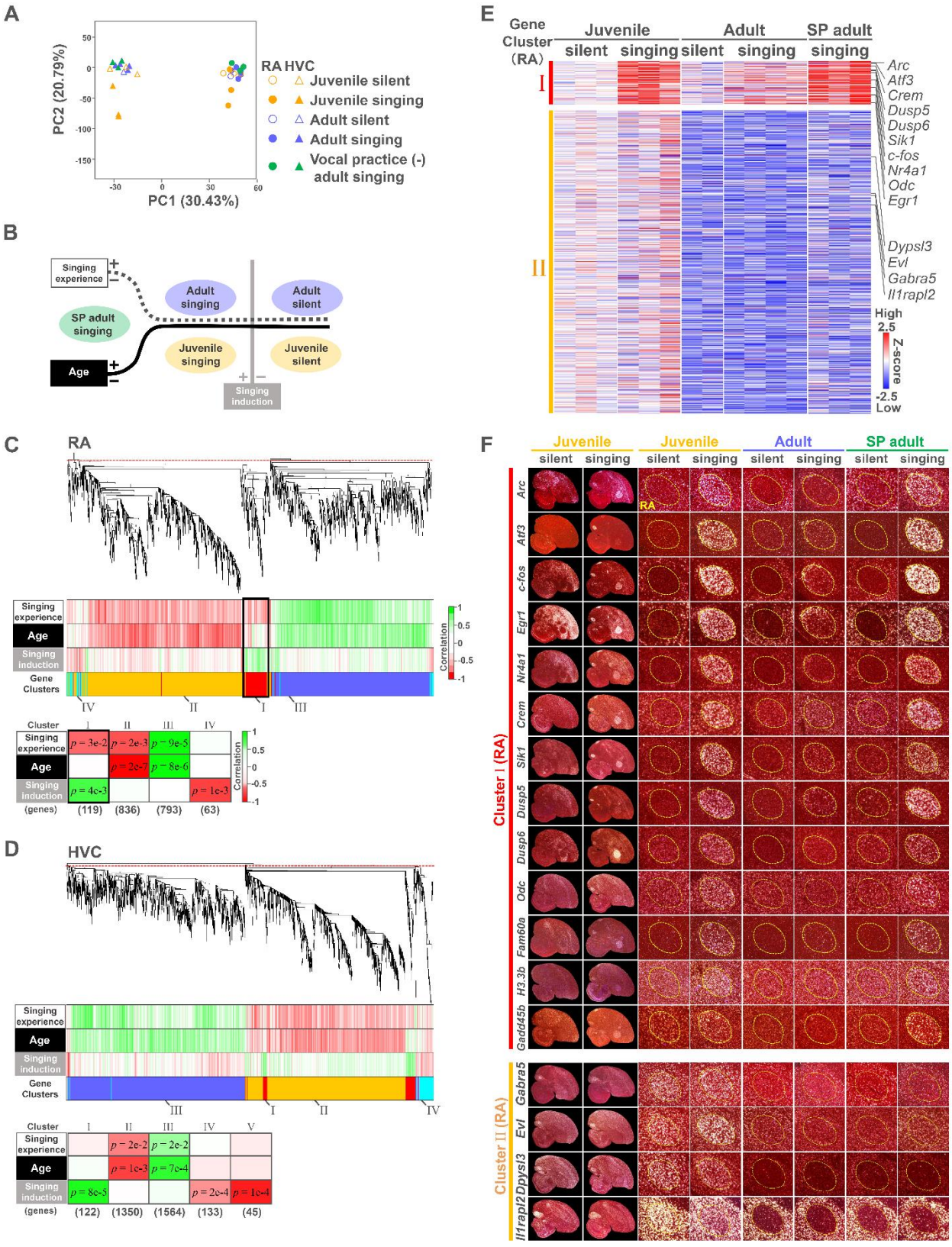
A
PC2 (20.79%)
PC1 (30.43%)
RA HVC
Juvenile silent
Juvenile singing
Adult silent
Adult singing
Vocal practice (-)
adult singing
B
Singing experience
Age
Adult singing
Adult silent
SP adult singing
Juvenile singing
Juvenile silent
Singing induction
C
RA
Singing experience
Age
Singing induction
Gene Clusters
Correlation
Cluster
(genes)
(119)
(836)
(793)
(63)
D
HVC
(122)
(1350)
(1564)
(133)
(45)
E
Gene Cluster (RA)
Juvenile
Adult
SP adult
silent
singing
Arc
Atf3
Crem
Dusp5
Dusp6
Sik1
c-fos
Nr4a1
Odc
Egr1
Dypsl3
Evl
Gabra5
Il1rapl2
High
Z-score
Low
F
Cluster I (RA)
Cluster II (RA)
RA
Arc
Atf3
c-fos
Egr1
Nr4a1
Crem
Sik1
Dusp5
Dusp6
Odc
Fam60a
H3.3b
Gadd45b
Gabra5
Evl
Dypsl3
Il1rapl2

Figure 14. Cumulative singing experience regulates a cluster of singing activity-dependent genes in RA

(A) Principal component analysis (PCA) using 12,156 transcripts for all brain samples.

(B) Sampling conditions for RNA-seq to extract transcriptome information on singing experience, age, and singing induction.

(C, D) (Upper panels) dendrogram of average linkage hierarchical clustering of differentially regulated genes in RA **(C)** and HVC **(D)** (1,811 and 3,214 genes, respectively). Red dotted line indicates the height at which the tree was cut. (Middle panels) correlation heat maps between gene expression levels and each parameter: singing experience, age, or singing induction. Colored bands indicate positive (green) and negative (red) correlations. (Lower pannels) Regulation relationships of Gene Clusters in RA and HVC for singing experience, age, and singing induction. Heat colors show correlations with parameters for each Gene Clusters. *P* values in each cell; student's asymptotic *P* value.

(E) Heat maps of Z scores of RA cluster I and II genes (119 and 836 genes, respectively), normalized by juvenile silent condition.

(F) Induction of Cluster I and II genes by singing in RA of juveniles, normal adults, and SP adults.

(Figure 15)

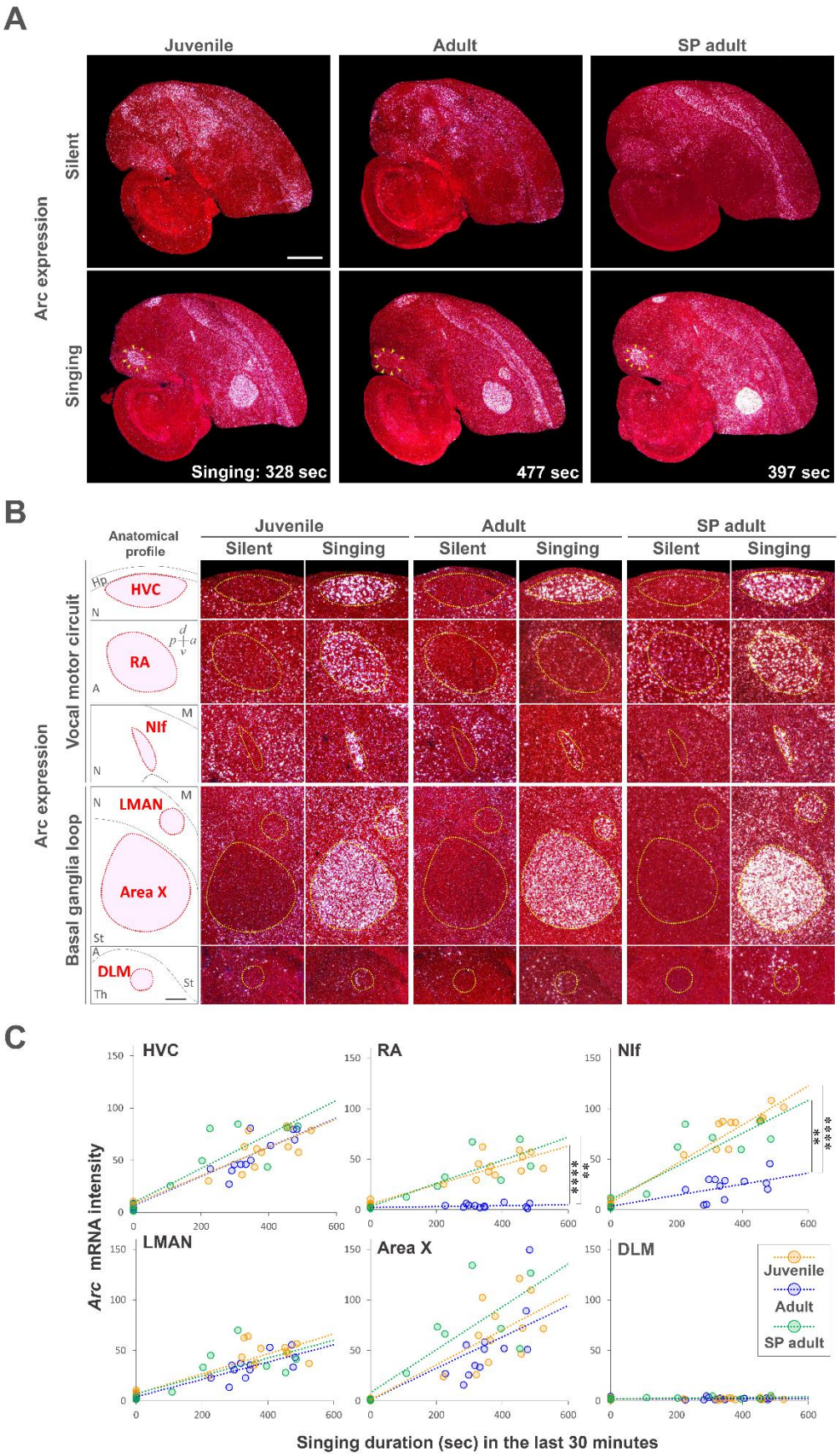
A
Juvenile
Adult
SP adult
Arc expression
Silent
Singing
Singing: 328 sec
477 sec
397 sec
B
Anatomical profile
Juvenile
Adult
SP adult
Silent
Singing
Vocal motor circuit
Basal ganglia loop
HVC
RA
NIf
LMAN
Area X
DLM
C
HVC
RA
NIf
LMAN
Area X
DLM
Arc mRNA intensity
Juvenile
Adult
SP adult
Singing duration (sec) in the last 30 minutes

Figure 15. Singing experience-dependent regulation of *Arc* inducibility

(A) Expression of *Arc* mRNA in juveniles (silent, 52 phd; singing, 47 phd), adults (silent, 124 phd; singing, 112 phd), and SP adults (silent, 100 phd; singing, 100 phd). Singing duration (sec) is shown at the bottom. White dot: *Arc* mRNA expression. Red: cresyl violet counter stain. Scale bar = 1.5 mm.

(C) Higher magnification images of *Arc* mRNA expression in the song nuclei. Scale bar = 200 μm.

(D) Induction intensity of *Arc* mRNA in the song nuclei in SP adults (n = 11) and juveniles (n = 17) compared with those of adults (n = 17). Lines represent linear approximation curve. $^{**}p < 0.001$, $^{****}p < 0.00001$, ANCOVA with Bonferroni correction.

(Figure 16)

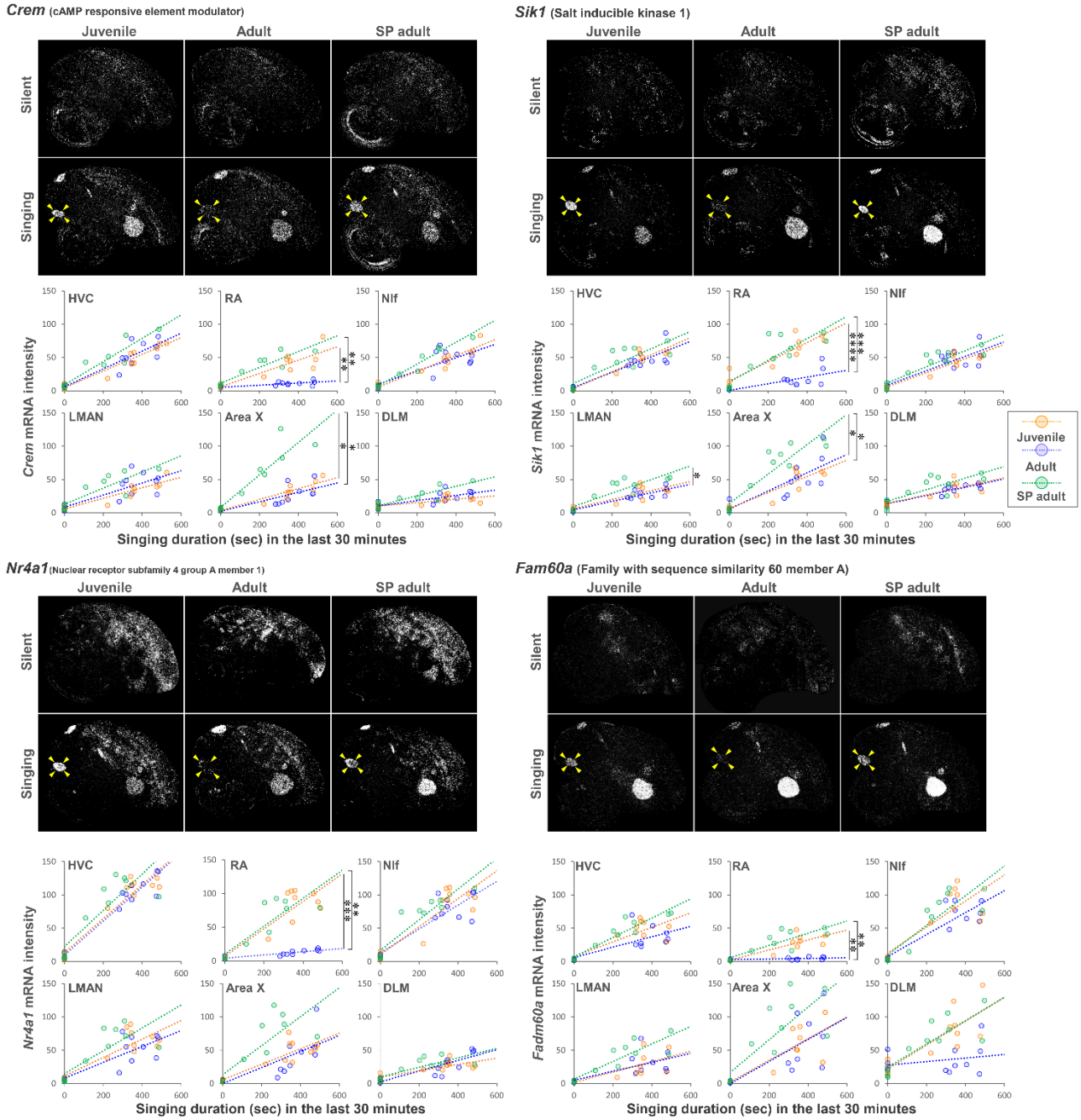
Crem (cAMP responsive element modulator)
Sik1 (Salt inducible kinase 1)
Nr4a1 (Nuclear receptor subfamily 4 group A member 1)
Fam60a (Family with sequence similarity 60 member A)
Juvenile
Adult
SP adult
Silent
Singing
HVC
RA
NIf
LMAN
Area X
DLM
Crem mRNA intensity
Sik1 mRNA intensity
Nr4a1 mRNA intensity
Fadm60a mRNA intensity
Singing duration (sec) in the last 30 minutes

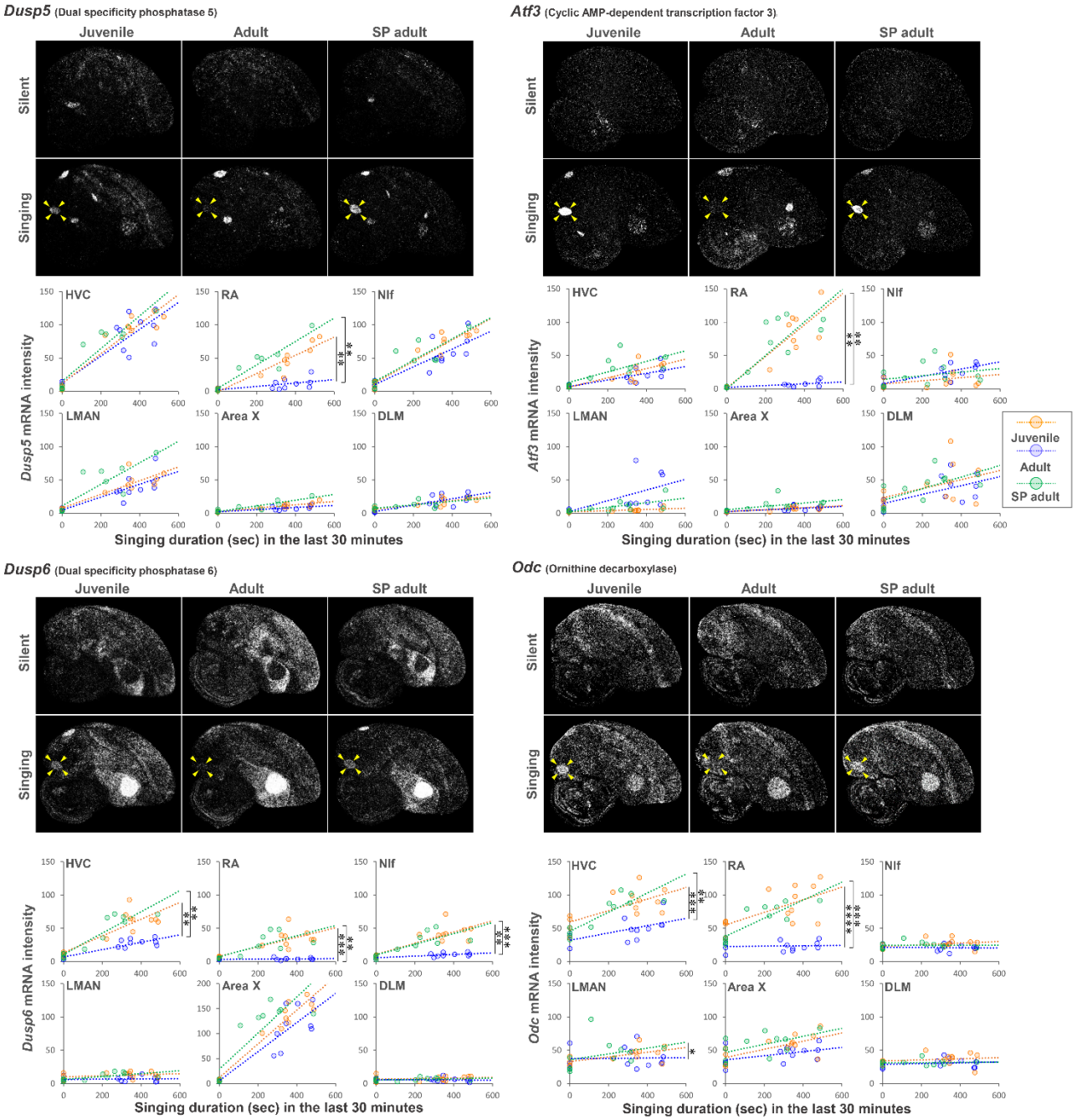
Dusp5 (Dual specificity phosphatase 5)
Atf3 (Cyclic AMP-dependent transcription factor 3)
Dusp6 (Dual specificity phosphatase 6)
Odc (Ornithine decarboxylase)
Juvenile
Adult
SP adult
Silent
Singing
HVC
RA
NIf
LMAN
Area X
DLM
Dusp5 mRNA intensity
Atf3 mRNA intensity
Dusp6 mRNA intensity
Odc mRNA intensity
Singing duration (sec) in the last 30 minutes

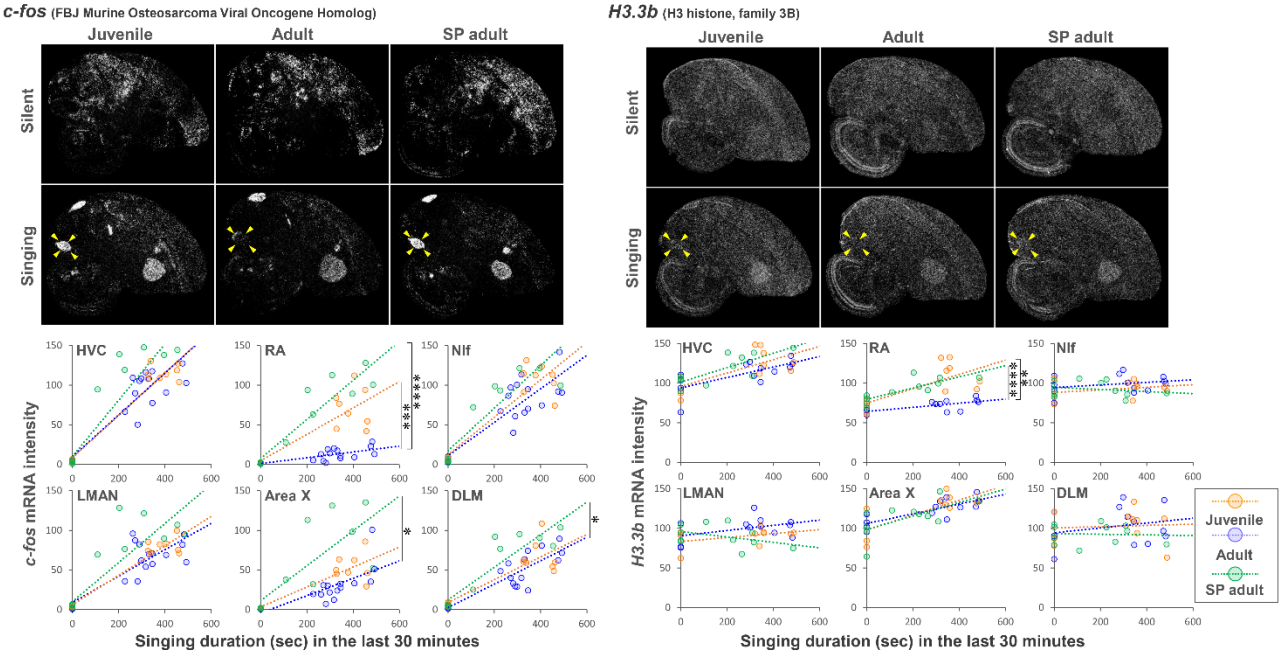
c-fos (FBJ Murine Osteosarcoma Viral Oncogene Homolog)
H3.3b (H3 histone, family 3B)
Juvenile
Adult
SP adult
Silent
Singing
HVC
RA
Nlf
LMAN
Area X
DLM
c-fos mRNA intensity
H3.3b mRNA intensity
Singing duration (sec) in the last 30 minutes
Juvenile
Adult
SP adult

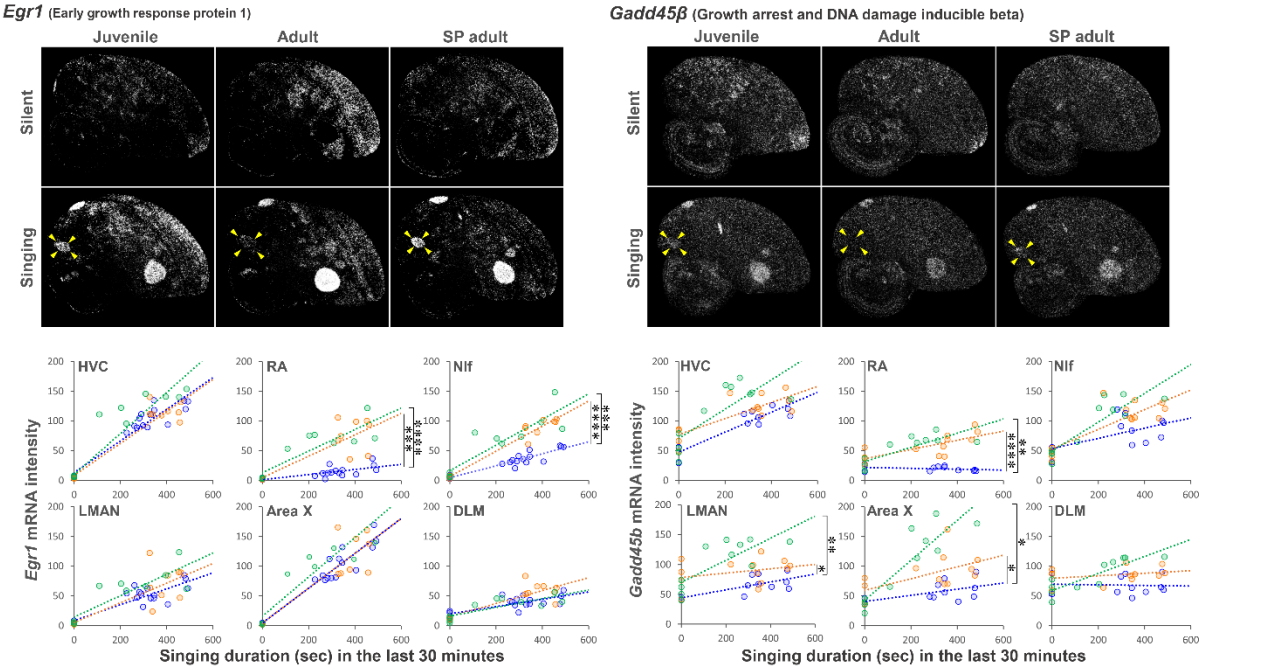
Egr1 (Early growth response protein 1)
Gadd45β (Growth arrest and DNA damage inducible beta)
Juvenile
Adult
SP adult
Silent
Singing
HVC
RA
Nlf
LMAN
Area X
DLM
Egr1 mRNA intensity
Gadd45b mRNA intensity
Singing duration (sec) in the last 30 minutes

Figure 16. Induction of RA Cluster I genes by singing in the song nuclei

(Upper panels of each gene) Expression patterns of the 12 tested genes (*Atf3*, *c-fos*, *Egr1*, *Nr4a1*, *Crem*, *Sik*1, *Dusp5*, *Dusp6*, *Odc*, and *Fam60a*, *H3.3b*, and *Gadd45β*) in silent and singing conditions of juveniles, adults, and SP adults. (Lower panels of each gene) Induction of the genes in juveniles (orange: n = 10–13), adults (blue: n = 11–18), and SP adults (green: n = 10–12) in the song nuclei. Lines represent linear approximation curve. (*$p < 0.01$, **$p < 0.001$, ***$p < 0.0001$, ****$p < 0.00001$; ANCOVA with Bonferroni correction).

(Figure 17)

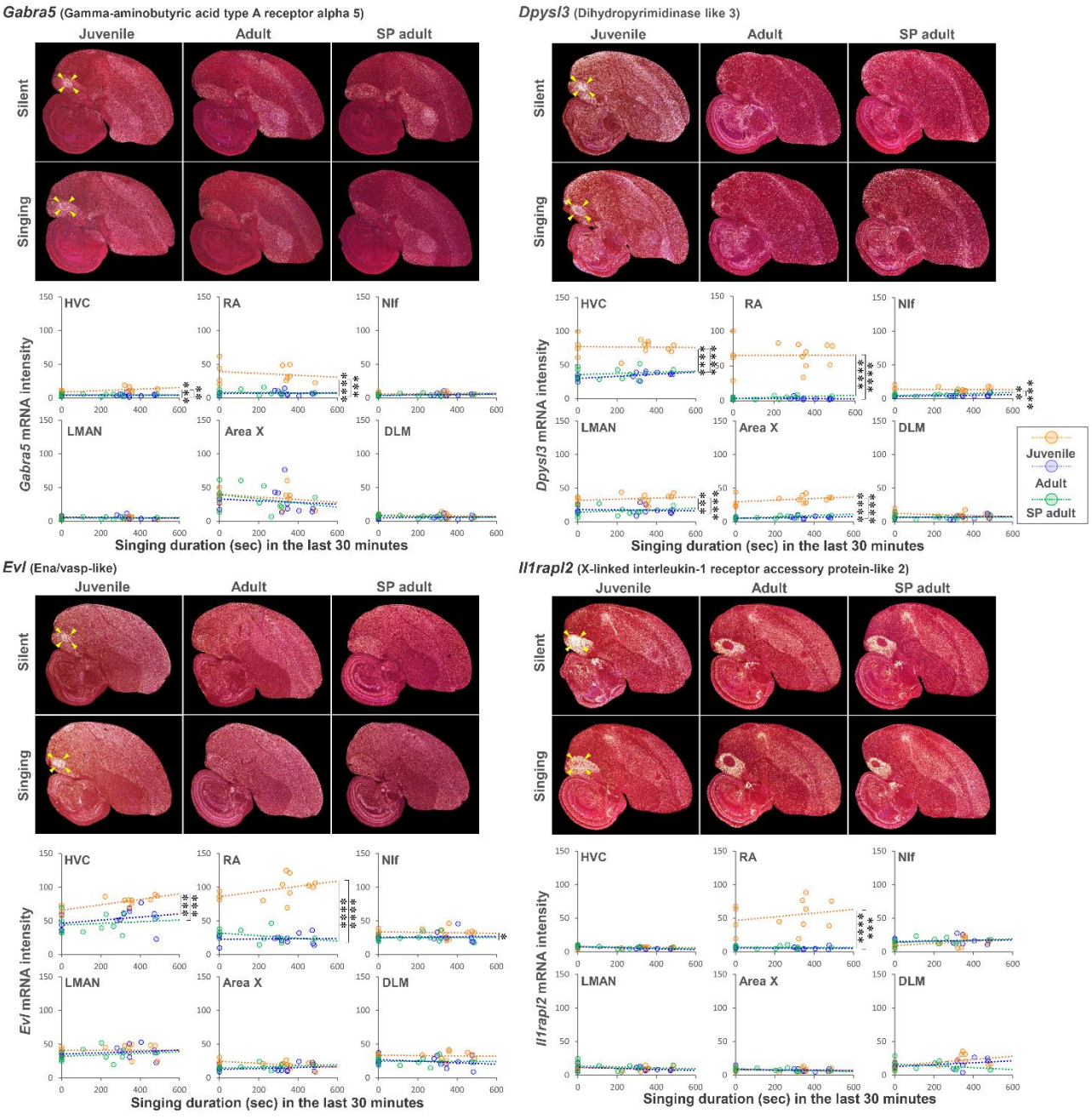
Gabra5 (Gamma-aminobutyric acid type A receptor alpha 5)
Dpysl3 (Dihydropyrimidinase like 3)
Evl (Ena/vasp-like)
Il1rapl2 (X-linked interleukin-1 receptor accessory protein-like 2)
Juvenile
Adult
SP adult
Silent
Singing
HVC
RA
NIf
LMAN
Area X
DLM
Gabra5 mRNA intensity
Dpysl3 mRNA intensity
Evl mRNA intensity
Il1rapl2 mRNA intensity
Singing duration (sec) in the last 30 minutes

Figure 17. Expression of age-regulated genes from RA Gene cluster II in SP adults

(Upper panels in each gene) Expression patterns of *Gabra5*, *Evl*, *Dpysl3*, and *Il1rapl2* from RA Cluster II genes, regulated by aging under silence and singing conditions in juveniles, adults, and SP adults. (Lower panels in each gene) Induction of the RA Cluster II genes in juveniles (orange: n = 10–13), adults (purple: n = 11–13), and SP adults (green: n = 11) in the song nuclei. Lines represent linear approximation curve. (*$p < 0.01$, **$p < 0.001$, ***$p < 0.0001$, and ****$p < 0.00001$; ANCOVA with Bonferroni correction).

(Figure 18)

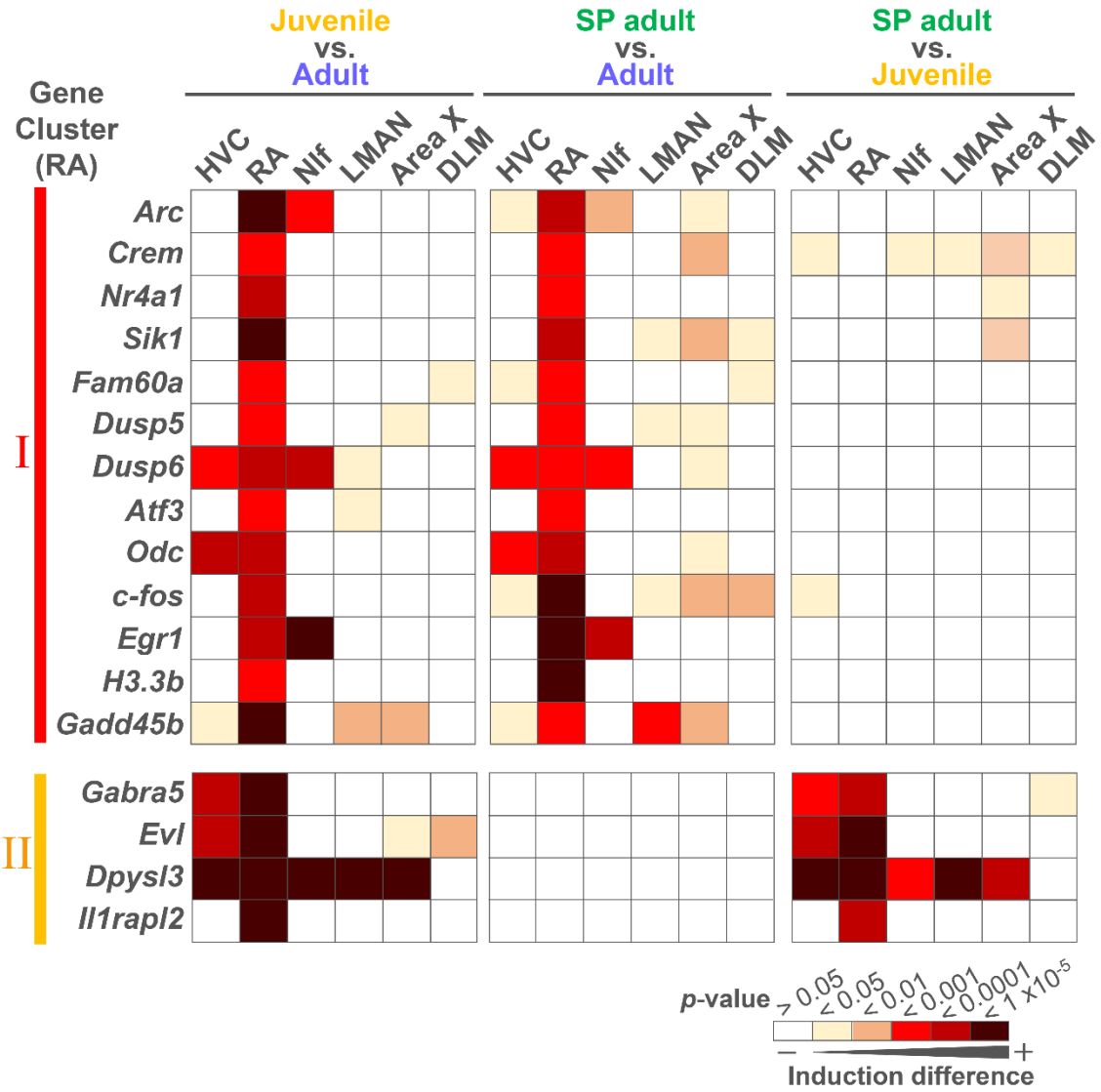

Figure 18. RA as a hotspot of experience-dependent gene regulation

Heat maps showing induction differences of Cluster I and II genes in the song nuclei between normal adults, juveniles, and SP adults (ANCOVA with Bonferroni correction, also see Fig. 16; Fig. 17).

(Figure 19)

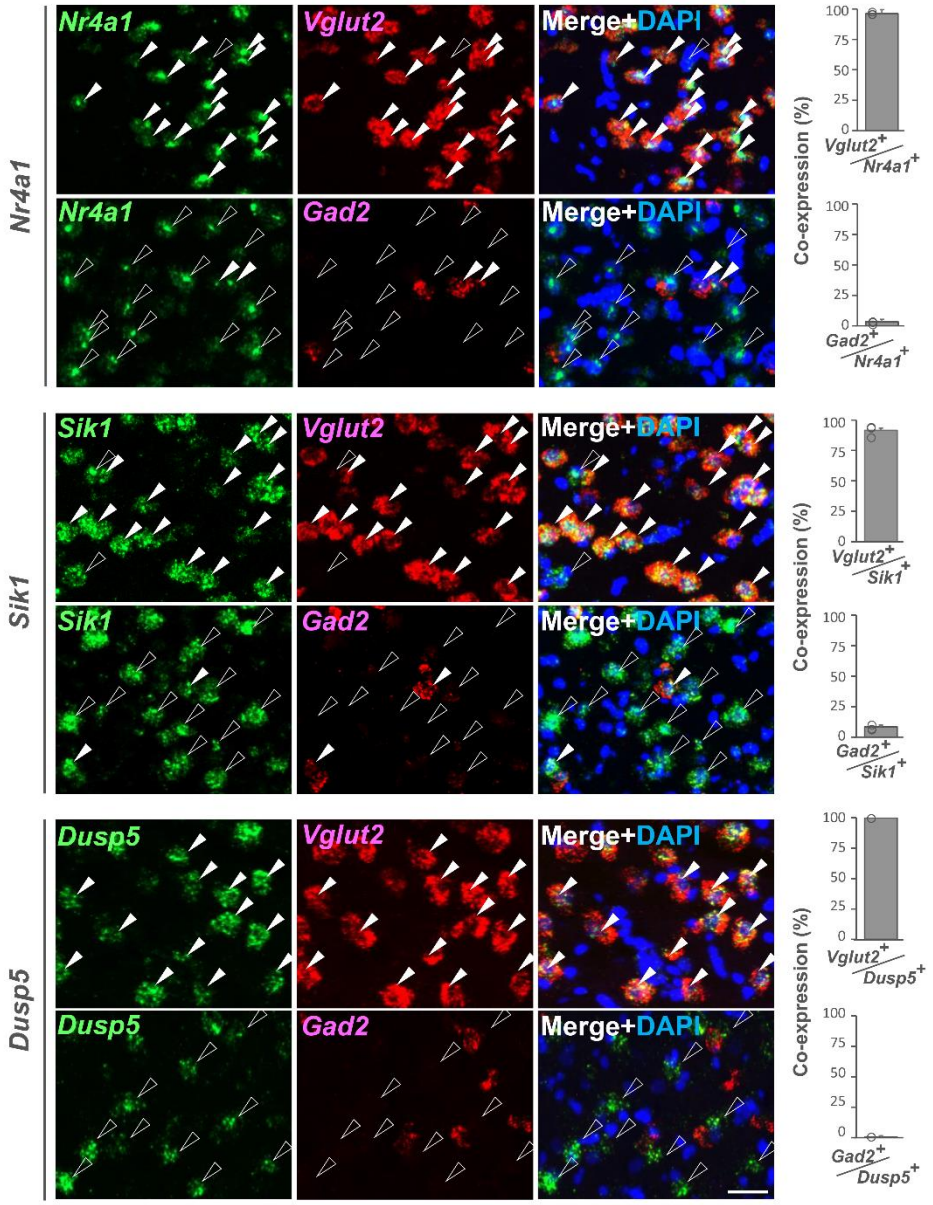

Figure 19. Co-induction of RA cluster I genes in RA

(Left panels) Co-induction of RA cluster I genes *Nr4a1*, *Sik1*, and *Dusp5* in glutamatergic neurons with *Vglut2* (+), but not GABAergic neurons with *Gad2* (+). Cell nuclei (blue, DAPI). Filled arrowheads: cells that co-expressed with Cluster I (RA) genes and marker genes. Empty arrowheads: cells that expressed Cluster I (RA) genes but not marker genes. Scale bar = 40 μm. (Right bar graphs) Proportion of each subpopulation in cells that express the mRNA of RA Cluster I genes (n = 491–770 cells).

(Figure 20)

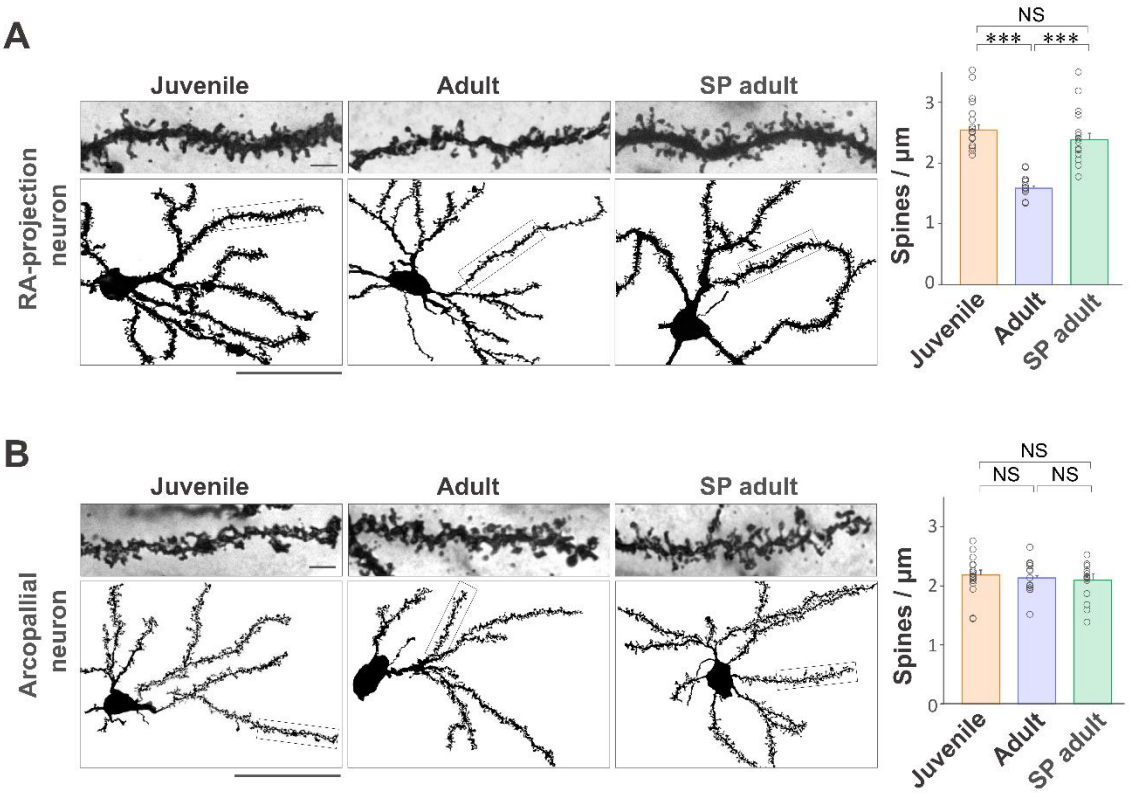

Figure 20. Dendritic spine density in RA projection neruons

(Left panels) Golgi-stained RA projection neurons **(A)** and RA-surrounding arcopallial neurons **(B)** in juvenile (55 phd), adult (105 phd), and SP adult birds (101 phd). Scale bars = 5 µm (upper) and 50 µm (lower). (Right bar graphs) Spine density of RA projection neurons and RA-surrounding arcopallial neurons in juveniles (n = 18), adults (n = 15), and SP adults (n = 15). ***$p < 0.0001$, $^{NS}p > 0.1$, unpaired *t* test with Bonferroni correction. Error bars: SEM.

(Figure 21)

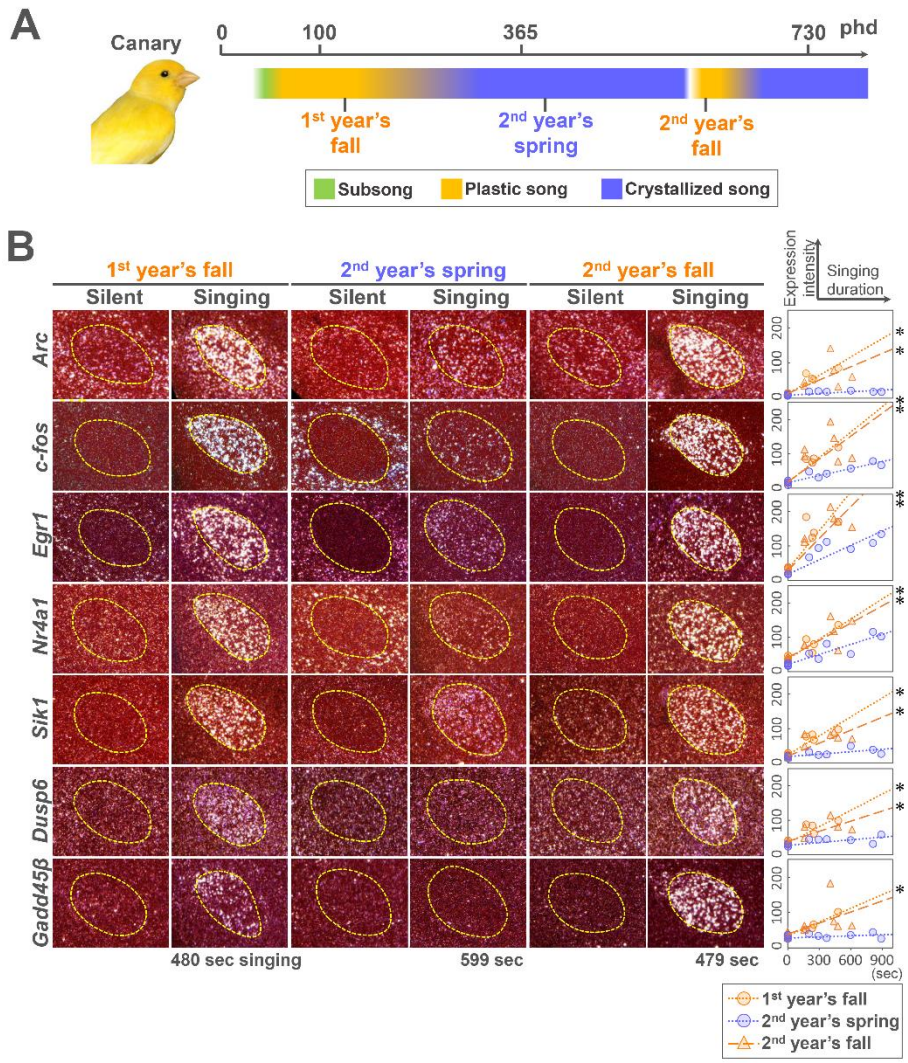

Figure 21. Expression dynamics of activity-dependent genes in RA of the canary

(A) The critical period of vocal learning in the canary.

(B) Re-induction of activity-dependent genes in RA during the 2nd plastic song phase (2nd year's fall) for song re-development in adult in the canary. Last 30 min of the singing duration of each bird is shown at the bottom. Lines represent linear approximation curve. *p < 0.05, ANCOVA with Bonferroni correction.

2.6 Tables

(Table 1)

	Sample title	Conditions	Species	Age	Singing duration (sec)	Brain region	RIN	DDBJ accession #	DRA accession #	Library preparateion
1	ZF_RA_adult_silent_1	45min_silent_after_light_on	*Taeniopygia guttata*	104	0.0	Robust nucleus of arcopallium	6.6	DRA005559	DRX081502	Oligo-dT-based qualtz-amp method + LIM prep (Sasagawa et al., 2013)
2	ZF_RA_adult_silent_2	45min_silent_after_light_on	*Taeniopygia guttata*	101	0.0	Robust nucleus of arcopallium	7.3	DRA005559	DRX081503	Oligo-dT-based qualtz-amp method + LIM prep (Sasagawa et al., 2013)
3	ZF_RA_adult_singing_1	45min_singing_after_light_on	*Taeniopygia guttata*	338	273.9	Robust nucleus of arcopallium	7.1	DRA005559	DRX081504	Oligo-dT-based qualtz-amp method + LIM prep (Sasagawa et al., 2013)
4	ZF_RA_adult_singing_2	45min_singing_after_light_on	*Taeniopygia guttata*	110	343.5	Robust nucleus of arcopallium	7.1	DRA005559	DRX081505	Oligo-dT-based qualtz-amp method + LIM prep (Sasagawa et al., 2013)
5	ZF_RA_adult_singing_3	45min_singing_after_light_on	*Taeniopygia guttata*	114	618.3	Robust nucleus of arcopallium	6.8	DRA005559	DRX081506	Oligo-dT-based qualtz-amp method + LIM prep (Sasagawa et al., 2013)
6	ZF_RA_adult_singing_4	45min_singing_after_light_on	*Taeniopygia guttata*	254	344.4	Robust nucleus of arcopallium	7	DRA005559	DRX081507	Oligo-dT-based qualtz-amp method + LIM prep (Sasagawa et al., 2013)
7	ZF_RA_juvenile_silent_1	45min_silent_after_light_on	*Taeniopygia guttata*	47	0.0	Robust nucleus of arcopallium	6.7	DRA005559	DRX081508	Oligo-dT-based qualtz-amp method + LIM prep (Sasagawa et al., 2013)
8	ZF_RA_juvenile_silent_2	45min_silent_after_light_on	*Taeniopygia guttata*	48	0.0	Robust nucleus of arcopallium	7.2	DRA005559	DRX081509	Oligo-dT-based qualtz-amp method + LIM prep (Sasagawa et al., 2013)
9	ZF_RA_juvenile_silent_3	45min_silent_after_light_on	*Taeniopygia guttata*	48	0.0	Robust nucleus of arcopallium	6.5	DRA005559	DRX081510	Oligo-dT-based qualtz-amp method + LIM prep (Sasagawa et al., 2013)
10	ZF_RA_juvenile_singing_1	45min_singing_after_light_on	*Taeniopygia guttata*	50	608.9	Robust nucleus of arcopallium	6.7	DRA005559	DRX081511	Oligo-dT-based qualtz-amp method + LIM prep (Sasagawa et al., 2013)
11	ZF_RA_juvenile_singing_2	45min_singing_after_light_on	*Taeniopygia guttata*	45	534.3	Robust nucleus of arcopallium	7.2	DRA005559	DRX081512	Oligo-dT-based qualtz-amp method + LIM prep (Sasagawa et al., 2013)
12	ZF_RA_juvenile_singing_3	45min_singing_after_light_on	*Taeniopygia guttata*	40	431.2	Robust nucleus of arcopallium	7.4	DRA005559	DRX081513	Oligo-dT-based qualtz-amp method + LIM prep (Sasagawa et al., 2013)
13	ZF_RA_singing-practice(-)_adult_singing_1	45min_singing_after_light_on	*Taeniopygia guttata*	96	453.8	Robust nucleus of arcopallium	7.1	DRA005559	DRX081514	Oligo-dT-based qualtz-amp method + LIM prep (Sasagawa et al., 2013)
14	ZF_RA_singing-practice(-)_adult_singing_2	45min_singing_after_light_on	*Taeniopygia guttata*	100	226.6	Robust nucleus of arcopallium	7.4	DRA005559	DRX081515	Oligo-dT-based qualtz-amp method + LIM prep (Sasagawa et al., 2013)
15	ZF_RA_singing-practice(-)_adult_singing_3	45min_singing_after_light_on	*Taeniopygia guttata*	101	309.2	Robust nucleus of arcopallium	7.2	DRA005559	DRX081516	Oligo-dT-based qualtz-amp method + LIM prep (Sasagawa et al., 2013)
16	ZF_HVC_adult_silent_1	45min_silent_after_light_on	*Taeniopygia guttata*	104	0.0	HVC	6.8	DRA005559	DRX081517	Oligo-dT-based qualtz-amp method + LIM prep (Sasagawa et al., 2013)
17	ZF_HVC_adult_silent_2	45min_silent_after_light_on	*Taeniopygia guttata*	101	0.0	HVC	6.7	DRA005559	DRX081518	Oligo-dT-based qualtz-amp method + LIM prep (Sasagawa et al., 2013)
18	ZF_HVC_adult_singing_1	45min_singing_after_light_on	*Taeniopygia guttata*	338	273.9	HVC	7.1	DRA005559	DRX081519	Oligo-dT-based qualtz-amp method + LIM prep (Sasagawa et al., 2013)
19	ZF_HVC_adult_singing_2	45min_singing_after_light_on	*Taeniopygia guttata*	110	343.5	HVC	6.9	DRA005559	DRX081520	Oligo-dT-based qualtz-amp method + LIM prep (Sasagawa et al., 2013)
20	ZF_HVC_adult_singing_3	45min_singing_after_light_on	*Taeniopygia guttata*	114	618.3	HVC	6.6	DRA005559	DRX081521	Oligo-dT-based qualtz-amp method + LIM prep (Sasagawa et al., 2013)
21	ZF_HVC_adult_singing_4	45min_singing_after_light_on	*Taeniopygia guttata*	254	344.4	HVC	6.9	DRA005559	DRX081522	Oligo-dT-based qualtz-amp method + LIM prep (Sasagawa et al., 2013)
22	ZF_HVC_juvenile_silent_1	45min_silent_after_light_on	*Taeniopygia guttata*	47	0.0	HVC	6.9	DRA005559	DRX081523	Oligo-dT-based qualtz-amp method + LIM prep (Sasagawa et al., 2013)
23	ZF_HVC_juvenile_silent_2	45min_silent_after_light_on	*Taeniopygia guttata*	48	0.0	HVC	7.2	DRA005559	DRX081524	Oligo-dT-based qualtz-amp method + LIM prep (Sasagawa et al., 2013)
24	ZF_HVC_juvenile_silent_3	45min_silent_after_light_on	*Taeniopygia guttata*	48	0.0	HVC	6.5	DRA005559	DRX081525	Oligo-dT-based qualtz-amp method + LIM prep (Sasagawa et al., 2013)
25	ZF_HVC_juvenile_singing_1	45min_singing_after_light_on	*Taeniopygia guttata*	50	608.9	HVC	6.9	DRA005559	DRX081526	Oligo-dT-based qualtz-amp method + LIM prep (Sasagawa et al., 2013)
26	ZF_HVC_juvenile_singing_2	45min_singing_after_light_on	*Taeniopygia guttata*	45	534.3	HVC	6.8	DRA005559	DRX081527	Oligo-dT-based qualtz-amp method + LIM prep (Sasagawa et al., 2013)
27	ZF_HVC_juvenile_singing_3	45min_singing_after_light_on	*Taeniopygia guttata*	40	431.2	HVC	6.5	DRA005559	DRX081528	Oligo-dT-based qualtz-amp method + LIM prep (Sasagawa et al., 2013)
28	ZF_HVC_singing-pHVCctice(-)_adult_singing_1	45min_singing_after_light_on	*Taeniopygia guttata*	96	453.8	HVC	7.1	DRA005559	DRX081529	Oligo-dT-based qualtz-amp method + LIM prep (Sasagawa et al., 2013)
29	ZF_HVC_singing-pHVCctice(-)_adult_singing_2	45min_singing_after_light_on	*Taeniopygia guttata*	100	226.6	HVC	7.1	DRA005559	DRX081530	Oligo-dT-based qualtz-amp method + LIM prep (Sasagawa et al., 2013)
30	ZF_HVC_singing-pHVCctice(-)_adult_singing_3	45min_singing_after_light_on	*Taeniopygia guttata*	101	309.2	HVC	6.4	DRA005559	DRX081531	Oligo-dT-based qualtz-amp method + LIM prep (Sasagawa et al., 2013)
31	ZF_total_RNA_1	morning_silent_and_dark	*Taeniopygia guttata*	239	0.0	Pallium and pallidum region	9.3	DRA005548	DRX026410	TruSeq DNA Sample Prep Kits
32	ZF_total_RNA_2	morning_silent_and_dark	*Taeniopygia guttata*	786	0.0	Pallium and pallidum region	9.5	DRA005548	DRX026411	TruSeq DNA Sample Prep Kits
33	ZF_total_RNA_3	morning_silent_and_dark	*Taeniopygia guttata*	234	0.0	Pallium and pallidum region	9.4	DRA005548	DRX026412	TruSeq DNA Sample Prep Kits
34	ZF_total_RNA_4	morning_silent_and_dark	*Taeniopygia guttata*	311	0.0	Pallium and pallidum region	9.3	DRA005548	DRX026413	TruSeq DNA Sample Prep Kits

(Table 2)

Gene short name	Full gene name	Cloned length (bp)	Forward primer seq	Reverse primer seq
Arc	activity-regulated cytoskeleton-associated protein	1607	5'-ATTCAAGGTGCTGAGAGC-3'	5'-TTGCAGCAGATATTTCAAAG-3'
Vglut2	vesicular glutamate transporter 2	1365	5'-AATGGAGTCGGTAAAACAAAG-3'	5'-TGAAGCAAATATGCCATAGA-3'
Gad2	glutamic acid decarboxylase 2	782	5'-ATATTTTCACCTGGTGGTG-3'	5'-TTTCCATCAAACACCATTTCA-3'
Atf3	cyclic AMP-dependent transcription factor 3 like	1604	5'-TGCTCATGCAGATAGCTC-3'	5'-GTGACCTTGAGTACCATC-3'
c-fos	FBJ Murine Osteosarcoma Viral Oncogene Homolog	247	5'-CTAGGCCGGATTTGCAGTG-3'	5'-TTTGCAGCTGCCATTTTGTTC-3'
Egr1	early growth response protein 1	1652	5'-GGAGCCCGGCGCTCTCAT-3'	5'-GCCTTGCAACGTATGGTGTTG-3'
Nr4a1	nuclear receptor subfamily 4 group A member 1	1364	5'-GTTGGCATGGTCAAAGAAG-3'	5'-AAGAAGACTCAGGCATCTG-3'
Crem	cAMP responsive element modulator	1030	5'-CTGAGAACCATATCCAGAG-3'	5'-AGTCTCAGCTCTCTCTTG-3'
Sik1	salt inducible kinase 1	1344	5'-CATCAGTGAGGAAGTGAG-3'	5'-TCACTTGACCAGCACGAAC-3'
Dusp5	dual specificity phosphatase 5	1449	5'-CAAGATCCTGGTGCACTG-3'	5'-CATTCTGAACTCCCTGTG-3'
Dusp6	dual specificity phosphatase 6	923	5'-AATGTTACTCCTAACCTGC-3'	5'-TACTACCAAGCTCCTAGC-3'
Odc	ornithine decarboxylase	1331	5'-CAAACATGCTGCCAGCAG-3'	5'-GTAGGTCACAAAGCACTAAG-3'
Fam60a	family with sequence similarity 60 member A	1514	5'-CCAAGTCAGGTGTAGATG-3'	5'-GATTACAAGTGTCTGAACAG-3'
H3.3b	H3 histone, family 3B	352	5'-AAGTGAAGGCTGTTTTTATGG-3'	5'-AAGTCATAACCAGTTTTATTGC-3'
Gadd45β	growth arrest and DNA damage inducible beta	629	5'-TTCCCGGCCTGCACTTGGA-3'	5'-TAAACGTTATTTTACAGACTGC-3'
Gabra5	gamma-aminobutyric acid type A receptor alpha 5	1166	5'-CAACTAATACATACAGCAC-3'	5'-AACACAGTCTTCTTCTTGG-3'
Evl	ena/vasp-like	719	5'-ACGATGGGTCAGTGTCAG-3'	5'-AAGCGAATCCAAGGCAGC-3'
Dpysl3	dihydropyrimidinase like 3	1045	5'-TGTGACTATGCCTTGCAC-3'	5'-GCTTGTAGACGTAGTCAG-3'
Il1rapl2	X-linked interleukin-1 receptor accessory protein-like 2	1044	5'-CAGGTCTTAGGCTTATGTG-3'	5'-ATCTAACGCATCAGGATCC-3'

Table2, Primers information

Chapter III

Contribution of singing experience to cheek plumage maturation in male zebra finches

3.1 Introduction

Following singing prevention in Chapter II, I observed that some of the SP adult zebra finches had delayed cheek plumage development (Fig. 22B), whereas breast bands and rust-colored side plumage developed normally. This phenomenon suggested that individual variations in cheek plumage development of normal birds might occur as a result of differences in their cumulative singing experience. To examine this idea, I recorded cheek plumage development and the total amount of singing practice in 12 intact juvenile zebra finches from 30-35 phd until 60 phd. Then, I analyzed the correlation between the total amount of singing experience and cheek plumage development. As a potential regulatory mechanisms for the molting of cheek plumage, I examined testis size and serum testosterone concentration at 60 phd. To further examine the experience-dependence of the cheek plumage, I evaluated the development of cheek plumage in RA-lesioned birds (60-76 phd) which could not produce songs. To estimate the effect of stress by the lesion manipulation, I measured serum corticosterone concentration in RA-lesioned birds.

A previous study in peacock showed testosterone-independent mechanisms for the plumage molt in castrated males (Owens and Short, 1995). In zebra finches, early-castration (< 35 phd) did not completely inhibit singing behavior (Arnold, 1975). However, the development of cheek plumage in castrated zebra finch juveniles has not been quantitatively evaluated. To examine the contribution of testis development to the singing experience-dependent development of cheek plumage, I examined whether castrated juveniles (35 phd) developed cheek plumage or not.

3.2 Materials and methods

Continuous song recording

To quantify total singing experience, juvenile zebra finches were individually housed in a cage inside a sound-attenuating box from 30 until 60 phd (intact, n = 12). To reduce the effects of social isolation, a mirror (290×160 mm) was placed inside the box and conspecific songs that recorded from an adult zebra finch were played back 14 times per day. See also p.12.

Quantification of development cheek plumage development

I took pictures of left and right cheeks for each intact bird at a 5 days interval from 35 to 60 phd using a digital camera (16 M pixels, Olympus, PEN lite E-PL7). In a cage for photographing (200 x 200 x 160 mm, hand-made) with a perch, birds freely moved and were photographed when they sat on the perch. Pictures were taken under the same light intensity and each session ended within 1 h. Cropped images of cheek patch area were separated into RGB histograms of color intensity using Photoshop (Adobe) and color saturation was measured as (max RGB intensity) - (min RGB intensity). To normalize for individual differences in the baseline color of juvenile feather, saturations were normalized (deducted) by the first photo at 30-35 phd (before molting) for each bird.

Determination of serum testosterone concentration and testis volume

At 60 phd, birds were sacrificed by decapitation under silent and dark condition and blood was sampled from the carotid artery. Serum was separated by centrifugation (1000 g, 10 min), and stored at –80 ^{o}C until use. Serum testosterone concentration or testosterone was determined using a testosterone enzyme-linked immunosorbent assay

kit (Enzo ADI-900-097, ADI-900-065), according to the manufacturer's instructions. Testis volume (mm^3) was measured as $4\pi/3 \times (\text{major axis}/2) \times (\text{minor axis}/2)^2$.

Bilateral lesion of RA

Juvenile zebra finches (30-35 phd; n = 8) were anesthetized with pentobarbital and RA was lesioned by local injection of 120 nL / hemisphere of 1 % ibotenic acid dissolved in 1 M NaCl using a Nanoject 2 injector (Drummond Scientific). RA was targeted with stereotaxic coordinates in mm: 1.4 caudal, 2.5 lateral, and 1.8-2.0 ventral from the bifurcation of the central sinus at the border of the forebrain and cerebellum. Lesioned birds were housed individually in a cage inside a sound-attenuating box until 60-76 phd under the same conditions as intact juveniles. Although I ensured that all lesioned birds did not produce songs during this experiment by continuous recording, RA lesion % was not evaluated in these birds.

Castration

Juvenile zebra finches (30-35 phd; n = 7) were anesthetized with pentobarbital and their testes were removed bilaterally through intercostal spoke using tweezers and a retractor (2×2, Muromachi Kikai). The wound was stitched with a surgical needle and suturing thread (Suprylon, Vomel). All birds recovered and started flying within a few hours after surgery. Birds were housed individually in a cage inside a sound-attenuating box from 35 to 60 phd under the same conditions as intact juveniles. I then counted the number of song bouts of all castrated birds until 60 phd.

3.3 Results

Cheek plumage and testis development in zebra finch juveniles under free-singing condition

Zebra finches with little singing experience showed delayed development of cheek plumage. As expected, intact zebra finches showed wide individual variations in both total amount of singing (bouts number) and cheek plumage development (color saturation) at 60 phd (Fig. 23A, B). Particularly, 3 out of 12 birds (light singers) showed lower frequency of singing (< 5500 bouts until 60 phd), compared with normal singers (n = 9, > 16500 bouts until 60 phd). The body weight of light singers was not significantly reduced (p = 0.6, Mann-Whitney U-test, Fig. 23C) and age (dph) at first singing was not significantly delayed (p = 0.32, Mann-Whitney U-test) compared to normal singers. These light singers showed remarkable delay in molting of cheek plumage (p = 0.009, Mann-Whitney U-test, Fig. 23B, D, and E). However, there was no significant correlation between singing amount and development of cheek plumage (rho = 0.21, p = 0.51, Spearman's correlation test, Fig. 23E) in the 12 juveniles. I did not analyze breast-band and rust-colored side plumage because these feathers were removed during preening in some birds. Light singers had lower serum testosterone levels and testis sizes compared with normal singers (serum testosterone level: p = 0.009, testis size: p = 0.063, Mann-Whitney U-test, Fig. 23F, and G).

RA lesion-mediated singing inhibition prevented cheek plumage development.

Singing experience was needed for development of cheek plumage. RA lesion successfully inhibited singing behavior and birds showed low corticosterone level like normal juveniles even during singing prevention (Fig. 24B). These RA-lesioned birds

showed delayed cheek plumage at 60-76 phd compared with intact birds (including light singers) (p = 0.025, Mann-Whitney U-test, Fig. 24A and C).

Testis-independent development of cheek plumage in zebra finch

During the free singing period (35-60 phd), castrated juveniles tended to sing a small number of times compared with intact birds (p = 0.00048, Mann-Whitney U test, Fig. 25A). However, even in castrated birds, there was individual variations in the amount of singing: castrated singers (n = 4, totally more than 2000 bouts until 60 phd, Fig. 25B) and castrated light singers (n = 3, less than 50 bouts until 60 phd). Although greater sample size like for intact birds may be necessary, castrated singers developed cheek plumages with wide individual variations and castrated light singers tended to have delayed molting of cheek plumage (p = 0.057, Mann-Whitney U-test, Fig. 25C, D). This result indicates that the development and individual variations of cheek plumage are not inhibited by castration.

3.4 Discussion

Singing experience was necessary, but not sufficient for cheek molting in zebra finch

Lack of singing practice delayed cheek plumage development (Fig. 23; Fig. 24), indicating that singing experience has a specific contribution to the development of cheek plumage. However, individual variations in cheek molting cannot be explained solely by singing experience because it did not correlate with cheek plumage development in normal singers (Fig. 23E). These results suggest a complex regulation in cheek plumage development.

Potential mechanisms for the development of cheek plumage

What molecular mechanisms could mediate singing experience and molting of cheek plumage? A potential mechanism is singing-driven hormonal regulation. Serum testosterone concentration and testis volume were lower in light singers compared with normal singers (Fig. 23F and G). These results suggest that singing experience also contribute to testis development. However, testis size and testosterone level may be alternately regulated by singing and not influence cheek plumage development, since castrated birds could normally develop cheek plumage through singing experience (Fig. 25).

Castrated singers developed cheek plumage even with less singing experience compared with normal birds (Fig. 25A and C). This result suggests that lower testosterone level may enhance the development of cheek plumage. Previous studies revealed that testosterone (T) implantation inhibits molting of plumage in avian species (Nolan et al., 1992; Dawson 1994; Ketterson et al., 2001). These facts suggest a mediated factor “X” which is regulated by singing, enhances testis size, induces molting of cheek plumage,

and is suppressed by T-implantation (Fig. 26).

Previous studies showed that secretion of serum luteinizing hormone (LH) is photoperiodically induced in seasonally-molting species, such as Starlings, chukar partridge and willow ptarmigan just before plumage molting (Dawson, 1997; Stokkan and Sharp, 1980). Furthermore, it is known that T-implant reduces the synthesis of additional LH hormone (Davies and Bicknell, 1976). These studies suggested that LH hormone secretion may contribute to plumage molting independent of testis development (Fig. 26). Since light singers in this study showed delayed testis development and lower serum testosterone concentration (Fig. 23G and H), they might produce lower LH levels. Future examination of singing-driven LH secretion or direct LH injection-mediated cheek molting may reveal such mechanisms for the development of cheek plumage in zebra finch.

3.5 Figures

(Figure 22)

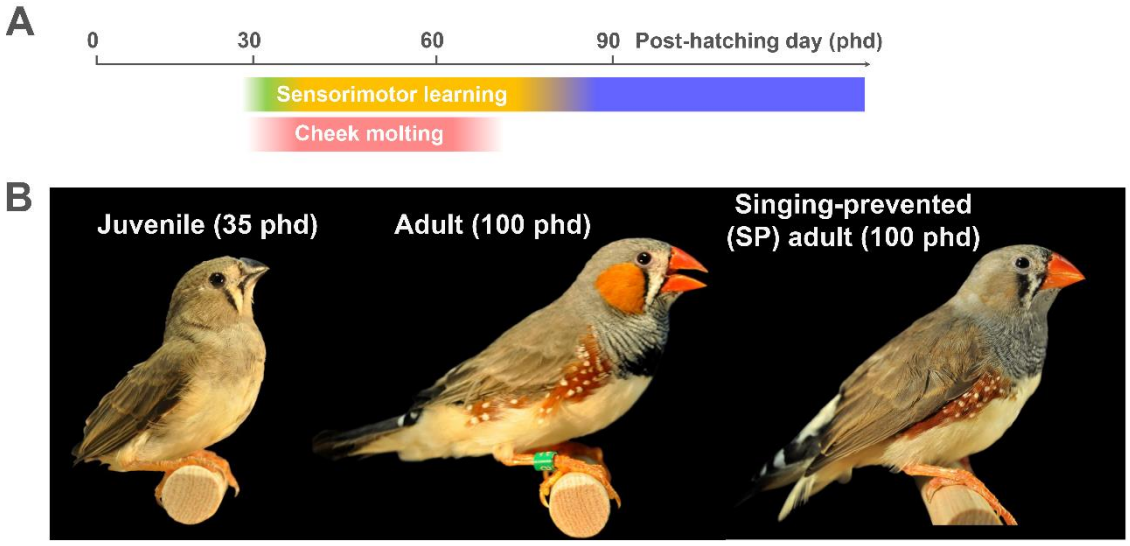

Figure 22. Developmental period of cheek patch and cheek plumage in SP adult

(A) Developmental period of cheek plumage in male zebra finch.

(B) Cheek plumage of juvenile (35 phd), adult (100 phd), and SP adult (100 phd).

(Figure 23)

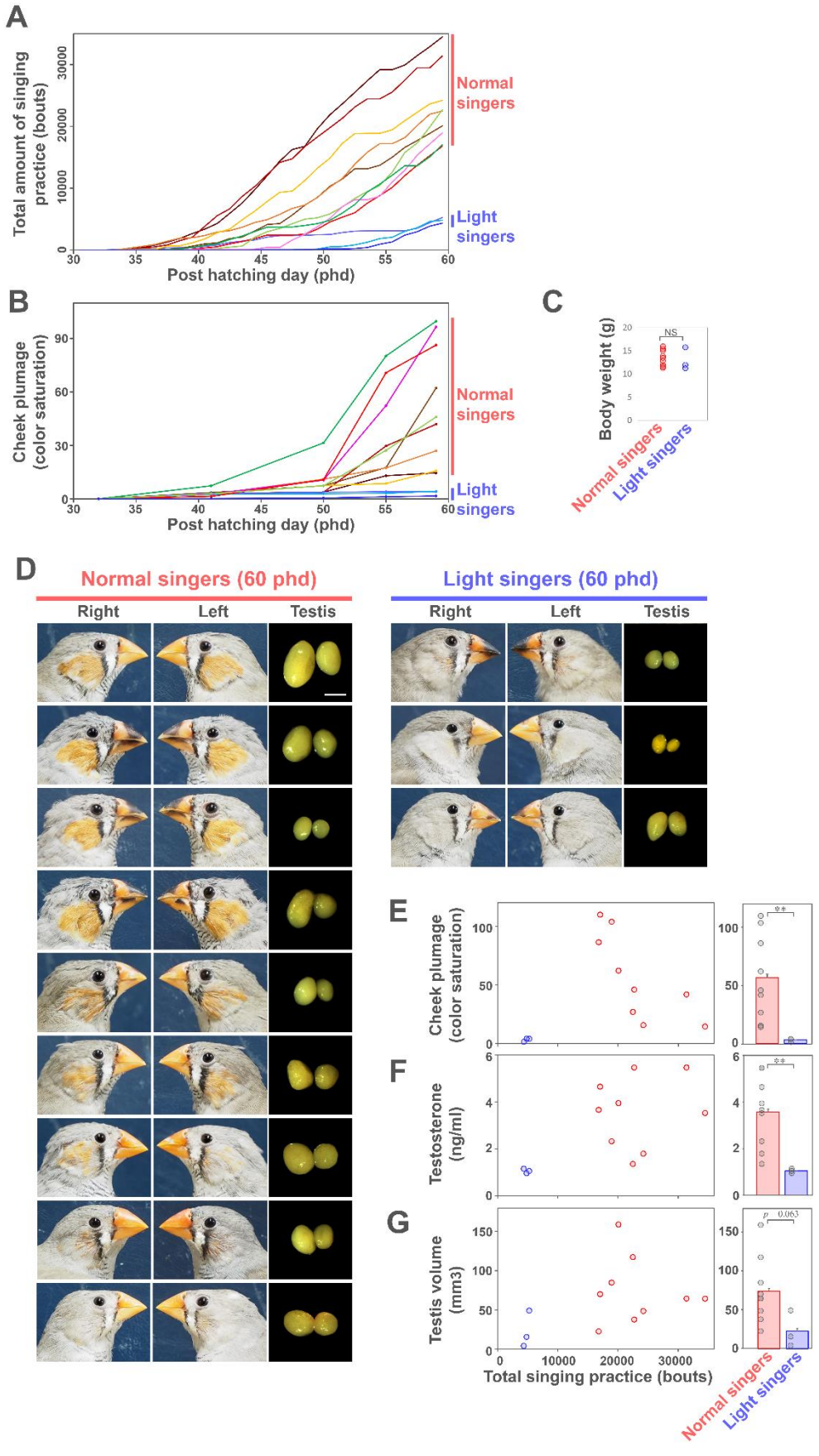
A
Total amount of singing practice (bouts)
Post hatching day (phd)
Normal singers
Light singers
B
Cheek plumage (color saturation)
Post hatching day (phd)
Normal singers
Light singers
C
Body weight (g)
NS
Normal singers
Light singers
D
Normal singers (60 phd)
Light singers (60 phd)
Right
Left
Testis
E
Cheek plumage (color saturation)
F
Testosterone (ng/ml)
G
Testis volume (mm3)
p 0.063
Total singing practice (bouts)
Normal singers
Light singers

Figure 23. Delay in cheek patch development in light singers

(A) Total accumulated amount of singing practice in juvenile birds (n = 12) from 30 until 60 phd.

(B) Color saturation of cheek patch of the 12 juvenile birds at 60 phd (n = 12).

(C) Body weight of normal singers (red, n = 9) and light singers (blue, n = 3). $^{NS}p > 0.1$, Mann-Whitney *U* test

(D) Bird faces (left panels) and testis (right panels) of the normal singers (n = 9) and light singers (n = 3) at 60 phd. Scale bar = 1.2 mm.

(E) (Left panel) Plot indicates color saturation of cheek plumage against amount of total singing (bouts) in each individuals (normal singers: red, light singers: blue, rho = 0.21, $p = 0.51$, Spearman's correlation test). (Right panel) Cheek color saturation in normal singers (red, n = 9) and light singers (blue, n = 3). $^{**}p < 0.01$, Mann-Whitney *U* test

(F) Plot indicates serum testosterone concentration (ng/ml) against amount of total singing (bouts) in each individuals (normal singers: red, light singers: blue, rho = 0.57, $p = 0.054$, Spearman's correlation test). (Right panel) Serum testosterone concentration (ng/ml) in normal singers (red, n = 9) and light singers (blue, n = 3). $^{***}p < 0.001$, Mann-Whitney *U* test

(G) Plot indicates testis volume (mm^3) against amount of total singing (bouts) in each individuals (normal singers: red, light singers: blue, rho = 0.44, $p = 0.15$, Spearman's correlation test). (Right panel) Testis volume (mm^3) in normal singers (red, n = 9) and light singers (blue, n = 3). Mann-Whitney *U* test

(Figure 24)

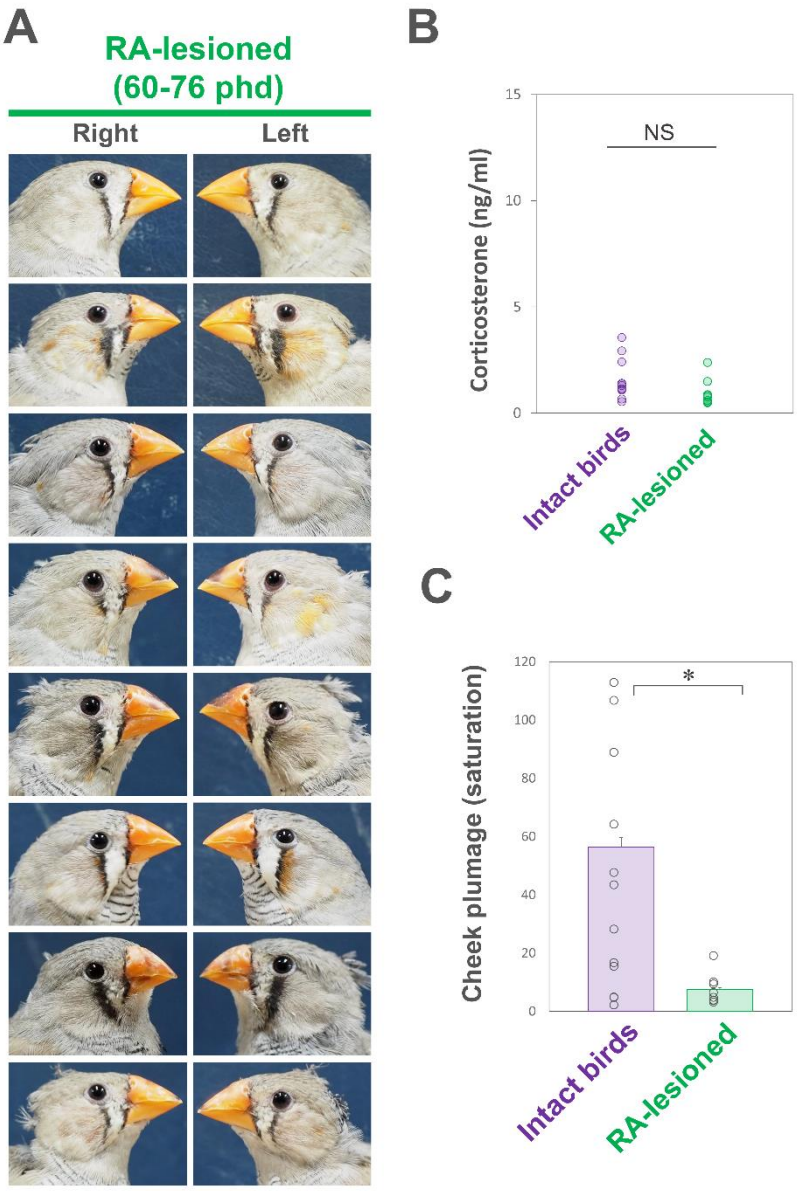

Figure 24. Delay in cheek patch development in RA-lesioned birds

(A) Faces of RA-lesioned birds.

(B) Serum corticosterone level of intact (purple, n = 12) and RA-lesioned birds (green. n = 8). $^{NS}p < 0.1$, Mann-Whitney *U* test

(C) Color saturation of cheek patch in intact (purple, n = 12, 60 phd) and RA-lesioned birds (green, n = 8, 60-76 phd). $*p < 0.05$, Mann-Whitney *U* test

(Figure 25)

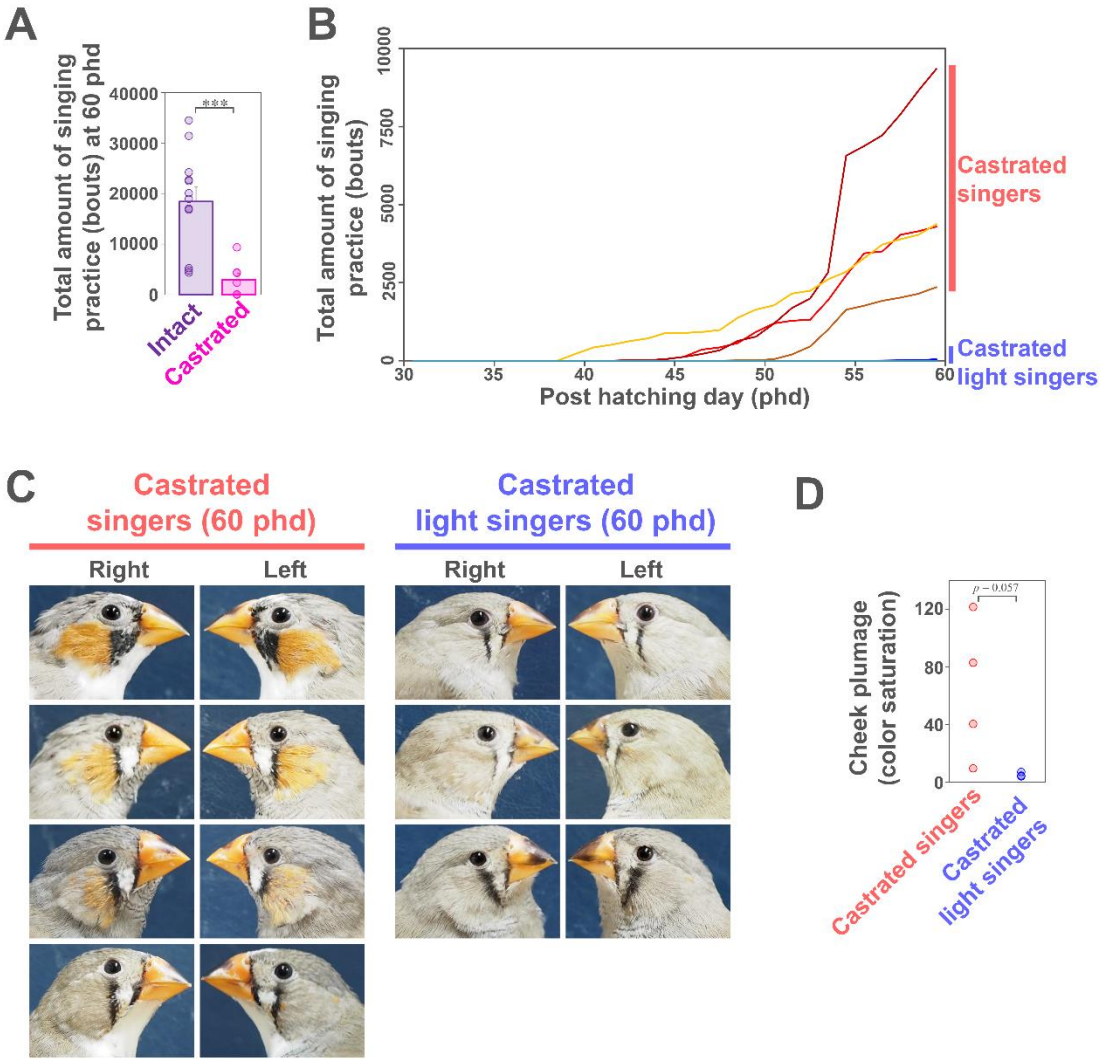

Figure 25. Molting of cheek plumage in castrated birds

(A) Total amount of singing practice in intact (purple, n = 12) and castrated birds (pink, n = 7). ***$p < 0.001$, Mann-Whitney *U* test

(B) Total accumulated amount of singing practice in the juvenile birds (n = 7) from 30 until 60 phd.

(C) Faces of the castrated singers (n = 4) and castrated light singers (n = 3) at 60 phd.

(D) Cheek color saturation in castrated singers (red, n = 4) and castrated light singers (blue, n = 3), Mann-Whitney *U* test

(Figure 26)

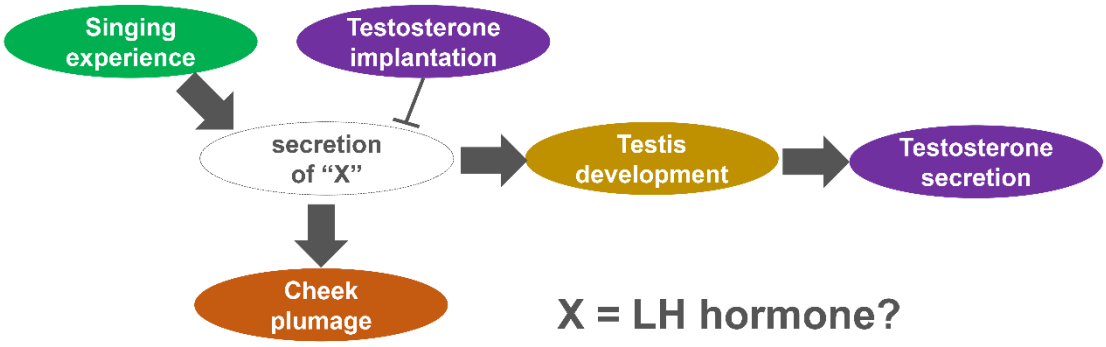

Figure 26. Potential mechanisms for cheek plumage development

General discussion

Self-generated singing experience for maturation

The critical period, a time when neuroplasticity is transiently enhanced after birth, acts as a temporal gate of learning, or rearrangement of brain circuits (Hensch, 2005). Unusual experiences during this period cause psychiatric or sensory diseases, such as schizophrenia or amblyopia which are not cured by later rehabilitation (Weinberger, 1996, Rapoport et al., 2012). Therefore, the regulatory mechanisms underlying the closure of the critical period are of importance. However, the contributions of experience and the molecular mechanisms behind the critical period in motor area still remains unclear. In this thesis, by controlling singing behavior, I examined the contributions of self-generated experience to the gene expression dynamics in particular brain regions and the regulation of song plasticity. As a by-product of this study, I found that molting of plumage also requires singing experience in zebra finch.

In Chapter I, *Arc* induction in the projection neurons in RA and NIf was synchronized with song plasticity both daily and developmentally through the critical period. The diurnal *Arc* induction dynamics was regulated by singing experience in the day. In Chapter II, singing-prevented (SP) adults generated juvenile-like plastic songs, and retained the ability to mimic the tutor song. These results indicate that the critical period of song learning is closed by singing experience, not by age. I showed that both the induction of a cluster of singing activity-dependent genes and dendritic morphology in the projection neurons in RA were strictly regulated by cumulative singing experience. Such transcriptional regulation was also observed in the canary, an open-ended learner characterized by the re-induction of the similar set of activity-dependent genes during seasonal song plasticity in adulthood. In Chapter III, I found the specific function of

singing experience on development of cheek plumage, one of secondary sex characteristics of male zebra finch.

Based on these, I conclude that cumulative singing experience during juvenile stage contribute to not only song development, but also various aspects of development (i.e. the closure of the critical period of song learning, gene expression dynamics in brain, and molting of cheek plumage) in the zebra finch. In other words, singing behavior was an essential element for normal development of zebra finch.

Potential contribution of sleep to the regulation of the critical period

During the early plastic song stage, the induction of *Arc* was down-regulated by singing experience in a day (Chapter I). However, the diurnal change was recovered every morning during the critical period. Since the developmental attenuation of Cluster I genes did not occur in SP adults (Chapter II), these daily cycles by practice-dependent reduction and recovery of activity-dependent genes may play an important role in the long-term regulation of the critical period. Therefore, the contribution of sleep to the regulation of the critical period should not be ignored.

Previous studies in rodents revealed sleep-dependent neuroplasticity during the critical period for ocular dominance in the visual system (Frank, 2011). In cortical layer II/III of the rat visual cortex, long-term potentiation (LTP) is evoked especially during rapid eye movement (REM) sleep (Frank, 2001) during the critical period (P 20~30), but not in adult (Kirkwood et al., 1995). This critical period is prolonged by REM sleep deprivation (Shaffery et al., 2002). These studies suggest an important contribution of sleep to the closure of the critical period in the visual cortex. Therefore, in zebra finch, sleep deprivation studies may also reveal the contribution of sleep to the closure of the

critical period of song plasticity.

Potential gene regulations of motor skill learning processes in other animals

In RA, analogous to the layer V pyramidal neurons in mammalian motor cortex region (Jarvis, 2004a), induction of activity-dependent genes was regulated along with song plasticity across songbird species (Chapter I and II). These results support a hypothesis that the regulation of activity-dependent genes may modulate the improvement of motor skill in various species including mammals.

During motor skill learning or adaptation process in mammal, repeated practice in a day tends to slow down skill improvement (Zhou et al., 2003; Buitrago et al., 2004; Robinson et al., 2006; Yin et al., 2009; Malone et al., 2011; Cao et al., 2015) as observed in zebra finch (Chapter I). Mammals acquire motor skills using similar brain circuits to songbird including the basal ganglia-thalamocortical loops (Reiner et al., 1998; Jarvis, 2004a; Shmuelof & Krakauer, 2011). However, most of these skills are acquired not with distinct neural circuits, but rather unspecialized circuits which contribute to multiple tasks. Training-dependent neuronal plasticity in the primary motor cortex (M1) has been associated with various complex motor skill learning (Karni et al., 1998; Costa et al., 2004; Dayan & Cohen, 2011), and these skills share same subpopulations of M1 neurons (Hayashi-Takagi et al., 2015). Such mixed motor circuits might present difficulties in evaluating the induction changes of activity-dependent gene through practice. Recent studies have revealed the existence of task-responsible cells and dendritic spines in the motor cortex, thanks to the development of live-cell imaging and cell- or spine-labelling technologies (Ren et al., 2014; Cao et al., 2015; Hayashi-Takagi et al., 2015; Mastwal et al., 2016). A previous study implemented learned motor skill-specific disruption by

shrinkage of responsible dendritic spines using optogenetic approach (Hayashi-Takagi et al., 2016). With research focus on such interspersed task-responsible cells, the diurnal practice-dependent regulation of genes may also be observed in the mammalian motor cortex.

Acknowledgment

First of all, I wish to express my sincere gratitude to my supervisor, Dr. **Kazuhiro Wada**, for giving me great support, insightful comments and providing opportunity for me to explore new and various experimental methods including fluorescence *in-situ* hybridization, transcriptome sequencing, chip-sequencing, one-cell level DNA extraction, dye injection into nXIIts, micro dialysis, and Golgi-staining. Though I could not succeed in all of these, these experiences significantly endowed me with more capability as a scientist. I also learned theoretical thinking, and the importance of deep observation of raw data from him.

I appreciate Ms. **Eri Ohgushi** for her great effort in producing the first case of the vocal practice (-) adult zebra finch. Without her work, I might not have performed singing-prevention experiment in Chapters II. She also provided brain samples of the first case of evening-singing juvenile birds. Using the samples, I got ideas about diurnal gene regulation shown in Chapter III. I also thank Mr. **Raimu Imai** and Mr. **Daisuke Sato** for giving me nice ideas on the method of singing-prevention procedures.

I appreciate Dr. **Chihiro Mori** for teaching me basic skills of animal treatment, breeding, birdsong analysis, and WGCNA method. Her hardworking and careful treatment of experimental animals were good examples for me.

I appreciate Dr. **Haruhito Horita** for providing the preliminary data of *Arc* mRNA induction in juvenile and adult zebra finches. His finding about the induction change of *Arc* lead me to better understand gene dynamics in the songbird brain. I also appreciate Dr. **Erich D. Jarvis** for deep discuss on my data.

I thank Mr. **Masahiko Kobayashi** for teaching me molecular biological techniques and tips for *in-situ* hybridization. He also provided the preliminary data on strong *Arc* induction in RA of VP (-) adult and the re-induction of *Arc* in canary RA.

I appreciate Dr. **Wan-chun Liu** for providing canary brain samples. Using his

carefully-sampled canary brains, I successfully evaluated the re-induction of Cluster I genes in RA in Chapter II.

I appreciate Dr. **Yutaka Suzuki** and members of MEXT for providing the first chance to perform RNA-sequence in zebra finch using next generation sequence. I also appreciate Dr. **Katsuhiko Mineta** for helping the first analysis of the next-generation sequence data. Although I did not use these data finally, this first analysis clearly indicated potential problems in sample preparation methods and uploaded gene/genome database of zebra finch. Based on the results, I could improve the gene library and sample preparation methods (Chapter II, Materials and Methods).

I appreciate Dr. **Yohei Sasagawa** and members of Platform Project for Supporting Drug Discovery and Life Science Research for giving me the chance to perform next generation sequencing (NGS) again and also helping to analyze the data. This program provided me not only clean data, but also deep understand of the preparation methods for NGS samples and data analysis. I also appreciate Dr. **Norikazu Monma** and Dr. **Kazuho Ikeo** for providing the computing pipeline, MASER, to analyze NGS read data. Their MASER system was very useful and really accelerated my analysis in Chapter II.

I thank Mr. **Chinweike Norman Asogwa** and **Sanchez-Valpuesta Miguel** for their kindly supports for checking English in this thesis. Daily discussion with them improved grammar in this write up.

I thank Ms. **Azusa Sawai** for improving the methods to remove background noise in song files. This behavioral analysis made it easier to analyze daily shifts of syllable acoustics in Chapter I. Additionally, her RNA-seq data of whole-brain were used for improving the database of zebra finch genes (Chapter II, Materials and Methods). Her non-amplified RNA-seq data was necessary to make good annotation file.

I thank Ms. **Yuika Suzuki** and Ms. **Yukino Shibata** for their great help in

counting singing bouts of juvenile birds in Chapter III (Fig. 22).

I thank Dr. **Nao Ota** for her critical suggestion on the experimental design in cheek-plumage analysis in Chapter III (Fig. 22).

I appreciate Dr. **Toshiya Matusima** and Dr. **Hiroto Ogawa** for useful suggestions on my data and manuscript to accomplish this thesis.

I appreciate Dr. **Miwako Yamasaki** for providing the protocol for fluorescence *in-situ* hybridization experiment (Chapter I, Materials and Methods).

I thank Dr. **Hidetoshi Amita** for his critical suggestion on statistical analysis for the *in-situ* hybridization experiment (Chapter I, II). I also thank members of Animal Behavior and Intelligence in Hokkaido University for their advices and kind supports.

This work was supported by MEXT KAKENHI (No. 221S0002).

This work was supported by JSPS KAKENHI Grant Number JP26001737

This research is supported by Platform Project for Supporting Drug Discovery and Life Science Research (Basis for Supporting Innovative Drug Discovery and Life Science Research (BINDS)) from Japan Agency for Medical Research and Development (AMED).

References

Abe, K., Matsui, S., & Watanabe, D. (2015). Transgenic songbirds with suppressed or enhanced activity of CREB transcription factor. *Proceedings of the National Academy of Sciences*, *112*(24), 7599–7604.

Alvarez-buylla, A., Kirn, J. R., & Notrebohm, F. (1990). Birth of Projection Neurons in Adult Avian Brain May Be Related to Perceptual or Motor Learning. *Science*, *249*(4975), 1444–1446.

Andalman, A. S., & Fee, M. S. (2009). A basal ganglia-forebrain circuit in the songbird biases motor output to avoid vocal errors. *Proceedings of the National Academy of Sciences*, *106*(30), 12518–12523.

Arnold, A. P. (1975). The effects of castration on song development in zebra finches (*Poephila guttata*). *Journal of experimental zoology*, 191, 261-278

Arnold, A. P. (1980). Quantitative analysis of sex differences in hormone ccumulation in the zebra finch brain: Methodological and theoretical issues. *J. Comp Neurol*. 189:421-36

Andersson, M. (1982). Female choice selects for extreme tail length in a widowbird. *Nature*, 299, 818-820

Balmer, T. S., Carels, V. M., Frisch, J. L., & Nick, T. A. (2009). Modulation of perineuronal nets and parvalbumin with developmental song learning. *The Journal of Neuroscience : The Official Journal of the Society for Neuroscience*, *29*(41), 12878–85.

Bardin, J. (2012). Neurodevelopment: Unlocking the brain. *Nature*, *487*(7405), 24–26.

Bengtsson, S. L., Nagy, Z., Skare, S., Forsman, L., Forssberg, H., & Ullén, F. (2005). Extensive piano practicing has regionally specific effects on white matter development. *Nature Neuroscience*, *8*(9), 1148–1150.

Bohner, J. (1990). Early acquisition in the zebra finch (*Taeniopygia guttata*). *Animal Behavior*, *39*, 369–374.

Bottjer, S.W. (1993) The distribution of tyrosine hydroxylase immunoreactivity in the brains of male and female zebra finches. *Developmental Neurobiology*, 24(1), 51-69

Bottjer, S.W., Miesner, E.A. & Arnold, A.P. (1984) Forebrain lesions disrupt development but not maintenance of song in passerine birds. *Science*, 224, 901-903.

Bramham, C. R., Worley, P. F., Moore, M. J., & Guzowski, J. F. (2008). The Immediate Early Gene *Arc/Arg3.1*: Regulation, Mechanisms, and Function. *Journal of Neuroscience*, *28*(46), 11760–11767.

Brenowitz, E. A., & Larson, T. A. (2015). Neurogenesis in the Adult Avian Song-Control System. *Cold Spring Harb Perspect Biol*, *7*(6), 1–23.

Buitrago, M. M., Schulz, J. B., Dichgans, J., & Luft, A. R. (2004). Short and long-term motor skill learning in an accelerated rotarod training paradigm. *Neurobiology of Learning and Memory*, *81*(3), 211–216.

Cao, V. Y., Ye, Y., Mastwal, S., Ren, M., Coon, M., Liu, Q., Costa, R.M., Wang, K. H. (2015). Motor Learning Consolidates *Arc*-Expressing Neuronal Ensembles in Secondary Motor Cortex. *Neuron*, *86*(6), 1385–1392.

Chang, E.F., Merzenich, M.M. (2003) Environmental Noise Retards Auditory Cortical Development. *Science*, 300, 498-502

Chowdhury, S., Shepherd, J. D., Okuno, H., Lyford, G., Petralia, R. S., Plath, N., Kuhl, D., Huganir, R.L., Worley, P. F. (2006). *Arc/Arg3.1* interacts with the endocytic machinery to regulate AMPA receptor trafficking. *Neuron*, *52*(3), 445–59.

Costa, R.M., Cohen, D., Nicolelis, M.A.L. (2004) Differential Corticostriatal Plasticity during Fast and Slow Motor Skill Learning in Mice. Current biology, 14, 1124-1134

Davis, M. F., Figueroa Velez, D. X., Guevarra, R. P., Yang, M. C., Habeeb, M., Carathedathu, M. C., & Gandhi, S. P. (2015). Inhibitory Neuron Transplantation into Adult Visual Cortex Creates a New Critical Period that Rescues Impaired Vision. *Neuron*, *86*(4), 1055–1066.

Davison, A. N. (1968). The developing brain, *Applied neurochemistry*, Blackwell Oxford, 253-286

Dawson, A. (1997). Plasma-luteinizing hormone and prolactin during circannual rhythms of gonadal maturation and molt in male and female European starlings. *J. Biol. Rhythms*, *12*(4), 371–377.

Dayan, E., & Cohen, L. G. (2011). Neuroplasticity subserving motor skill learning. *Neuron*, *72*(3), 443–454.

Derégnaucourt, S., Mitra, P. P., Fehér, O., Pytte, C., & Tchernichovski, O. (2005). How sleep affects the developmental learning of bird song. *Nature*, *433*(7027), 710–6.

Ding, L. & Perkel, D. (2004). Long-Term Potentiation in an Avian Basal Ganglia Nucleus Essential for Vocal Learning. *Journal of Neuroscience*, *24*(2), 488–494.

Doupe, a J., & Kuhl, P. K. (1999). Birdsong and human speech: common themes and mechanisms. *Annual Review of Neuroscience*, *22*, 567–631.

Drnevich, J., Replogle, K. L., Lovell, P., Hahn, T. P., Johnson, F., Mast, T. G., Nordeen, E., Nordeen, K., Strand, C., London, S. E., Mukai. M., Wingfield, J.C., Arnold, A. P., Ball, G. F., Brenowitz, E. A., Wade, J., Mello, C. V., Clayton, D. F. (2012). Impact of experience-dependent and -independent factors on gene expression in songbird brain. *Proceedings of the National Academy of Sciences of the United States of America*, *109 Suppl*, 17245–52.

Eales, L. A. (1985). Song learning in zebra finches: some effects of song model availability on what is learnt and when. *Animal Behaviour*, *33*(4), 1293–1300.

Elbert, T., Pantev, C., Wienbruch, C., Rockstroh, B., & Taub, E. (1995). Increased cortical representation of the fingers of the left hand in string players. *Science*, *270*(5234), 305–7.

Farris, S., Lewandowski, G., Cox, C. D., & Steward, O. (2014). Selective Localization of *Arc* mRNA in Dendrites Involves Activity- and Translation-Dependent mRNA Degradation. *Journal of Neuroscience*, *34*(13), 4481–4493.

Fee, M. S., Kozhevnikov, A. a, & Hahnloser, R. H. R. (2004). Neural mechanisms of vocal sequence generation in the songbird. *Annals of the New York Academy of Sciences*, *1016*, 153–70.

Feenders, G., Liedvogel, M., Rivas, M., Zapka, M., Horita, H., Hara, E., Wada, K., Mouritsen, H., Jarvis, E. D. (2008). Molecular mapping of movement-associated areas in the avian brain: A motor theory for vocal learning origin. *PLoS ONE*, *3*(3).

Frank, M. G., Issa, N. P., & Stryker, M. P. (2001). Sleep enhances plasticity in the developing visual cortex. *Neuron*, *30*(1), 275–287.

Frank, M. G. (2011) Sleep and developmental plasticity not just for kids. *Prog Brain Res*, 193, 221-32

Garst-Orozco, J., Babadi, B., Ölveczky, B. (2014) A neural circuit mechanism for regulating 1 vocal variability during song learning in zebra finches. *elife*, 3, e03697

Funabiki, Y., & Konishi, M. (2003). Long Memory in Song Learning by Zebra Finches. *The Journal of Neuroscience*, *23*(17), 6928–35.

Goldman, S. A., & Nottebohm, F. N. (1983). Neuronal production, migration, and differentiation in a vocal control nucleus of the adult female canary brain.

Proceedings of the National Academy of Sciences of the United States of America, *80*(8), 2390–2394.

Gordon, J. A., & Stryker, M. P. (1996). Experience-dependent plasticity of binocular responses in the primary visual cortex of the mouse. *The Journal of Neuroscience*, *16*(10), 3274–86.

Greer, P. L., & Greenberg, M. E. (2008). From Synapse to Nucleus: Calcium-Dependent Gene Transcription in the Control of Synapse Development and Function. *Neuron*, *59*(6), 846–860.

Guo, J. U., Ma, D. K., Mo, H., Ball, M. P., Jang, M.-H., Bonaguidi, M. A., Balazer, J .A., Eaves, H. L., Xie, B., Ford, E., Zhang, K., Ming, G., Gao, Y., Song, H. (2011). Neuronal activity modifies the DNA methylation landscape in the adult brain. *Nature Neuroscience*, *14*(10), 1345–51.

Hahnloser, R. H. R., Kozhevnikov, A. A., & Fee, M. S. (2003). An ultra-sparse code underlies the generation of neural sequences in a songbird. *Nature*, *421*(6920), 294–294.

Hagelin, J. C., & Kimball, R. T. (1997). A female Gambel's Quail with Partial Male Plumage. *The Wilson Bulletin*, 109 (3). 544-546

Hayashi-takagi, A., Yagishita, S., Nakamura, M., Shirai, F., Wu, Y., Loshbaugh, A. L., Kuhlman, B., Hahn, K. M., Kasai, H. (2016). Labelling and optical erasure of synaptic memory traces in the motor cortex. *Nature*, *525*(7569), 333–338.

Hensch, T. K. (2005). Critical period plasticity in local cortical circuits. *Nature Reviews Neuroscience*, *6*(11), 877–888.

Herrmann, K. and Arnold, A. P. (1991) The Development of Afferent Projections to the Robust Archistriatal Nucleus in Male Zebra Finches: A Quantitative Electron Microscopic Study. *The Journal of Neuroscience*, 11(7), 2063–74

Hill, G. E., & Montgomerie, R. (1994). Plumage Colour Signals Nutritional Condition in the House Finch. *Proceedings of the Royal Society B: Biological Sciences*, *258*(1351), 47–52.

Hilliard, A., Miller, J., Fraley, E. R., Horvath, S., & White, S. (2012). Molecular microcircuitry underlies functional specification in a basal ganglia circuit dedicated to vocal learning. *Neuron*, *73*(3), 537–552.

Houtman, A. M. (1990). Female zebra finches choose extra-pair copulations with genetically attractive males. *Proc. R. Soc. Lond,* 249, 3-6.

Hubel, D. H., Wiesel, T. N. (1965) Binocular interaction in striate cortex of kittens reared with artificial squint. *Journal of Neurophysiology,* 28 (6), 1041-1059

Hultsch, H. & Todt, D. (2004) Learning to sing-Chapter 3, *Nature's Music*, Elsevier Inc. 80-107

Immelmann, K. (1969) Song development in the zebra finch and other estrildid finches. In Hinde, R. (ed) *Bird Vocalizations*. Cambridge University Press, Cambridge, pp. 61–74.

Jarvis, E. D., & Nottebohm, F. (1997). Motor-driven gene expression, PNAS, *94*(April), 4097–4102.

Jarvis, E. D. (2004a) Learned birdsong and the neurobiology of human language, *N.U.Acad.Sci*, 1016, 749-777

Jarvis, E. D. (2004b) Brains and birdsong-Chapter 8, *Nature's Music,* Elsevier Inc. 226-271

Jin, H., & Clayton, D. F. (1997). Localized changes in immediate-early gene regulation during sensory and motor learning in zebra finches. *Neuron*, *19*(5), 1049–59.

Johnson, F., Soderstrom, K., Whitney, O. (2002) Quantifying song bout production during zebra finch sensory-motor learning suggests a sensitive period for vocal practice. *Behav Brain Res*. 131, 57–65.

Kao, M. H., Doupe, A. J., & Brainard, M. S. (2005). Contributions of an avian basal ganglia–forebrain circuit to real-time modulation of song. *Nature*, *433*(7026), 638–643.

Karni, A., Meyer, G., Rey-Hipolito, C., Jezzard, P., Adams, M. M., Turner, R., & Ungerleider, L. G. (1998). The acquisition of skilled motor performance: Fast and slow experience-driven changes in primary motor cortex. *Proceedings of the National Academy of Sciences*, *95*(3), 861–868.

Kelleher III, R. J., Govindarajan, A., & Tonegawa, S. (2004). Translational regulatory mechanisms in persistent forms of synaptic plasticity. *Neuron*, *44*(1), 59–73.

Kigar, S. L., Chang, L., & Auger, A. P. (2015). Gadd45b is an epigenetic regulator of juvenile social behavior and alters local pro-inflammatory cytokine production in the rodent amygdala. *Brain, Behavior, and Immunity*, *46*, 60–69.

Kimball, R. T., & Ligon, J. D. (1999). Evolution of Avian Plumage Dichromatism from a Proximate Perspective. *The American Naturalist*, *154*(2), 182–193.

Kirkwood, a., Lee, H. K., & Bear, M. F. (1995). Co-regulation of long-term potentiation and experience-dependent synaptic plasticity in visualcortex by age and experience. *Nature*.

Kittelberger, J. M., & Mooney, R. (1999). Lesions of an avian forebrain nucleus that disrupt song development alter synaptic connectivity and transmission in the vocal premotor pathway. *J Neurosci*, *19*(21), 9385–9398.

Knudsen, I. E. (2004). Sensitive periods in the development of the brain and behavior. *Journal of Cognitive Neuroscience*, 16:8, 1412-1425

Korsia, S., & Bottjer, S. W. (1991). Chronic testosterone treatment impairs vocal learning in male zebra finches during a restricted period of development. *The Journal of Neuroscience : The Official Journal of the Society for Neuroscience*, *11*(8), 2362–2371.

Krause, E., & Naguib, M. (2015). Zebra finch males compensate in plumage ornaments at sexual maturation for a bad start in life. *Frontiers in Zoology*, *12*(Suppl 1), S11.

Kruse, A. A., Stripling, R., & Clayton, D. F. (2004). Context-specific habituation of the zenk gene response to song in adult zebra finches. *Neurobiology of Learning and Memory*, *82*(2), 99–108.

Kubikova, L., Wada, K., & Jarvis, E. D. (2010). Dopamine receptors in a songbird brain. *Journal of Comparative Neurology*, *518*(6), 741–769.

Lampe, H. M. H., & Espmark, Y. Y. O. (1994). Song structure reflects male quality in pied flycatchers, *Ficedula hypoleuca*. *Animal Behaviour*.

Langfelder, P., & Horvath, S. (2008). WGCNA: an R package for weighted correlation network analysis. *BMC Bioinformatics*, *9*(1), 559.

Leader, N., & Nottebohm, F. (2006). Delayed plumage maturation in socially isolated juvenile zebra finches, *Taeniopygia guttata*. *Animal Behaviour*, *72*(1), 113–121.

Lifjeld, J. T. & Slagsvold, T (1988). Plumage color and sexual selection in the Pied Flycatcher Ficedula hypoleuca. *Animal Behaviour*, *36*(2), 395–407.

Lorenz, K. (1958). The Evolution of Behavior. *Scientific American*, 199(6), 67-78.

Ma, D. K., Jang, M.-H., Guo, J. U., Kitabatake, Y., Chang, M.-L., Pow-Anpongkul, N., Flavell, R. A., Lu, B., Ming, G-L., Song, H. (2009). Neuronal activity-induced Gadd45b promotes epigenetic DNA demethylation and adult neurogenesis. *Science*, *323*(5917), 1074–7.

Malone, L. A., Vasudevan, E. V. L., & Bastian, A. J. (2011). Motor Adaptation Training for Faster Relearning. *Journal of Neuroscience*, *31*(42), 15136–15143.

Marler, P. (1970) A comparative approach to vocal learning: Song development in white-crowned sparrows. *Journal of Comparative and Physiological Psychology*, 71(2), 1-25.

Marler, P., Peters, S., Ball, G. F., Dufty, a M., & Wingfield, J. C. (1988). The role of sex steroids in the acquisition and production of birdsong. *Nature*, *336*, 770–772.

Mastwal, S., Cao, V., & Wang, K. H. (2016). Genetic Feedback Regulation of Frontal Cortical Neuronal Ensembles Through Activity-Dependent Arc Expression and Dopaminergic Input. *Frontiers in Neural Circuits*, *10*(December), 1–10.

Matsunaga, E., & Okanoya, K. (2008). Expression analysis of cadherins in the songbird brain: Relationship to vocal system development. *Journal of Comparative Neurology*, *508*(2), 329–342.

Maze, I., Wenderski, W., Noh, K. M., Bagot, R. C., Tzavaras, N., Purushothaman, I., Elisasser, S. J., Guo, Y., Ionete, C., Hurd, Y. L., Tamminga, C. A., Halene, T., Farrelly, L., Soshnev, A. A., Wen, D., Rafii, S., Birtwistle, M. R., Akbarian, S., Buchholz, B. A., Blitzer, R. D., Nestler, E. J., Yuan, Z-F., Garcia, B. A., Shen, L., Molina, H., & Allis, C. D. (2015). Critical Role of Histone Turnover in Neuronal Transcription and Plasticity. *Neuron*, *87*(1), 77–94.

Mehaffey, W. H., & Doupe, A. J. (2015). Naturalistic stimulation drives opposing heterosynaptic plasticity at two inputs to songbird cortex. *Nature Neuroscience*, *18*(9), 1272–1280.

Mello, C., Nottebohm, F., & Clayton, D. (1995). Repeated exposure to one song leads to a rapid and persistent decline in an immediate early gene's response to that song in zebra finch telencephalon. *The Journal of Neuroscience : The Official Journal of the Society for Neuroscience*, *15*(10), 6919–25.

Mello, C. V., Pinaud, R., & Ribeiro, S. (1998). Noradrenergic system of the zebra finch brain: Immunocytochemical study of dopamine-β-hydroxylase. *Journal of Comparative Neurology*, *400*(2), 207–228.

Messaoudi, E., Kanhema, T., Soule, J., Tiron, A., Dagyte, G., da Silva, B., & Bramham, C. R. (2007). Sustained *Arc/Arg3.1* Synthesis Controls Long-Term Potentiation Consolidation through Regulation of Local Actin Polymerization in the Dentate Gyrus In Vivo. *Journal of Neuroscience*, *27*(39), 10445–10455.

Mori, C., & Wada, K. (2015). Audition-Independent Vocal Crystallization Associated with Intrinsic Developmental Gene Expression Dynamics. *Journal of Neuroscience*, *35*(3), 878–889.

Mower, G. D., Berry, D., Burchfiel, J. L., & Duffy, F. H. (1981). Comparison of the effects of dark rearing and binocular suture on development and plasticity of cat visual cortex. *Brain Research*, *220*(2), 255–267.

Møller, A. P. (1989) Natural and sexual selection on a plumage signal of status and on morphology in house sparrows, *Passer domesticus*. *Journal of Evolutionary Biology*, *2*(2), 125–140.

Nottebohm, F., Stokes, T.M. & Leonard, C.M. (1976) Central control of song in the canary, Serinus canarius. *The Journal of comparative neurology*, **165**, 457-486.

Nottebohm, F., Nottebohm, M. E., Crane, L. A., & Wingfield, J. C. (1987). Seasonal changes in gonadal hormone levels of adult male canaries and their relation to song. *Behavioral and Neural Biology*, *47*(2), 197–211.

Ohgushi, E., Mori, C., & Wada, K. (2015). Diurnal oscillation of vocal development associated with clustered singing by juvenile songbirds. *The Journal of Experimental Biology*, *218*(Pt 14), 2260–8.

Okubo, T. S., Mackevicius, E. L., Payne, H. L., Lynch, G. F., & Fee, M. S. (2015). Growth and splitting of neural sequences in songbird vocal development. *Nature*, *528*(7582), 352–357.

Okuno, H., Akashi, K., Ishii, Y., Yagishita-Kyo, N., Suzuki, K., Nonaka, M., Kawashima, T., Fujii, H., Takemoto-Kimura, S., Abe, M., Natsume, R., Chowdhury, S., Sakimura, K., Worley, P. F., Bito, H. (2012). Inverse synaptic tagging of inactive synapses via dynamic interaction of Arc/Arg3.1 with CaMKIIβ. *Cell*, *149*(4), 886–898.

O'Leary, D. D. M., Ruff, N. L., & Dyck, R. H. (1994). Development, critical period plasticity, and adult reorganizations of mammalian somatosensory systems. *Current Opinion in Neurobiology*, *4*(4), 535–544.

Ölveczky, B. P., Otchy, T. M., Goldberg, J. H., Aronov, D., & Fee, M. S. (2011). Changes in the neural control of a complex motor sequence during learning. *Journal of Neurophysiology*, *106*(1), 386–97.

Owens, I. P. F., & Short, R. V. (1995). Hormonal basis of sexual dimorphism in birds: implications for new theories of sexual selection. *Trends in Ecology & Evolution*, *10*(1), 44–47.

Plath, N., Ohana, O., Dammermann, B., Errington, M. L., Schmitz, D., Gross, C., Mao, X., Engelsberg, A., Mahlke, C., Welzl, H., Kobalz, U., Stawrakakis, A., Fernandez, E., Waltereit, R., Bick-Sander, A., Therstappen, E., Cooke, S. F., Blanquet, V., Wurst, W., Salmen, B., Bosl, M. R., Lipp, H-P., Grant, S. G. N., Bliss, T. V. P., Wolfer, D. P., Kuhl, D. (2006). *Arc/Arg3.1* is essential for the consolidation of synaptic plasticity and memories. *Neuron*, *52*(3), 437–44.

Portman, O.W., Alexander, M., & Illingworth, D.R. (1972). Changes in Brain and Sciatic Nerve Composition With Development of the Rhesus Monkey (*Macaca Mulatta*), *Brain research*, *43*, 197–213.

Price, P. (1979) Developmental Deterrininants Of Structure in Zebra Finch Song. *Journal of Comparative and Physiological Psychology*, 93, 260-277

Rapoport, J. L., Giedd, J. N., & Gogtay, N. (2012). Neurodevelopmental model of schizophrenia: update 2012. *Molecular Psychiatry*, *17*(12), 1228–1238.

Reiner, a, Medina, L., & Veenman, C. L. (1998). Structural and functional evolution of the basal ganglia in vertebrates. *Brain Research. Brain Research Reviews*, *28*(3), 235–85.

Ren, M., Cao, V., Ye, Y., Manji, H. K., & Wang, K. H. (2014). Arc Regulates Experience-Dependent Persistent Firing Patterns in Frontal Cortex. *Journal of Neuroscience*, *34*(19), 6583–6595.

Roberts, T. F., Tschida, K. A., Klein, M . E., & Mooney, R. (2010). Rapid spine stabilization and synaptic enhancement at the onset of behavioural learning. *Nature.* Vol.463, 08759

Robinson, F. R., Soetedjo, R., & Noto, C. (2006). Distinct Short-Term and Long-Term Adaptation to Reduce Saccade Size in Monkey. *Journal of Neurophysiology; Journal of Neurophysiology*, *96*(3), 1030–1041.

Sasagawa, Y., Nikaido, I., Hayashi, T., Danno, H., Uno, K. D., Imai, T., & Ueda, H. R. (2013). Quartz-Seq: a highly reproducible and sensitive single-cell RNA sequencing method, reveals non-genetic gene-expression heterogeneity. *Genome Biology*, *14*(4), 3097.

Sato, M., & Stryker, M. P. (2008). Distinctive features of adult ocular dominance plasticity. *Journal of Neuroscience*, *28*(41), 10278–86.

Scharff, C., & Nottebohm, F. N. (1991). A comparative study of the behavioral deficits following lesions of various parts of the zebra finch song system: implications for vocal learning. *The Journal of Neuroscience : The Official Journal of the Society for Neuroscience, 11*(9), 2896–913.

Senar, J. C. (1999). Plumage coloration as a signal of social status. *Proceedings of the International Ornithological Congress*, (22), 1669–1686.

Shaffery, J. P., Sinton, C. M., Bissette, G., Roffwarg, H. P., & Marks, G. A. (2002). Rapid eye movement sleep deprivation modifies expression of long-term potentiation in visual cortex of immature rats. *Neuroscience*, *110*(3), 431–443.

Shank, S. S., & Margoliash, D. (2009). Sleep and sensorimotor integration during early vocal learning in a songbird, *Nature*, *458*(7234), 73–77.

Shepherd, J. D., & Bear, M. F. (2011). New views of Arc, a master regulator of synaptic plasticity. *Nature Neuroscience*, *14*(3), 279–84.

Shmuelof, L., & Krakauer, J. W. (2011). Are we ready for a natural history of motor learning? *Neuron*, *72*(3), 469–476.

Sizemore, M., & Perkel, D. J. (2008). Noradrenergic and GABAB Receptor Activation Differentially Modulate Inputs to the Premotor Nucleus RA in Zebra Finches. *Journal of Neurophysiology*, *100*(1), 8–18.

Sizemore, M., & Perkel, D. J. (2011). Premotor synaptic plasticity limited to the critical period for song learning. PNAS, 108(42), 17492-17497

Snow, C. E., & Hoefnagel-Hohle, M. (1978). The Critical Period for Language Acquisition : Evidence from Second Language Learning. *Child Development*, *49*(4), 1114–1128.

Sober, S. J., Wohlgemuth, M. J., & Brainard, M. S. (2008). Central Contributions to Acoustic Variation in Birdsong. *Journal of Neuroscience*, *28*(41), 10370–10379.

Soha, J. A., Shimizu, T., & Doupe, A. J. (1996). Development of the catecholaminergic innervation of the song system of the male zebra finch. *Journal of Neurobiology*, *29*(4), 473–489.

Spiro, J. E., Dalva, M. B., & Mooney, R. (1999). Long-range inhibition within the zebra finch song nucleus RA can coordinate the firing of multiple projection neurons. *Journal of Neurophysiology*, *81*(6), 3007–20.

Stark, L. L., & Perkel, D. J. (1999). Two-stage, input-specific synaptic maturation in a nucleus essential for vocal production in the zebra finch. *The Journal of Neuroscience*, *19*(20), 9107–9116.

Steward, O., Wallace, C. S., Lyford, G. L., & Worley, P. F. (1998). Synaptic activation causes the mRNA for the leg Arc to localize selectively near activated postsynaptic sites on dendrites. *Neuron*, *21*(4), 741–751.

Stokkan, K. A., & Sharp, P. J. (1980). Seasonal changes in the concentrations of plasma leutinizing hormone and testosterone in willow ptarmigan (Lagopus lagopus lagopus) with observations on the effects of permanent short days. *General & Comparative Endocrinology*, *40*, 109–115.

Stryker, M. P., & Harris, W. a. (1986). Binocular impulse blockade prevents the formation of ocular dominance columns in cat visual cortex. *The Journal of Neuroscience : The Official Journal of the Society for Neuroscience*, *6*(8), 2117–2133.

Tchernichovski, O. (2001). Dynamics of the Vocal Imitation Process: How a Zebra Finch Learns Its Song. *Science*, *291*(5513), 2564–2569.

Tchernichovski, O., Nottebohm, F., Ho, C., Pesaran, B., & Mitra, P. (2000). A procedure for an automated measurement of song similarity. *Animal Behaviour*, *59*(6), 1167–1176.

Vicario, D. S., Nottebohm, F. (1988) Organization of the zebra finch song control system: I. Representation of syringeal muscles in the hypoglossal nucleus. *J. Comp Neurol*. 271, 346-354

Vyssotski, A. L., Stepien, A. E., Keller, G. B., & Hahnloser, R. H. R. (2016). A Neural Code That Is Isometric to Vocal Output and Correlates with Its Sensory Consequences. *PLoS Biology*, *14*(10), 1–21.

Wada, K., Howard, J.T., McConnell, P., Whitney, O., Lints, T., Rivas, M.V., Horita, H., Patterson, M.A., White, S.A., Scharff, C., Haesler, S., Zhao, S., Sakaguchi, H., Hagiwara, M., Shiraki, T., Hirozane-Kishikawa, T., Skene, P., Hayashizaki, Y., Carninci, P. & Jarvis, E.D. (2006) A molecular neuroethological approach for identifying and characterizing a cascade of behaviorally regulated genes. *Proceedings of the National Academy of Sciences of the United States of America*, **103**, 15212-15217.

Weinberger, D. R. (1996). On the plausibility of "the neurodevelopmental hypothesis" of schizophrenia. *Neuropsychopharmacology*. 14, 35

West, A. E., Griffith, E. C., & Greenberg, M. E. (2002). Regulation of transcription factors by neuronal activity. *Nature Reviews Neuroscience*, *3*(12), 921–931.

Whitney, O., Pfenning, A. R., Howard, J. T., Blatti, C. A., Liu, F., Ward, J. M., Wang, R., Audet, J-N., Killis, M., Mukherjee, S., Sinha, S., Hertemink, A. J., West, A. E., Jarvis, E. D. (2014). Core and region-enriched networks of behaviorally regulated genes and the singing genome. *Science*, *346*(6215), 1256780–1256780.

Wiesel, T. N., & Hubel, D. H. (1963). Responses in Striate Deprived of Vision Cortex of One Eye. *Journal of Neurophysiology*, *26*, 1003–1017.

Wild, J. M. (1993) Descending projections of the songbird nucleus robustus archistriatalis. *J. Comp Neurol*. 338 (28), 225-241

Wood, W. E., Lovell, P. V., Mello, C. V., Perkel, D. J. (2011) Serotonin, via HTR2 receptors, excites neurons in a cortical-like pre-motor nucleus necessary for song learning and production. *J Neurosci.* 31(39), 13808–13815.

Ye, Y., Mastwal, S., Cao, V. Y., Ren, M., Liu, Q., Zhang, W., Elkahloun, A. G., Wang, K. H. (2017). Dopamine is Required for Activity-Dependent Amplification of Arc mRNA in Developing Postnatal Frontal Cortex. *Cerebral Cortex*, *27*(7), 3600–3608.

Yin, H. H., Mulcare, S. P., Hilário, M. R. F., Clouse, E., Holloway, T., Davis, M. I., Hansson, A. C., Lovinger, D.M., Costa, R. M. (2009). Dynamic reorganization of striatal circuits during the acquisition and consolidation of a skill. *Nature Neuroscience*, *12*(3), 333–341.

Zann, R. A. (1997) The Zebra Finch. Oxford University Press.

Zhang, L. I., Bao, S., & Merzenich, M. M. (2002). Disruption of primary auditory cortex by synchronous auditory inputs during a critical period. *Proceedings of the National Academy of Sciences*, *99*(4), 2309–2314.

Zhou, W., Weldon, P., Tang, B., & King, W. M. (2003). Rapid motor learning in the translational vestibulo-ocular reflex. *Journal of Neuroscience*, *23*(10), 4288–4298.